DISTRIBUTION, CHARACTERIZATION, & TEMPORAL STUDY OF BIOSIGNATURES AT THE DYNGJUSANDUR, ICELAND MARS ANALOG

A Dissertation
Presented to
The Academic Faculty

by

Scot M Sutton II

In Partial Fulfillment
of the Requirements for the Degree
Doctor of Philosophy in the
School of Chemistry & Biochemistry

Georgia Institute of Technology
May 2022

DISTRIBUTION, CHARACTERIZATION, & TEMPORAL STUDY OF BIOSIGNATURES AT THE DYNGJUSANDUR, ICELAND, MARS ANALOG

Approved by:

Dr. Amanda Stockton, Advisor
School of Chemistry & Biochemistry
Georgia Institute of Technology

Dr. Julia Kubanek
School of Chemistry & Biochemistry
Georgia Institute of Technology

Dr. Neha Garg
School of Chemistry & Biochemistry
Georgia Institute of Technology

Dr. Matthew Torres
School of Biology
Georgia Institute of Technology

Dr. James Wray
School of Earth and Atmospheric Sciences
Georgia Institute of Technology

Date Approved: [April 21, 2022]

This thesis is dedicated to my wife Lauren, whose support and encouragement made this possible.

ACKNOWLEDGEMENTS

The following work was made possible by a countless number of people. First and foremost, I would like to thank Dr. Amanda Stockton for gambling on me as an undergraduate student and giving me the opportunity to continue my research in her lab as a graduate student. As expected, graduate school has seemed impossible at times, and writing this document seemed equally impossible. Thank you, Amanda, for keeping me on track, being available to answer my questions, giving me invaluable feedback, and providing me the expertise to grow as a scientist, writer, mentor, and researcher.

During my time in the Stockton lab I met numerous incredible post docs, graduate students, and undergraduate students that have shaped me during this journey. I learned how to be a graduate student from Zach Duca, Thomas Cantrell, Giorgio Morbioli, George Tan, Aaron Pital, and Dedra Eichstedt. Watching my lab-mates experience literature exams, candidacy, six-month reviews, and thesis defenses gave me the ability to better prepare myself for these hurdles. I then struggled through these obstacles alongside Marshall Seaton, Carlie Novak, and Chinmayee Raj as we experienced the PhD program together. Research can be daunting, but the expertise of Nick Speller, Mike Cato, and Anna Simpson taunt me how to approach new problems, even those in other disciplines.

I would like to thank my Thesis Committee of Dr. Julia Kubanek, Dr. Neha Garg, Dr. Matthew Torres, and Dr. James Wray for providing me excellent feedback, support, and encouragement during my PhD. You helped me to see that there was a light at the end of the tunnel and equipped me with the tools to get there.

I would like to thank Dr. Christy O'Mahony for being an incredible TA advisor. I never needed or wanted to teach for a different lab. Thank you for teaching me so much and helping me learn to deal with high stress situations calmly and effectively.

I am thankful for Mr. David Bostwick for teaching me Mass Spectroscopy. You are a fountain of knowledge, and I am grateful I got to work with you before your retired.

I am thankful for Jerry Wagner, Kathy Wagner, Elise Meyer, Colin Meyer, Jessica Green, and Scotty Green and the support they have offered me since undergrad. You are my Georgia family, and I appreciate you putting up with my years of complaining about graduate school.

I am thankful for my high school chemistry teachers Mr. Jason Cammann and Mr. Darrell Feebeck for exposing me to the subject and helping me as I struggled with the more challenging concepts. I was not your most talented student, but you still had faith in me.

I am thankful for my Mom, Dad, and brother Taylor for checking up on me and supporting me from far away. Thank you for helping me through undergrad as I struggled finding my path and supporting me through the endless years of graduate school. You've had to watch from afar, but I appreciate the time and effort you have invested in me.

Finally, I need to thank my wife, Lauren, for supporting me through years of graduate school and study. This would not have been possible without you. Thank you for listening to my ramblings as I told you more about Icelandic lava fields than you would ever have cared to know.

TABLE OF CONTENTS

LIST OF TABLES

LIST OF FIGURES

CHAPTER 1. INTRODUCTION

1.1 Astrobiology & Extraterrestrial Study

Extraterrestrial exploration and the possibility of discovering extant life has captured the fascination of scientists and the general public for decades. Excitement for space exploration reached a peak with the Viking Missions to Mars in the 1970s, which incorporated chemical assays in the search for potential biosignatures. However, analysis of the Viking results was anticlimactic, if not discouraging, with the findings being inconclusive in the search for microorganisms and findings of only trace organics by the onboard gas chromatography-mass spectrometer (GC-MS) casting doubt on the possibility of biological systems [1-3]. Interest in Mars tapered following the Viking Missions until the late 90s and early 2000s when a series of missions including the Mars Pathfinder, Mars Exploration Rovers Spirit and Opportunity, Mars Odyssey and Phoenix Lander missions returned evidence of water ice on the Mars surface [4-9]. The discovery of water on Mars, and its biological relevance on Earth, renewed interest in the red planet in the hopes of uncovering present or past microbial activity.

For approaching this system, NASA has future missions and proposals in place with the goal of identifying biosignatures [10]. The Mars 2020 mission uses the Perseverance Rover to sample multiple locations at the Jezero Crater, with the ability to analyze samples using an onboard instrumental suite and the intent to cache samples for future missions. All NASA missions have requirements that constrain sampling return and analysis. Physical space, planetary protection requirements, and monetary cost are all factors that influence a mission's sample capacity, and the instruments that can be included. In the case of Mars 2020, the mission goal is to recover at least 20 samples, with a maximum of 43 sampling containers on board the rover. With a limited number of potential samples, several questions must be addressed during mission planning.

The first question that must be addressed is: how can an ideal sampling site be determined? NASA spent five years analyzing data to select the Jezero Crater as the target landing location, but once the rover touches down, what factors must be considered to select a specific sampling location? Should the spatial separation between samples be accounted for? These sorts of questions are concerned with the physical process of sample excavation, but with the goal of finding biosignatures, they imply a need for understanding the factors that make a particular environment habitable. Habitability requirements of microorganisms can be characterized by analyzing the correlations between an environment's chemistry, minerology, and bioactivity. While extraterrestrial life may not necessarily be constrained by the same processes as terrestrial biology, an understanding of the processes that contribute to the distribution and persistence of life on Earth represents a key step for informing future extraterrestrial missions [11-18].

1.2 Analog Research

Terrestrial analogs of extraterrestrial systems are a primary source of information when defining potential habitable zones on Earth and beyond [19-21]. The habitability requirements of terrestrial organisms inform sampling decisions in current and future NASA missions, while also providing valuable information about the adaptations microorganisms can employ to survive extreme terrestrial conditions. Numerous potential analogs exist for Martian systems, presenting unique habitats and environmental stresses.

Areas like the Atacama Desert in Chile present an extremely dry environment with high levels of UV radiation that limits habitability to the most robust organisms [22]. Other locations, such as the Rio Tinto in Spain, present a highly acidic and anoxic environment where adapted organisms are able to thrive [23, 24].

Icelandic volcanic regions are of growing interest to the astrobiology community as analog sites. Icelandic lava fields offer an environment with extreme temperatures, limited nutrient availability, desiccation, glacial activity, and isolation from anthropogenic activity, and the plains of basaltic tephra have spectroscopic similarities analogous to geological features observed on Mars [25-30]. The Icelandic lava fields are also in close proximity to hot springs and fumaroles that make analysis of hydrothermal systems a possibility. While Mars analog research is prevalent, it is primarily focuses on hydrothermal systems and the geological characteristics of analog sites [31-34]. Relatively little work has been done regarding biosignature distribution at analog sites, leaving room for analyses of sampling protocols to improve efficiency and science return for future Mars missions. A recent review by Cockell et al. in 2019 synthesized much of the previously published work in this area, highlighting the heterogeneity of microorganism distribution within analog samples [35]. In light of this work, understanding how biomass varies across a larger analog site and the environmental factors best correlated with habitability are critical steps for planning sampling protocols for future extraterrestrial missions.

Since 2013, the PSTAR funded Field Exploration and Life Detection Sampling through Planetary Analog Research (FELDSPAR) team has visited numerous Mars analog locations in Iceland to evaluate the operations and analytical techniques employed by the Mars 2020 Perseverance Rover. In addition to sampling containers, the Perseverance Rover is equipped with instruments for site photography (Mastcam-Z), environmental measurements and sediment morphology (MEDA), and mineralogical and elemental spectroscopy (SHERLOC, SuperCam, and PIXL) [36-40]. The FELDSPAR team attempted to mirror these techniques during their Icelandic field campaigns, performing site mapping by quadcopter and individual site photography, in situ visible near infrared (VNIR) and x-ray fluorescence (XRF) spectroscopy, and grain size and moisture measurements. DNA and adenosine triphosphate (ATP) were also measured for collected samples, enabling comparisons between abiotic site factors and bulk biomass and bioactivity.

The FELDSPAR team visited Dyngjusandur, Iceland, a Mars analog basaltic plain in the Central Highlands of Iceland, from 2016 to 2019 [15, 16, 18]. Dyngjusandur is located south of the Askja volcano and is composed of a fine black sand of basaltic origin (Figure 1-1). Large lava rocks are uncommon at Dyngjusandur, resulting in large expanses of visually and morphologically homogenous sediment. Katabatic winds arise from southern glaciers to disrupt the Dyngjusandur sediment, forming frequent sandstorms that resurface the site. Previous mineralogical analysis of the Dyngjusandur sediment has revealed a similar composition to Martian basalts, however the impacts on these conditions on sample habitability have yet to be determined [41].

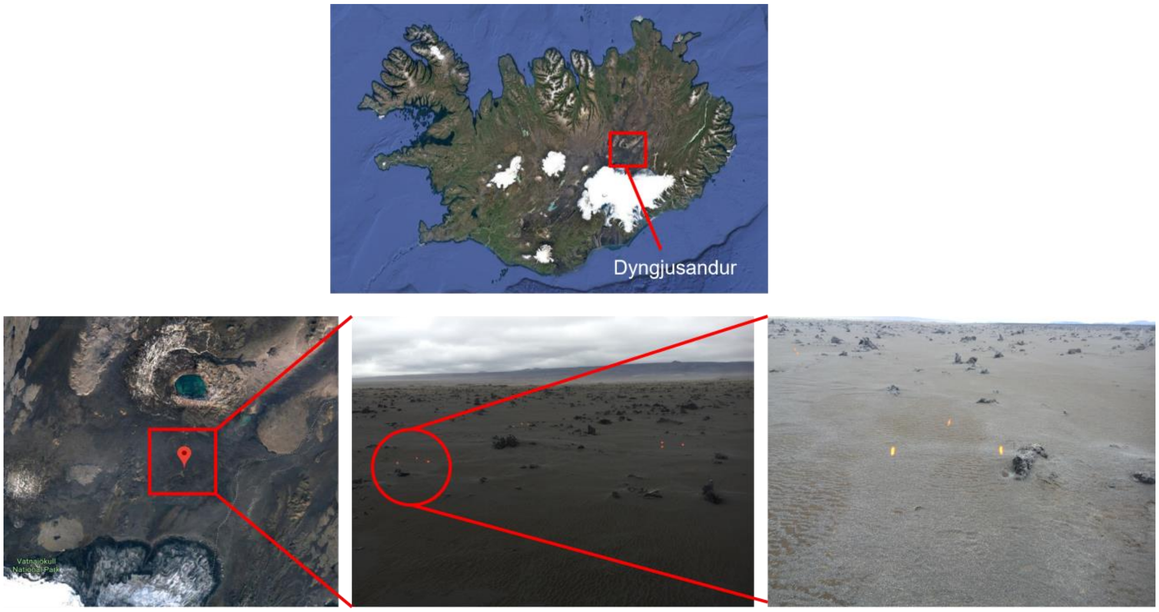

Figure 1-1 – The Dyngjusandur Mars Analog. *Dyngjusandur is located in the Central Highlands of Iceland, and is primarily composed of fine, black tephra. Large lava rocks were infrequently dispersed across Dyngjusandur's plains, resulting in an analog that is often dispersed by southern Katabatic winds.*

1.3 Thesis Objectives

This work aims to inform future extraterrestrial sampling protocols by determining the spatial distributions that capture the most biological variability at the Dyngjusandur Mars analog. Moreover, this work seeks to identify the abiotic sample factors that correlate with terrestrial life to characterize sample habitability, making this study applicable for extraterrestrial paradigms where life may have formed using different means of data storage and metabolism. Finally, this work considers samples from three years of expeditions at three samplings sites with a 5 km diameter, enabling the identification of temporal shifts at Dyngjusandur within the confined area.

Chapter 2 considers the 2016 expedition and includes a preliminary depth profile study and amplicon sequencing study. Chapter 3 introduces the 2017 field campaign, which considers the largest Dyngjusandur sampling area and presents unique site heterogeneity not observed in 2016. After the 2017 data is presented, it is compared with the 2016 data to identify parallels and discrepancies in the correlations uncovered from year to year. Chapter 4 focuses on the 2018 Dyngjusandur expedition, visiting one of the subsites from 2017. The overlapping sites from 2017 and 2018 allow for direct comparison of the site factors from year to year, while providing an additional year to observe the evolution of the sampling area. Chapter 4 also includes a three-year summary of the trends identified at the Dyngjusandur Mars analog, followed by lessons learned. The final chapter of this work, chapter 5, summarizes the key lessons learned from three years of Dyngjusandur study, and the implications of these lessons for future extraterrestrial missions. Chapter 5 also presents suggestions for future work to bolster the results presented here.

1.4 Citations

1. Klein, H.P., The Viking biological experiments on Mars. Icarus, 1978. 34(3): p. 666 - 674.

2. Biemann, K., On the ability of the Viking gas chromatograph-mass spectrometer to detect organic matter. Proceedings of the National Academy of Sciences of the United States of America, 2007. 104(25): p. 10310-10313.

3. Mazur, P., et al., Biological implications of the Viking mission to Mars. Space Science Reviews, 1978. 22(1): p. 3-34.

4. Golombek, M.P., et al., Overview of the Mars Pathfinder Mission and assessment of landing site predictions. Science, 1997. 278(5344): p. 1743-1748.

5. Boynton, W.V., et al., Distribution of hydrogen in the near surface of Mars: Evidence for subsurface ice deposits. Science, 2002. 297(5578): p. 81-85.

6. Mitrofanov, I., et al., Maps of subsurface hydrogen from the high energy neutron detector, Mars Odyssey. Science, 2002. 297(5578): p. 78-81.

7. Smith, P.H., et al., Introduction to special section on the Phoenix Mission: Landing Site Characterization Experiments, Mission Overviews, and Expected Science. Journal of Geophysical Research-Planets, 2008. 113: p. 16.

8. Ming, D.W., et al., Geochemical and mineralogical indicators for aqueous processes in the Columbia Hills of Gusev crater, Mars. Journal of Geophysical Research-Planets, 2006. 111(E2): p. 23.

9. Grotzinger, J.P., et al., Stratigraphy and sedimentology of a dry to wet eolian depositional system, Burns formation, Meridiani Planum, Mars. Earth and Planetary Science Letters, 2005. 240(1): p. 11-72.

10. Mustard, J., et al., Report of the Mars 2020 Science Definition Team. 2013.

11. Hays, L.E., et al., Biosignature Preservation and Detection in Mars Analog Environments. Astrobiology, 2017. 17(4): p. 363-400.

12. Amador, E.S., et al., Synchronous in-field application of life-detection techniques in planetary analog missions. Planetary and Space Science, 2015. 106: p. 1-10.

13. Gentry, D.M., et al., Correlations Between Life-Detection Techniques and Implications for Sampling Site Selection in Planetary Analog Missions. Astrobiology, 2017. 17(10): p. 1009-1021.

14. Rader, E., et al., Preferably Plinian and Pumaceous: Implications of Microbial Activity in Modern Volcanic Deposits at Askja Volcano, Iceland, and Relevancy for Mars Exploration. Acs Earth and Space Chemistry, 2020. 4(9): p. 1500-1514.

15. Sutton, S.M.S., A. C.; Hanna, A. M.; Tan, G. K.; Gentry, D. M.; Cable, M. L.; Rader, E.; Cullen, D.; Geppert, W.; Stockton, A. M.; FELDSPAR Team, Microbial Population and Distribution at Dyngjusandur, Iceland a Mars Analog Alluvial Plain. 2021.

16. Sutton, S.V.H., S. R.; Tan, G. K.; Patel, A.; Hanna, A. M.; Simspon, A. C.; Gentry, D. M.; Cable, M. L.; Rader, E.; Cullen, D.; Geppert, W.; Stockton, A. M.; FELDSPAR Team, Biosignature Distribution & Characterization of the Dyngjusandur, Iceland Mars Analog Plain from 2016-2017. Submitted to Astrobiology, 2022.

17. Tan, G., et al., Spatial Variation in Results of Biosignatures Analyses of Apparently Homogenous Samples from Mars Analog Environments in Iceland. Acs Earth and Space Chemistry, 2021.

18. Sutton, S., et al., Lessons of Sampling & Sample Habitability at the Dyngjusandur, Iceland, Mars Analog from 2016-2018. Astrobiology, 2022.

19. Moissl-Eichinger, C., C.S. Cockell, and P. Rettberg, Venturing into new realms? Microorganisms in space. Fems Microbiology Reviews, 2016. 40(5): p. 722-737.

20. Preston, L.J. and L.R. Dartnell, Planetary habitability: lessons learned from terrestrial analogues. International Journal of Astrobiology, 2014. 13(1): p. 81-98.

21. Lammer, H., et al., What makes a planet habitable? Astronomy and Astrophysics Review, 2009. 17(2): p. 181-249.

22. Azua-Bustos, A., C. González-Silva, and A.G. Fairén, The Atacama Desert in Northern Chile as an Analog Model of Mars. Frontiers in Astronomy and Space Sciences, 2022. 8: p. 242.

23. Amaral-Zettler, L.A., et al., Microbial community structure across the tree of life in the extreme Rio Tinto. Isme Journal, 2011. 5(1): p. 42-50.

24. Fernández-Remolar, D.C., et al., Underground habitats in the Río Tinto basin: a model for subsurface life habitats on Mars. Astrobiology, 2008. 8(5): p. 1023-47.

25. Hartmann, W.K. and G. Neukum, Cratering chronology and the evolution of Mars. Space Science Reviews, 2001. 96(1-4): p. 165-194.

26. Baker, V.R., et al., ANCIENT OCEANS, ICE SHEETS AND THE HYDROLOGICAL CYCLE ON MARS. Nature, 1991. 352(6336): p. 589-594.

27. Bishop, J. Spectroscopic and geochemical analyses of ferrihydrite from springs in Iceland and applications to Mars in Geological Society, London, Special Publications. 2002.

28. Neukum, G., et al., Recent and episodic volcanic and glacial activity on Mars revealed by the High Resolution Stereo Camera. Nature, 2004. 432(7020): p. 971-979.

29. Bathgate, E.J., et al., Raman, FTIR and XRD study of Icelandic tephra minerals: implications for Mars. Journal of Raman Spectroscopy, 2015. 46(10): p. 846-855.

30. Kargel, J.S. and R.G. Strom, ANCIENT GLACIATION ON MARS. Geology, 1992. 20(1): p. 3-7.

31. Aerts, J.W., et al., Biosignature Analysis of Mars Soil Analogs from the Atacama Desert: Challenges and Implications for Future Missions to Mars. Astrobiology, 2020. 20(6): p. 766-784.

32. Stromberg, J.M., et al., Biosignature detection by Mars rover equivalent instruments in samples from the CanMars Mars Sample Return Analogue Deployment. Planetary and Space Science, 2019. 176.

33. Moreras-Marti, A., et al., Volcanic controls on the microbial habitability of Mars-analogue hydrothermal environments. Geobiology, 2021. 19(5): p. 489-509.

34. Bosak, T., et al., Searching for biosignatures in sedimentary rocks from early Earth and Mars. Nature Reviews Earth & Environment, 2021. 2(7): p. 490-506.

35. Cockell, C.S., et al., Sample Collection and Return from Mars: Optimising Sample Collection Based on the Microbial Ecology of Terrestrial Volcanic Environments. Space Science Reviews, 2019. 215(7): p. 44.

36. Allwood, A.C., et al., PIXL: Planetary Instrument for X-Ray Lithochemistry. Space Science Reviews, 2020. 216(8): p. 132.

37. Beegle, L., et al., Scanning Habitable Environments with Raman and Luminescence for Organics and Chemicals (SHERLOC) on Mars 2020. Abstracts of Papers of the American Chemical Society, 2019. 257: p. 2.

38. Hayes, A.G., et al., Pre-Flight Calibration of the Mars 2020 Rover Mastcam Zoom (Mastcam-Z) Multispectral, Stereoscopic Imager. Space Science Reviews, 2021. 217(2): p. 95.

39. Perez-Izquierdo, J., et al., The Thermal Infrared Sensor (TIRS) of the Mars Environmental Dynamics Analyzer (MEDA) instrument onboard Mars 2020, a general description and performance analysis. Measurement, 2018. 122: p. 432-442.

40. Wiens, R.C., S. Maurice, and F.R. Perez, The SuperCam Remote Sensing Instrument Suite for the Mars 2020 Rover: A Preview. Spectroscopy, 2017. 32(5): p. 50-55.

41. Sara, M.J., Dyngjusandur sand sheet, Iceland, as a depositional analog to the Stimson Fm. in Gale Crater, Mars. 2017. p. xii, 145 pages.

CHAPTER 2. MICROBIAL POPULATION AND DISTRIBUTION AT DYNGJUSANDUR, ICELAND A MARS ANALOG ALLUVIAL PLAIN

Adapted with permission from: "Microbial Population and Distribution at Dyngjusandur, Iceland a Mars Analog Alluvial Plain" Submitted to Astrobiology Fall 2021

2.1 Abstract

The limited nutrient availability, extreme temperatures, and desiccation of Arctic volcanic regions provide a unique opportunity to study environments with multiple similarities to extraterrestrial systems. Dyngjusandur, Iceland, is a plain of nutrient-poor volcanic basaltic tephra shaped by alluvial and aeolian action sharing spectroscopic similarities to analogous geological features observed on Mars[1]. Two regions of the Dyngjusandur plain separated by 1 km and selected for their homogenous appearance were sampled in this study. Sampling schemes each consisted of nested triangular grids of samples beginning at the 0.1 m scale and increasing to the 100 m scale[2, 3]. Additional samples were recovered at 1 cm increments to a depth of 7 cm. Biological and geophysical analyses were performed including: 16S qPCR, DNA quantification, amplicon sequencing, moisture quantification, and separation of grain size fractions. The two sampling sites were found to have significantly different dsDNA content by T-Test (p-value = 0.001) and Mann-Whitney U Test (p-value = 0.003). Biomass showed the greatest variation at 10 m of sample separation, and both total dsDNA content and bacterial DNA showed significant correlations with sample grain size. Grain size distribution also appeared to influence the abundance of several bacterial phyla, with positive and negative correlations observed, and the same dominant phyla were observed across all samples studied. This work suggests

that a sample set collected at small spatial separation may be sufficient to define a baseline level of biomass and moisture, however sampling a larger site at smaller intervals (10 m) provides important characterization of site heterogeneity with diminishing returns at increasingly smaller intervals.

2.2 Introduction

A goal of the Mars 2020 mission is to search for evidence of past life on the Martian surface. Such an undertaking requires the exploratory rover to be equipped with the analytical tools to analyze samples for potential biosignatures, then excavate and cache for potential future return to Earth. Onboard, the Mars 2020 rover carries a camera for field visualization (Mastcam-Z), sensors for identifying temperature, humidity, and mineral grain size and morphology (MEDA), an x-ray fluorescence spectrometer for elemental chemistry (PIXL), Raman spectrometers for mineralogical measurements (SHERLOC & SuperCam). In addition to these instruments, the Mars Reconnaissance Orbiter (MRO) has provided infrared spectroscopy measurements using the Compact Reconnaissance Imaging Spectrometer for Mars (CRISM), allowing for characterization of surface mineralogy in the search for water on Mars[4-9]. However, questions remain about the efficacy of these instruments for detecting or predicting biosignatures. When evaluating the instrument package of the Mars 2020 rover, and those of future missions, which metrics offer the greatest correlation with bioactivity and habitability?

Constructing an instrumental suite is only one part of achieving success when identifying signs of past life on Mars. The Mars 2020 rover is limited in the number of samples it can analyze and select for potential future return, increasing the importance of sample selection at the landing site[10]. When characterizing a sampling location, factors such as moisture content, grain size, and geochemistry of the sediment could result in vastly different habitability, and heterogeneity of any biomarkers might require large sampling sets to ensure collection of "the right" sample. Determining a sampling strategy is therefore a primary concern, not just for Mars 2020 but for any landed planetary mission.

Analog research is a primary way of testing instruments and sampling techniques in preparation for extraterrestrial missions[11-14]. As a result of its glacial and volcanic history, Iceland has long been considered an analog for regions of the Martian surface with similar minerology, harsh environmental conditions, and minimal anthropogenic activity[15-17]. One such location is Dyngjusandur, a plain in the Central Highlands of Iceland sculpted by a mix of alluvial and aeolian processes[1, 18, 19]. Dyngjusandur is largely composed of unconsolidated basaltic tephra, worn down to a fine sand, resulting in a location frequently disrupted by dust storms. Amidst the plains of black sand, larger chunks of lava are infrequently dispersed, resulting in an open and relatively homogenous field site ideal for testing the spatial scale heterogeneity of native ecology. While the minerology of Dyngjusandur has been investigated in other publications, the bioactivity at the site remains largely uncharacterized [1, 18, 19].

The PSTAR-funded Field Exploration and Life Detection Sampling through Planetary Analog Sampling (FELDSPAR) project is an international collaborative program aimed at testing operations and feasibility of a future Mars mission through field campaigns to various Icelandic lava fields [2, 3, 20]. The FELDSPAR team visited the Dyngjusandur sampling site annually starting in the summer of 2016, and this work identifies relationships between the geophysical and environmental characteristics of the sandy plain and its biosignatures. To estimate bioactivity at Dyngjusandur we analyzed DNA content as a bulk measurement given its ubiquitous use as genetic material by terrestrial organisms [21]. Quantitative polymerase chain reaction (qPCR) with universal 16S primers provides an additional bio-content measure with a specificity for prokaryotic organisms [22]. Biosignature abundances are important points of comparison for identifying shifts in habitability factors and paired with 16S amplicon sequencing changes in the microbial community can also be observed. These techniques are optimal for detecting terrestrial life but are likely insufficient on an extraterrestrial mission. Potential extraterrestrial organisms may have evolved unique methods of information storage making DNA content an incompatible point of comparison. However, determining the environmental factors that influence terrestrial biology informs our understanding of the characteristics that make a sampling site habitable, and potentially habitable on another planet.

Here, we characterize the Dyngjusandur sampling site and the correlation of bulk biosignatures with environmental measurements and determine spatial heterogeneity of biosignatures. Two analyses of bio-content were performed: total dsDNA concentration by fluorescence assay and quantitative polymerase chain reaction with bacteria-focused primers. These general measures are intended to act as an estimate of biomass and bioactivity, sequencing of the 16S amplicon was conducted to enable an estimate biodiversity. The results of these assays were compared at each spatial scale and juxtaposed with grain size and moisture content to determine the most biologically predictive characteristics of this Mars analog site.

2.3 Methods – Dyngjusandur Samples

2.3.1 Sampling: Nested Triangular Grids & Depth Profile

Sediment samples were recovered from a plain in Dyngjusandur, Iceland (64.92°N, 16.76°W) in June 2016. The sampling location was selected based on visual and morphological homogeneity, with a focus on sand sheets absent of larger sediment (Figure 2-1). Sampling was performed using a series of nested triangles with edges of 0.1 m, 1 m, 10 m, and 100 m at two locations separated by 1 km hereafter referred to as D1 and D2 (Figure 2-2). Sampling locations were marked using triangular tarps and flags, and then photographed aerially using a DJI Inspire 1 Quadcopter.

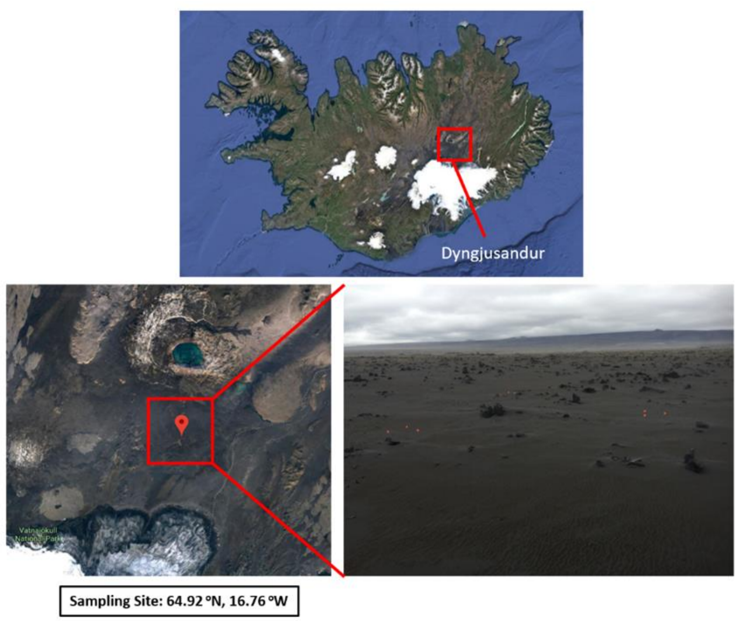

Figure 2-1 – The Dyngjusandur field site. *Dyngjusandur alluvial plain is located in the central highlands of Iceland, 16 km south of the Askja Caldera. The sand is composed of unconsolidated basaltic tephra, and while portions of the plains are morphologically homogenous, others are distributed with basaltic stone.*

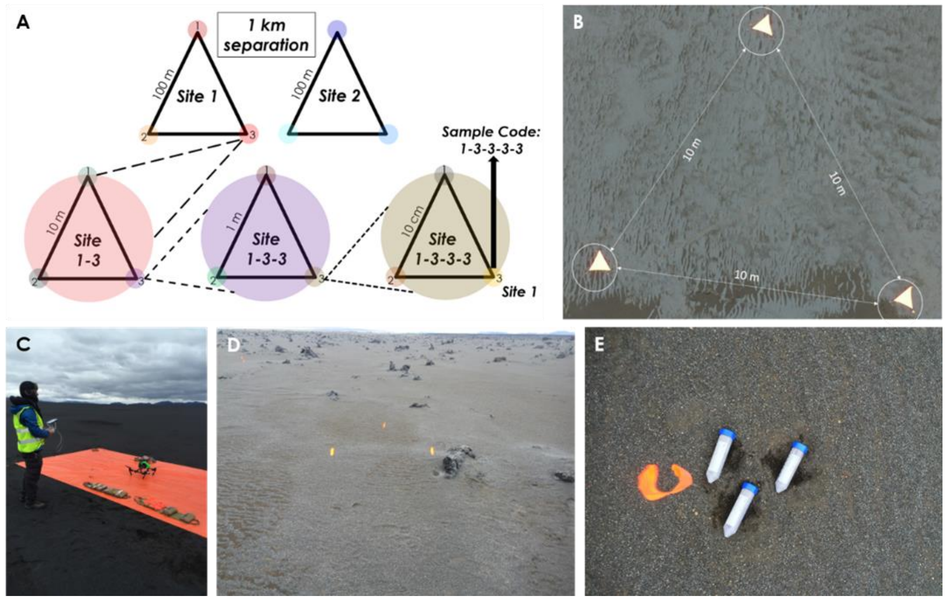

Figure 2-2 – Nested Triangular Grids Sampling System. *Two sampling sites were selected with a separation of 1 km. At each sampling site, a series of nested triangular grids was sampled to determine spatial heterogeneity of bioactivity. (A) The sampling schematic employed at Dyngjusandur. Each site was mapped into equilateral triangles, with the vertices separated by 100 m. The corner of each triangle was then mapped into a smaller triangle, with distributions of 10 m, 1 m, and 0.1 m. A code was generated for each sample based on its placement in the nested triangular grid. (B) A 10 m triangle from Site 1. Orange, triangular tarps with 1 m per side were placed at the corners of each 10 m triangle for visualization. (C) Aerial mapping of each site was obtained using a quadcopter for imaging. (D) The 1 m triangles prior to sample collection and aerial mapping were denoted in field by small orange flags. (E) Triplicate samples at 0.1 m spacing were recovered at the corners of each 1 m triangle after removing the top 1 cm of surface sediment.*

Following aerial photography, the top 1 cm layer of sediment from each site was removed using a sterilized spade. In a similar fashion, depth profile samples were recovered from a sampling site within 10 m of Site 1 in 1 cm increments from the surface to a depth of 7 cm. Spectroscopic data was obtained for each location using a field portable visible near infrared (VNIR) ASD spectrometer and a portable x-ray fluorescence spectrometer.

Mineralogical analysis will be presented in a sister paper currently in preparation. Sediment samples were deposited into 50 mL conical tubes, and bagged for return to Georgia Tech.

All work, including sampling, was performed with an attempt to minimize anthropogenic contamination. Face masks, non-linting arm sleeves, and nitrile gloves were worn by those taking samples, and considerations were made to work downwind from sampling sites.

Samples were returned to a field lab at the University of Akureyri where they were stored in laboratory freezers until they were shipped to Georgia Tech. Upon return to Georgia Tech, samples were stored in a -80 ^{o}C freezer until they were subject to characterization and bioassays.

2.3.2 Sample Bulk Characterization (Moisture Content and Grain Size Analysis)

Sediment samples were defrosted in a room sterilized and prepared for biological analysis, and several grams of each were measured into glass scintillation vials. The vials were prepared in triplicate and weighed prior to the introduction of field sample. Sample vials were placed in an oven at 100 ^{o}C for 24 hours, and then weighed to determine the contribution of moisture to total dry sample mass. This process was repeated until consistent masses were observed on multiple days.

After moisture content was determined, grain size analysis was performed using dry sieving. The sieves captured grains at scales greater than 2000 µm, 850 µm, 425 µm, and less than 425 µm. The sediment collected by each sieve was massed to estimate the grain size composition for each location in the nested triangle.

2.3.3 Biological Assays (dsDNA Content, qPCR, and Amplicon Sequencing)

DNA was extracted from sediment samples using a DNeasy PowerLyzer PowerSoil Kit from Qiagen (Hilden, Germany). The standard protocol for the PowerLyzer kit proved insufficient for recovering DNA from our samples, and instead, an alternative PowerSoil Protocol for Low Biomass Soil was used as provided by Qiagen and adapted from Hale et al [23]. Successful extraction was confirmed using a Qubit dsDNA High Sensitivity Assay by Thermo Fisher (Waltham, MA), which quantifies double stranded DNA with a fluorescent dye and standard curve. A Qubit fluorimeter was used for fluorescence measurements.

Bacterial copies were determined for each sample using qPCR with standards provided in the FEMTOTM Bacterial DNA Quantification Kit (Zymo Research, Irvine, CA). Bacterial primers 515F (5'-GTG CCA GCM GCC GCG GTAA) and 806R (5'-GGA CTA CHV HHH TWT CTA AT) were used to target the V4 region of the 16S rRNA gene [24, 25]. Samples were run in triplicate on a CFX96TM Real-Time System (Bio-Rad, Hercules, CA), with 20 µL reactions composed of 10 µL 1x SsoAdvanced Universal SYBR® Green Supermix (Bio-Rad), 1 µL of 10 µM forward and reverse primer, 1 µL of template DNA, and 8 µL of water. Cycling conditions were 95 ºC for 10 min; 40 cycles of 95 ºC for 30 s, 50 ºC for 30 s, and 72 ºC for 1min followed by a final step of 72 ºC for 7 min as recommended by the FEMTO kit.

A subset of extracts, one sample from each 1 m triangle at the D1 site, were prepared for 16S amplicon sequencing. Amplification of DNA was performed as outlined in Illumina's 16S Metagenomic Sequencing Library Preparation guide, and amplicons were sent to SeqMatic (Fremont, CA) for clean-up, indexing, and sequencing. Sequences were processed using the DADA2 pipeline and analyzed using the Phyloseq package. An in-depth analysis of the sequencing results will be explored in a future publication.

2.3.4 Statistical Analysis

Pairwise T and U tests were performed using R studio to compare moisture content, bacterial copies, and dsDNA content at each distance scale of the nested triangular grids[3]. The 1 m level involved the comparison of measurements using the corner 0.1 m sample at each 1 m triangle's apex as a grouping. Groupings were only compared within each parent 1 m triangle. P-values obtained for each comparison were adjusted using a Bonferroni correction, and significant differences were identified as adjusted P-values less than or equal to 0.05[26]. The percentage of statistically significant differences across all triangles was determined by comparing the number of statistically significant differences to the total number of comparisons. This process was repeated for the 10 m spacing level using the 1 m triangle corners of each 10 m triangle as groupings, while the 100 m spacing level used the 10 m triangle corners as groupings. Sites 1 and 2 were analyzed as individual sites and as a greater combined site.

Correlation plots were generated using the corrplot package in R and Spearman's rank correlation coefficients were calculated. Sequencing reads were scaled to remove the least abundant ASVs, and correlations between Phylum abundance and dsDNA content, bacterial copies, moisture content, and grain size were determined. Phyla demonstrating a positive or negative correlation with a parameter and a p-value less than 0.1 were included in a correlation plot. Correlations were also determined among dsDNA content, bacterial copies, moisture content, and grain size and presented in a separate correlation plot.

2.4 Results

Figure 2-3 shows bacterial copies, dsDNA content, and gravimetric moisture content at groupings of 0.1 m, 1 m, and 10 m. The difference in bioactivity between samples was quantified at each spatial separation using pairwise T-Tests and U-Tests to compare the within-group means and medians respectively. Two 100 m triangles separated by 1 km were sampled and analyzed as a single site. The two triangles were also considered as individual sites to distinguish trends at a smaller scale (Table 2-1).

2.4.1 Analysis of Combined Sites

As a combined site, variation was observed primarily at scales of 10 m and 100 m. For dsDNA content, both the T-Test and U-Test showed statistical differences at the 100 m and 10 m levels ranging from 16-33% significantly different comparisons, and no differences at the 1 m level. For bacterial copies and gravimetric moisture content, statistical differences were observed at the 10 m level, but not at the 100 m level. Both statistical tests revealed 11% significantly different comparisons for bacterial copies, and 28% significantly different comparisons for moisture content. Less than 2% of comparisons were considered statistically different at the 1 m scale.

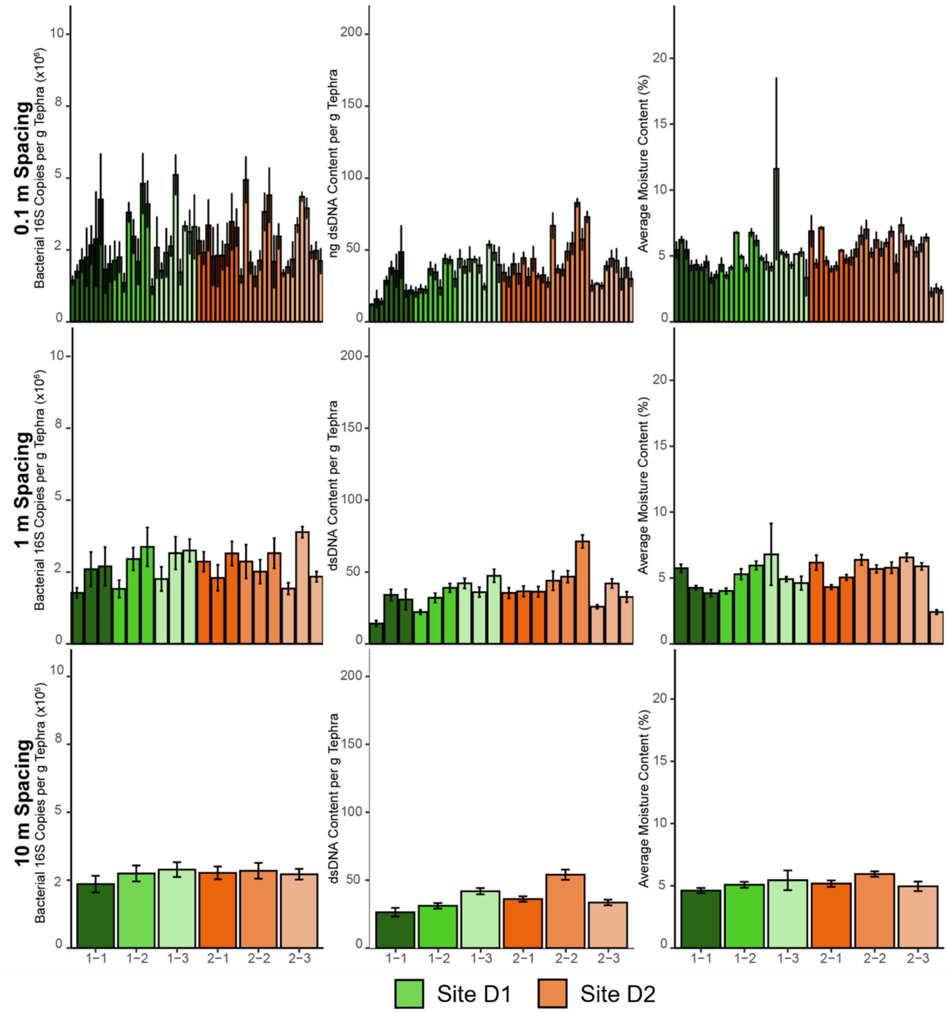

Figure 2-3 – Dyngusandur Characteristic Measurements. *16S copies, dsDNA content, and gravimetric moisture content at spatial distributions of 10 m, 1 m, and 10 cm. Shades of red and blue correspond to their respective x-axis value, denoting the 0.1 m and 1 m triangle. Three sub-samples of each sample at 0.1 m spacing were analyzed, thus error bars represent the heterogeneity of the sample. The measurements at the 0.1 m spacing were combined to yield the data presented for 1 m and 10 m spacing.*

Table 2-1. Comparison of Differences Between Nested Triangles at Each Spatial Scale Using Two Qualitative Tests

	Pairwise T-Test			Pairwise Mann-Whitney-U			
		Site 1			*Site 1*		
Separation	**100 m**	**10 m**	**1 m**	**100 m**	**10 m**	**1 m**	
DNA Content	67%	22%	3.7%	67%	33%	0.0%	*Significant Pairwise Comparisons*
16S Copies	0.0%	0.0%	0.0%	0.0%	0.0%	0.0%	
Grav Moist	0.0%	44%	3.7%	0.0%	44%	0.0%	
		Site 2			*Site 2*		
Separation	**100 m**	**10 m**	**1 m**	**100 m**	**10 m**	**1 m**	
DNA Content	67%	33%	0.0%	67%	33%	0.0%	*Significant Pairwise Comparisons*
16S Copies	0.0%	22%	0.0%	0.0%	22%	0.0%	
% Moisture	0.0%	33%	0.0%	33%	22%	0.0%	

**The table represents the percentage of different comparisons at each spatial scale. A comparison was considered statistically significant with $0.05 \geq p$.*

2.4.2 Analysis of Individual Sites

Table 2-1 shows sites D1 and D2 analyzed individually. In both sites, the 1 m scale showed less than 4% significant variation across each metric of measure based on the T-test and no statistically different comparisons based on the U-test. At the 10 m scale, the percentage of significant differences ranged from 22-44% when considering both tests for each metric except for 16S bacterial copies for Site 1, which showed no statistically significant differences between groupings. Only dsDNA content showed statistically significant differences at the 100 m level, with 67% different comparisons when comparing means and medians.

Variation at the 10 m scale ranged from 33-67% for each metric. Both tests showed no significant difference in comparisons at the 100 m scale for 16S copies, while gravimetric moisture content saw 33% significantly different comparisons at the 100 m scale based on medians in the U-Test for Site 2. For both sites, dsDNA content demonstrated nearly the same percentage of statistically significant comparisons at each separation distance and for both pairwise tests.

2.4.3 Correlations with Grain Size

Across all samples, the greatest proportion of each were grains less than 450 μm (dust), with mid-sized grains (larger than 850 μm and 450 μm) representing the next most abundant interval. Very little large sediment (larger than 2000 μm) was observed in all samples. The percentage of each division by mass was compared with each sample's respective DNA content, bacterial copies, and moisture content as seen in Figure 4. Across both sites, the grain size fraction greater than 2000 μm represented an average of 1.96% (±1.62% standard deviation) per sample. The fraction ranging from 850-2000 μm represented an average of 12.29% (±5.85% standard deviation) of each sample, while the fraction ranging from 425-850 μm represented an average of 13.57% (±7.26% standard deviation) of each sample. Finally, the fraction less than 425 μm was an average of 71.62%(±10.32% standard deviation) of each sample.

To determine the relationship of each grain size to DNA content, bacterial copies, and moisture content, a correlation matrix was made (Figure 2-4). A 90% confidence interval was used to determine the significance of correlations and revealed that larger sediment was inversely correlated with moisture content, bacterial copies, and dsDNA content. Both 16S copies and dsDNA content were strongly positively correlated, and a weak positive correlation was observed between moisture content and dsDNA content. All three variables, moisture, dsDNA, and 16S copies showed positive correlations with the dust grain size fraction, and weak negative correlations with the mid-sized sediment fractions. The mid-sized sediment fractions unsurprisingly displayed a strong negative correlation with the smallest sediment size, and the grain size fraction between 850 - 2000 µm was positively correlated with the largest sediment.

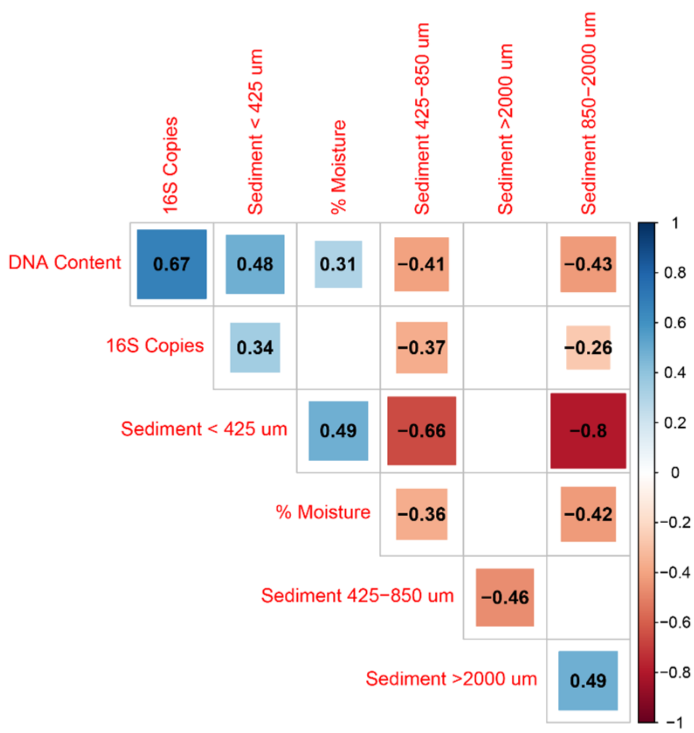

Figure 2-4 - Correlations between bacterial copies, dsDNA Content, moisture content, and grain size. *Blue represents positive correlations, while red represents an inverse correlation. Correlation coefficients are overlayed for significant comparisons. Significant comparisons are based on a 90% confidence interval. Empty boxes represent a lack of significant correlation.*

2.4.4 Depth Profile: Biosignature and Correlation

Figure 2-5 shows the 16S copies, dsDNA content, and gravimetric moisture content observed in samples taken at depths of 1 – 7 cm. Both DNA content and moisture content follow a similar trend of increasing beyond a depth of 1 cm. This trend is likely observed among the 16S copy data as well, however the significance of the trend is questionable given the larger heterogeneity of these samples for this parameter. A large increase in DNA content is observed between samples 2 and 3, ~15 ng/g of DNA to ~30 ng/g, and the remaining samples never fall below 20 ng/g. Moisture content fluctuates at depths 2 cm and below, but it remains close to 5% moisture for the remaining samples. While the heterogeneity in 16S bacterial copies obscures trends, the deepest sample (7 cm) appears to have the most copies of all the depth profile samples and is statistically different from samples taken in the top 4 cm. Samples taken from the top 2 cm were statistically different from the deepest sample based on a T-Test comparison (p-value = 0.002), while samples taken from a depth of 3-4 cm were also significantly different with a slightly higher p-value (p-value = 0.02). This suggests that as deeper sediment layers become more sheltered from the harsh winds of Dyngjusandur, the microbiome can support a greater density of organisms. The heterogeneity observed for samples taken at depths of 5-6 cm may be due to a shift in community composition towards organisms less adept at surviving in surface conditions, resulting in a higher variability in the qPCR measurements (Figure 2-5).

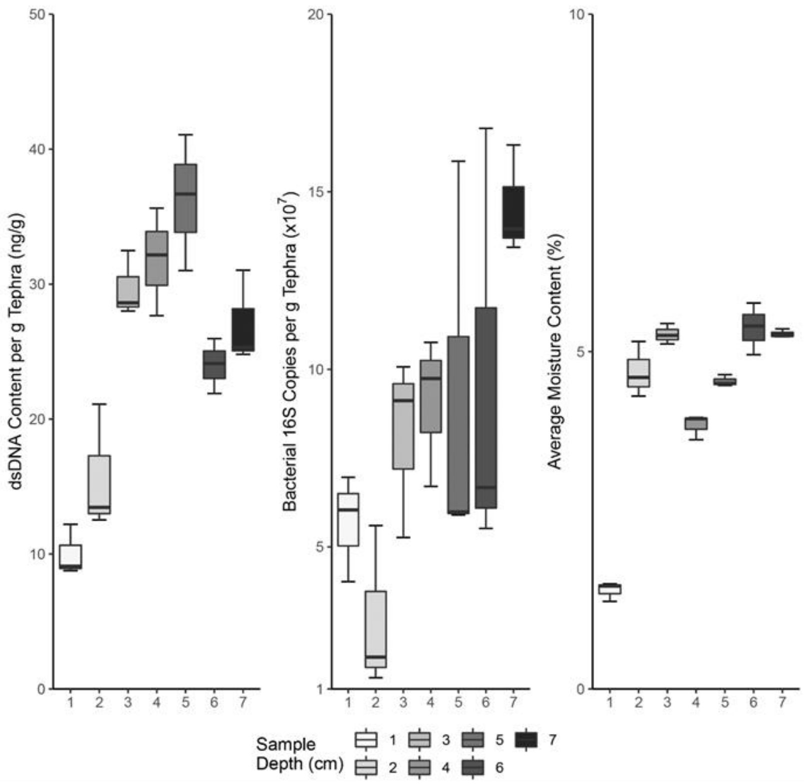

Figure 2-5 – Dyngjusandur Depth Profile Measurements. *DNA content, 16S Copies, and gravimetric moisture content from samples recovered from depths of 1-7 cm. Samples were taken in 1 cm increments. Triplicate sub-samples were analyzed for each data point.*

Grain size fractions followed a similar trend to the samples taken at varying spatial scales. The largest sediment (> 2000 µm) made up the smallest fraction of each sample, while the mid-sized sediment fractions (850-2000 µm and 425-850 µm) made up less than 25% of the samples respectively. The largest sediment fraction was made up of the smallest sediment (< 425 µm), with 50% composition across each sample.

Correlations were performed between the biosignature variables, moisture content, and grain size, Figure 2-6, and DNA content was shown to have a strong negative correlation with the largest sediment sizes. No other significant correlations were observed.

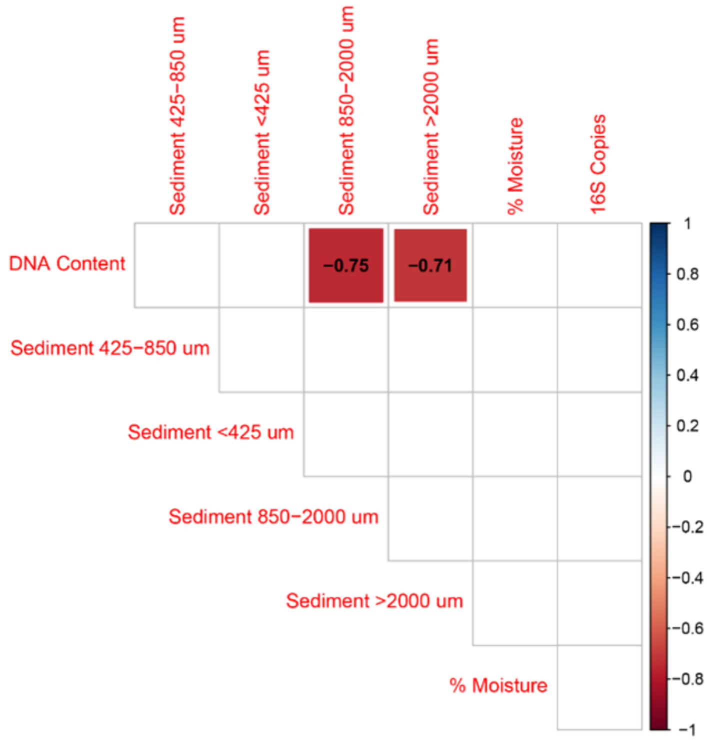

Figure 2-6 – Depth Profile Correlations Between Bacterial Copies, dsDNA Content, Moisture Content, and Grain Size. *Blue represents positive correlations, while red represents inverse correlation. Correlation coefficients are overlayed for significant comparisons. Significant comparisons are based on the 90% confidence interval. Empty boxes represent a lack of significant correlation.*

2.4.5 16S Amplicon Sequencing

After processing, 4465 ASVs representing putative individual bacterial or archaeal species were uncovered across all samples, and all phyla representing less than 3% of the total abundance were grouped together (Figure 2-7). Nine phyla with abundances greater than 3% were observed in the nine samples: Acidobacteria, Actinobacteria, Bacteroidetes, Chloroflexi, Gemmatimonadetes, Patescibacteria, Plantomycetes, Proteobacteria, and Verrucomicrobia. Of the abundant phyla, Actinobacteria, Proteobacteria, and Acidobacteria each had an average abundance greater than 10%, with shares of 37%, 23%, and 13% respectively. In depth exploration of Dyngjusandur's minerology and sequencing analysis will follow in subsequent manuscripts.

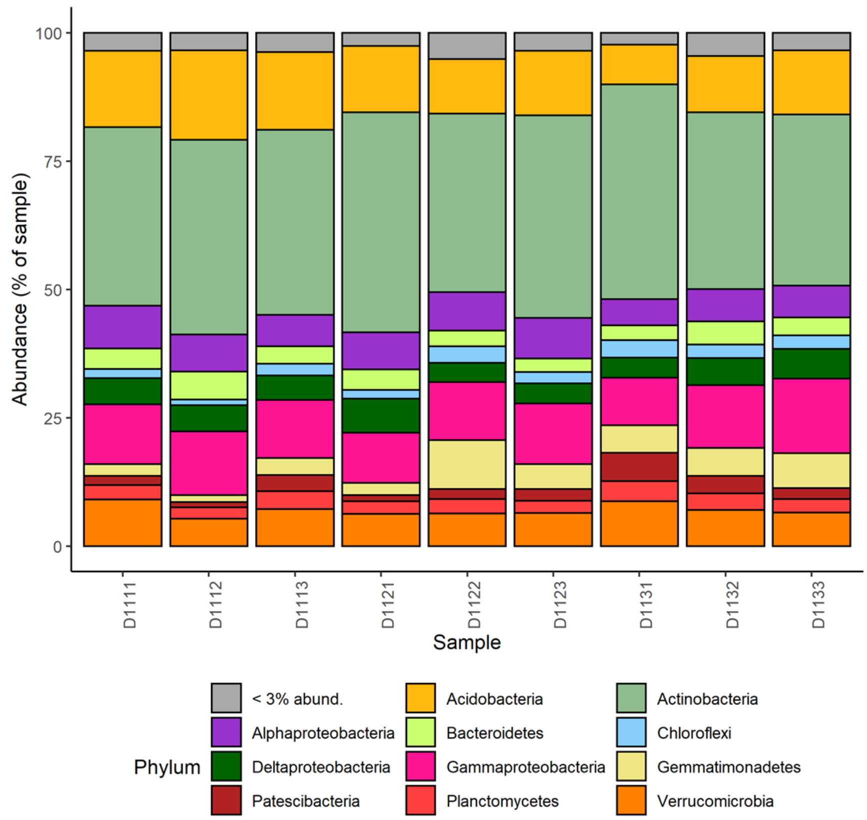

Figure 2-7 – Abundant Sequences in Dyngjusandur Samples. *Sequencing results from one sample from each 1 m triangular grid from Site D1, representing the phyla with greater than 3% abundance. Of the nine most abundant phyla, Actinobacteria, Proteobacteria, and Acidobacteria each accounted for more than 10% of the total population.*

2.4.6 Sequencing Correlations

Correlations were observed between phylum abundance and dsDNA content, bacterial copies, gravimetric moisture content, and grain size (Figure 2-8). A strong positive correlation was observed between 16S copies and Patescibacteria and a weak positive correlation was observed between DNA content and Cyanobacteria. Rokubacteria had negative correlations with both 16S moisture content and DNA content. However, the smaller grain size fractions demonstrated the strongest correlations with sequencing phyla. The sediment fraction smaller than 850 µm and larger than 450 µm demonstrated strong positive correlations with Acidobacteria, Armatimonadetes, and Abditibacteriota, and strong negative correlations with Chloroflexi, Cyanobacteria, Gemmatimonadetes, and Patescibacteria. The smallest sediment, less than 450 µm, showed a strong positive correlation with Cyanobacteria, and strong negative correlations with Rokubacteria and Actinobacteria.

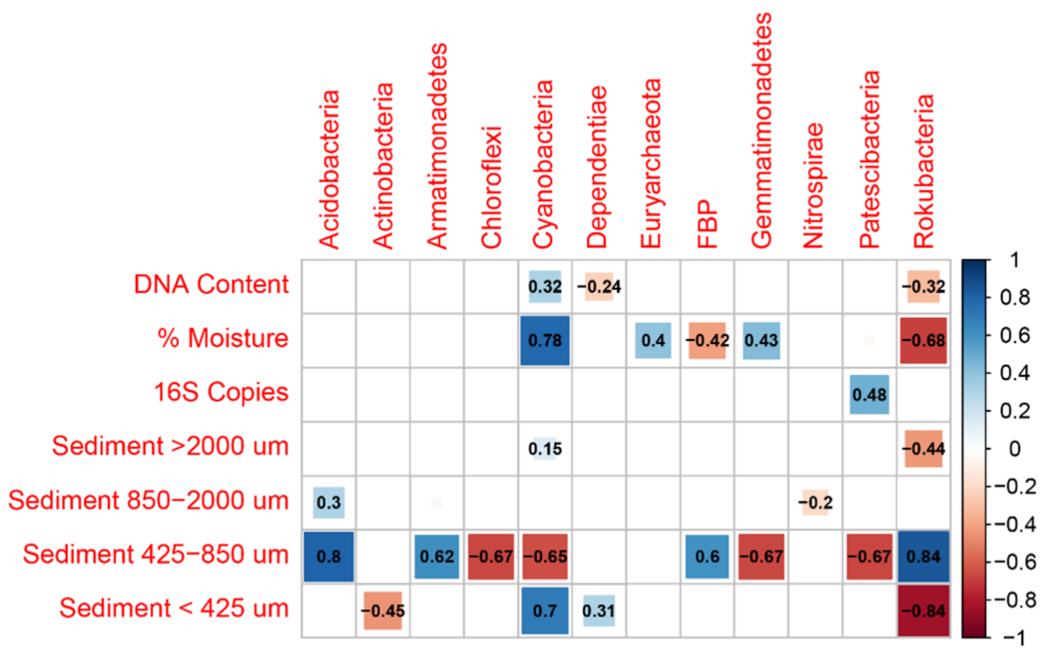

Figure 2-8 – Correlations Between Phyla and Primary Measures. *Phyla demonstrating a significant correlation (p-value less than 0.1) with dsDNA content, bacterial copies, moisture content, or grain size were included in the plot above. Shades of blue represent a positive correlation and shades of red represent a negative correlation. Correlation coefficients are overlayed for significant comparisons. Measurements were performed in triplicate. Empty boxes represent a lack of significant correlation.*

2.5 Discussion

2.5.1 Spatial Influences

Characterizing the impacts of spatial scale and environmental factors on bulk biomass is a key step towards understanding how biosignatures may be distributed at Mars analog sites. These results suggest that visually homogenous sampling sites can vary dramatically in biosignature and geochemical measurements at different spatial scales (Figure 2-1). Across both D1 and D2, the smallest grouping, 1 m, yielded less than 5% statistically different comparisons for each metric. Comparing 1 m triangles separated by 10 m, however, resulted in 22-44% statistically different comparisons for D1, and 22-33% comparisons for D2. The pairwise T-Tests and U-Tests were consistent for all sets of comparisons except for moisture content at D2 with 100 m separation. The differences between the two tests at 100 m separation represent disparate evaluations for the same comparison and are likely the result of the inherently different approaches of each test.

The large percentage of significant differences at the 10 m grouping point toward environmental shifts influencing biosignature measurements when moving beyond the relative closeness of the 1 m scale. These results also suggest that moisture content is an influencing factor for this microbial distribution, with a positive correlation between dsDNA content and moisture observed. A significant positive correlation between 16S copies and dust, and negative correlations with the mid-sized sediment fractions are observed, indicating the influence of grain size on the community (Figure 2-4). Similar correlations were also observed between moisture content and these grain size fractions. In this way, a relationship exists between microbial colonization and grain size with respect to the amount of moisture a sample can carry. The finest grain size fractions appear to be friendly to microbial colonization, while the large fractions demonstrate a negative trend for both biosignatures and moisture capacity.

Interestingly, the differences observed at the 10 m grouping were often averaged out at the 100 m grouping across both sites and both statistical tests. For D2, 16S copies show 22% statistically significant differences at the 10 m scale, but this drops to 0% different comparisons at the 100 m scale. Similarly, gravimetric moisture content at D1 dropped from 44% different comparisons to 0% different comparisons when shifting from 10 m to 100 m. This suggests that a baseline exists for the bioactivity Dyngjusandur can support, but stochasticity may still be the prevalent factor when comparing individual samples, as opposed to grouped samples. However, homogeneity was not a hard rule at the 100 m scale. For dsDNA content at both sites, the percentage of significantly different comparisons increased from 10 m to 100 m, changing from 22-33% to 67%. The magnitude of the percentage increase may be inflated due to the limited number of comparisons available at the 100 m scale (3 comparisons), but this highlights that one of three 10 m triangles at D1 had significantly more or less microbial colonization in comparison to its counterparts. This observation is maintained when considering the pairwise T-test results for 16S copies at both sites, which maintain the 67% difference from 10 m to 100 m, showing that a single 10 m triangle had significantly different microbial colonization than its neighbouring corners. These cases highlight the importance of recovering a multitude of samples from a sampling site given that biomass can vary dramatically even without apparent environmental differences.

2.5.2 Aeolian Resurfacing

Samples taken at depths several centimeters below the surface were shown to contain more dsDNA and 16S copies than samples taken closer to the surface (Figure 2-5). Given the consistent and frequent resurfacing of the Dyngjusandur plains by wind action, sediment exhumed closer to the surface is likely to primarily contain organisms robust enough to withstand the turbulent conditions and resettling [27-30]. Sequencing of these samples would provide greater insight into the shifts in community composition hinted at by this bulk biosignature data. While moisture content did not directly correlate to individual shifts in bulk biosignatures (Figure 2-4), moisture significantly increased after the first 1 cm of depth, mirroring the trends observed for the biosignatures quantified here. This suggests that, in addition to wind influences, a baseline level of moisture (~5%) may be a key element of the native community at Dyngjusandur. Sediment samples recovered for the spatial study also contained similar moisture levels across both sites, providing additional evidence for the importance of moisture across a much greater sample size.

The grain size fractions recovered from the depth profile closely mirror the trends observed during the spatial study, with smaller grain sizes making up the bulk of each sample. Again, the largest grain size composed the smallest fraction of each sample. Correlation tests also suggest grain size continues to have impact on bulk biomass, with DNA content showing strong negative correlations with the two largest sediment sizes. This trend could be influenced by the DNA extraction method, which uses bead tubes to disrupt the sample. It is possible this method is less efficient for larger grain sizes, however the larger grain sizes may also provide less surface area for microbial growth, resulting in respectively diminished DNA content among these fractions[31].

2.5.3 Microbial Community Impacts

The phyla uncovered from the D1 samples can provide a greater understanding of microbial distribution at the Dyngjusandur alluvial plane. At D1, clear variation is observed at the 10 m scale for dsDNA content, 16S copies, and moisture content, and interrogating the 100 m grouping reveals one of the corner 10 m triangles (D1-1) to have significantly less dsDNA content than its counterparts. Despite differences in these measurements, amplicon sequencing suggests that the community across D1 is somewhat homogenous, with the same three phyla (Proteobacteria, Acidobacteria, and Actinobacteria) comprising over 70% of the community of each sample on average. Searching for correlations between biosignature measurements and phyla revealed few strong correlations. DNA content showed a positive correlation with Cyanobacteria, and negative correlations with Dependentiae and Rokubacteria. Here, however, the impact of grain size fractions on bioactivity is pronounced, with the fraction between 425-850 μm showing both strong positive and negative correlations with several phyla. Positive correlations observed with this fraction include Acidobacteria, Armatimonadetes, Abditibacteriota, and Rokubacteria, and negative correlations were observed between Chloroflexi, Cyanobacteria, Gemmatimonadetes, and Patescibacteria. The importance of the 425-850 μm fraction was also documented in another FELDSPAR publication by Rader et al., finding that the rarer microorganisms were influenced by shifts in the abundance of this fraction in addition to mineral characteristics[20]. Previous studies, as noted by Rader et al., suggest that surface qualities of the sediment, such as concave areas and crevices, could provide protective environment from weathering, while other factors such as water retention, porosity, and mineral availability may also be influential[30, 32, 33]. The grain size fraction less than

450 μm showed negative correlations with Actinobacteria and Rokubacteria, and a positive correlation with cyanobacteria. The contrasting correlations displayed by these fractions is unsurprising given the strong negative correlation these fractions shared, but it suggests that the grain size of a sampling site could play a critical role in predicting the types of organisms in a sample. Even when bulk biomass fails to distinguish two sites, grain size distribution could be a dictating factor for community composition.

2.5.4 Implications for Astrobiology and Site Selection

Analyzing the microbiota and raw biomass of planetary analog environments with respect to geophysical limitations and spatial scale provides critical characterization for future extraterrestrial missions in search of life and for further terrestrial field studies. Missions like the Mars 2020 Perseverance Rover and campaigns to remote terrestrial environments are limited in their sampling capacity, and this work presents important insight into necessary considerations for producing a sampling strategy for these missions. These results suggest that sample separation, grain size fractions, and depth are important factors for identifying bulk biomass on an otherwise visually homogenous plain.

Sampling Dyngjusandur at 1 m of separation yielded few significantly different comparisons among moisture, dsDNA content, and 16S copies, suggesting a higher degree of homogeneity as samples sharing such close clustering. However, comparing these samples with those collected 10 m away yielded a much higher percentage of significant comparisons, while sampling at 100 m separation saw these differences mostly averaged out. The two sampling sites were compared, 1 km of separation, and both T-test and U-test showed statistically significant comparisons. These results imply an ideal separation range for sample gathering with site characterization in mind. Spatially tight clusters (sub 1 m) provide little characterization of a larger sampling site, while clusters separated by longer distances (10 m) covered a greater diversity of bulk biomass, 16S copies, and moisture measures represented by the high percentage of statistically significant comparisons. The lack of variability among samples separated by 100 m suggests that a rough characterization of a site's biomass may be possible with a smaller set of samples, although the finer details of a site, like geophysical relationships, will be lost without more comprehensive sampling.

The aeolian action at Dyngjusandur likely amplifies the impacts of sample depth on bulk biomass due to the near constant turnover of the top layers of sediment. The depth profile analysis shows significant differences between the top levels of sediment and the bottom levels when comparing dsDNA content. This result supports the hypothesis that upper levels of sediment are composed of a unique selection of the native biodiversity, primarily organisms robust enough to survive frequent weathering. This observation has implications for future Mars missions, an extraterrestrial target home to sediment storms like those observed at Dyngjusandur, and where sampling at depth has long been postulated to be highly important[34]. At Dyngjusandur, the majority of biomass was observed at depths of 3 cm and below. In comparison, Mars has additional factors influencing the anticipated depth profile of potential biosignatures, including persistent exposure to ionizing radiation, likely increasing optimal sampling depth significantly[35-37]. Sequencing of the Dyngjusandur samples would provide valuable details about shifts in community composition with respect to sediment depth, and additional geochemical measurements taken for each sample, such as pH, total organic carbon, and total nitrogen, would rigorously characterize the influence of environmental factors on life in Mars analog samples.

Despite this work focusing on terrestrial biosignatures, we do not necessarily expect potential extraterrestrial life to conform to our traditional understanding of biology. Rather, this work characterizes the qualities life adopts to maintain under extreme environmental pressures and the factors that must be considered when establishing an extraterrestrial or terrestrial sampling plan. Combined with further analysis of the amplicon sequencing data and mineralogical spectroscopy, this work aims to emulate and inform future extraterrestrial mission and terrestrial field campaign design from instrumental suite to sampling schemes to yield the most valuable science return possible for potential biosignature detection.

2.6 Citations

1. Sara, M.J., Dyngjusandur sand sheet, Iceland, as a depositional analog to the Stimson Fm. in Gale Crater, Mars. p. xii, 145 pages.

2. Amador, E.S., et al., Synchronous in-field application of life-detection techniques in planetary analog missions. Planetary and Space Science, 2015. 106: p. 1-10.

3. Gentry, D.M., et al., Correlations Between Life-Detection Techniques and Implications for Sampling Site Selection in Planetary Analog Missions. Astrobiology, 2017. 17(10): p. 1009-1021.

4. Allwood, A.C., et al., PIXL: Planetary Instrument for X-Ray Lithochemistry. Space Science Reviews, 2020. 216(8): p. 132.

5. Beegle, L., et al., Scanning Habitable Environments with Raman and Luminescence for Organics and Chemicals (SHERLOC) on Mars 2020. Abstracts of Papers of the American Chemical Society, 2019. 257: p. 2.

6. Hayes, A.G., et al., Pre-Flight Calibration of the Mars 2020 Rover Mastcam Zoom (Mastcam-Z) Multispectral, Stereoscopic Imager. Space Science Reviews, 2021. 217(2): p. 95.

7. Perez-Izquierdo, J., et al., The Thermal Infrared Sensor (TIRS) of the Mars Environmental Dynamics Analyzer (MEDA) instrument onboard Mars 2020, a general description and performance analysis. Measurement, 2018. 122: p. 432-442.

8. Wiens, R.C., S. Maurice, and F.R. Perez, The SuperCam Remote Sensing Instrument Suite for the Mars 2020 Rover: A Preview. Spectroscopy, 2017. 32(5): p. 50-55.

9. Murchie, S., et al., Compact reconnaissance Imaging Spectrometer for Mars (CRISM) on Mars Reconnaissance Orbiter (MRO). Journal of Geophysical Research-Planets, 2007. 112(E5): p. 57.

10. Mustard, J., et al., Report of the Mars 2020 Science Definition Team. 2013.

11. Hays, L.E., et al., Biosignature Preservation and Detection in Mars Analog Environments. Astrobiology, 2017. 17(4): p. 363-400.

12. Hoehler, T.M., An energy balance concept of habitability. Astrobiology, 2007. 7: p. 824.

13. Preston, L.J. and L.R. Dartnell, Planetary habitability: lessons learned from terrestrial analogues. International Journal of Astrobiology, 2014. 13(1): p. 81-98.

14. Lammer, H., et al., What makes a planet habitable? Astronomy and Astrophysics Review, 2009. 17(2): p. 181-249.

15. Thordarson, T. and A. Hoskuldsson, Postglacial volcanism in Iceland. Jokull, 2008. 58: p. 197-228.

16. Bathgate, E.J., et al., Raman, FTIR and XRD study of Icelandic tephra minerals: implications for Mars. Journal of Raman Spectroscopy, 2015. 46(10): p. 846-855.

17. Kargel, J.S. and R.G. Strom, ANCIENT GLACIATION ON MARS. Geology, 1992. 20(1): p. 3-7.

18. Baratoux, D., et al., Volcanic sands of Iceland - Diverse origins of aeolian sand deposits revealed at Dyngjusandur and Lambahraun. Earth Surface Processes and Landforms, 2011. 36(13): p. 1789-1808.

19. Arnalds, O., P. Dagsson-Waldhauserova, and H. Olafsson, The Icelandic volcanic aeolian environment: Processes and impacts — A review. Aeolian Research, 2016. 20: p. 176-195.

20. Rader, E., et al., Preferably Plinian and Pumaceous: Implications of Microbial Activity in Modern Volcanic Deposits at Askja Volcano, Iceland, and Relevancy for Mars Exploration. Acs Earth and Space Chemistry, 2020. 4(9): p. 1500-1514.

21. Direito, S.O.L., et al., A wide variety of putative extremophiles and large beta-diversity at the Mars Desert Research Station (Utah). International Journal of Astrobiology, 2011. 10(3): p. 191-207.

22. Isenbarger, T., et al., The Most Conserved Genome Segments for Life Detection on Earth and Other Planets. Origins of life and evolution of the biosphere : the journal of the International Society for the Study of the Origin of Life, 2008. 38: p. 517-33.

23. Hale, L. and D. Crowley, DNA extraction methodology for biochar-amended sand and clay. Biology and Fertility of Soils, 2015. 51.

24. Dowd, S.E., et al., Evaluation of the bacterial diversity in the feces of cattle using 16S rDNA bacterial tag-encoded FLX amplicon pyrosequencing (bTEFAP). BMC Microbiology, 2008. 8(1): p. 125.

25. Baldrian, P., et al., Active and total microbial communities in forest soil are largely different and highly stratified during decomposition. Isme Journal, 2012. 6(2): p. 248-258.

26. Dunn, O.J., MULTIPLE COMPARISONS AMONG MEANS. Journal of the American Statistical Association, 1961. 56(293): p. 52-&.

27. Mountney, N.P. and A.J. Russell, Sedimentology of cold-climate aeolian sandsheet deposits in the Askja region of northeast Iceland. Sedimentary Geology, 2004. 166(3-4): p. 223-244.

28. Rime, T., M. Hartmann, and B. Frey, Potential sources of microbial colonizers in an initial soil ecosystem after retreat of an alpine glacier. Isme Journal, 2016. 10(7): p. 1625-1641.

29. Weil, T., et al., Legal immigrants: invasion of alien microbial communities during winter occurring desert dust storms. Microbiome, 2017. 5: p. 11.

30. Acosta-Martinez, V., et al., Microbiology of wind-eroded sediments: Current knowledge and future research directions. Aeolian Research, 2015. 18: p. 99-113.

31. Bai, H.J., et al., Bacteria cell properties and grain size impact on bacteria transport and deposition in porous media. Colloids and Surfaces B-Biointerfaces, 2016. 139: p. 148-155.

32. Meslier, V., et al., Fundamental drivers for endolithic microbial community assemblies in the hyperarid Atacama Desert. Environmental Microbiology, 2018. 20(5): p. 1765-1781.

33. Probandt, D., et al., Microbial life on a sand grain: from bulk sediment to single grains. Isme Journal, 2018. 12(2): p. 623-633.

34. Sagan, C. and J.B. Pollack, DIFFERENTIAL TRANSMISSION OF SUNLIGHT ON MARS - BIOLOGICAL IMPLICATIONS. Icarus, 1974. 21(4): p. 490-495.

35. Keppler, F., et al., Ultraviolet-radiation-induced methane emissions from meteorites and the Martian atmosphere. Nature, 2012. 486(7401): p. 93-96.

36. Ertem, G., et al., Shielding biomolecules from effects of radiation by Mars analogue minerals and soils. International Journal of Astrobiology, 2017. 16(3): p. 280-285.

37. Fornaro, T., et al., UV Irradiation and Near Infrared Characterization of Laboratory Mars Soil Analog Samples. Frontiers in Astronomy and Space Sciences, 2020. 7(91).

CHAPTER 3. BIOSIGNATURE DISTRIBUTION & CHARACTERIZATION OF THE DYNGJUSANDUR, ICELAND MARS ANALOG PLAIN FROM 2016-2017

Adapted with permission from: "Biosignature Distribution & Characterization of the Dyngjusandur, Iceland Mars Analog Plain From 2016-2017" Submitted to Astrobiology Spring 2022

3.1 Abstract

Analog research represents one of the primary means of informing future extraterrestrial missions, enabling investigation into the factors that could influence sample habitability. The FELDSPAR team visited the Dyngjusandur, Iceland, alluvial plain from 2016-2019 in order to emulate the protocols and procedures employed by the Mars 2020 Perseverance Rover under analogous conditions. Dyngjusandur is a plain of basaltic sediment in central Iceland with limited nutrient availability, similar spectroscopic qualities to regions of the Martian surface, extreme temperatures, and visually and morphologically homogenous sediment. In 2017, a sampling site was selected 4 km southwest of the 2016 sites, and three subsites were established with 1 km separation. Samples were recovered using a schematic of nested triangles, where each sub-site was composed of a 100 m equilateral triangle, the corners of which were made of 10 m equilateral triangles. Additional nested triangles were mapped at 1 m and 0.1 m separation, with each sample at the 0.1 m scale assigned a barcode for processing. The following characteristic factors were determined for each sample procured: ATP, DNA, moisture

content, and grain size composition. Trends observed during the 2016 campaign were often realized in the 2017 sample set, with the 10 m scale demonstrating consistent biosignature variability, and grain size fractions correlating with biosignature content. The 2017 sample sites also presented a paradigm shift, with one of the subsites being heterogenous as a result of large lava chunks dispersed frequently across the sampling area. The uniqueness of this sampling site appeared to provide more protection from katabatic winds, resulting in pockets of increased bioactivity. This work provides additional support for many of the observations uncovered during the 2016 expedition, suggesting that replicate samples at close spacing can often be omitted in favor of additional samples at larger and variable sampling distances.

3.2 Introduction

As interest in extraterrestrial exploration expands with improved technology and scientific innovations, making the most of sample analysis and return is paramount. The recent Mars 2020 Perseverance Rover landed in early 2021 and houses analytical instruments for in situ sample analysis and 43 sampling tubes for specimen collection capable of carrying 9 cubic inches of sediment [1]. The choice of instruments on the Mars 2020 rover were selected considering size and power constraints, success of the proposed technique on previous missions, and applicability of the proposed technique for achieving NASA's mission goals [2-6]. With these constraints in mind, the Mars 2020 rover was equipped with an arsenal of spectroscopic instruments to perform mineralogical and elemental analysis of the Martian surface. However, as the search for indicators of past life becomes an increasing focus for extraterrestrial missions, the optimization of sample collection must also be considered to maximize the limited space available on future rovers.

Moreover, while currently employed techniques provide valuable environmental and mineralogical data, they do not directly measure biosignatures that would help confirm extinct (or even extant) microbial life. This work aims to emulate sampling procedures at a terrestrial Mars analog site to determine the most efficient sampling approach to capture the biological variability of a potential Mars sampling site while looking for trends in environmental factors that may be predictive of life as we know it.

Since 2013, the PSTAR-funded Field Exploration and Life Detection Sampling through Planetary Analog Research (FELDSPAR) team has been returning to Icelandic lava fields sites with some characteristics analogous to Martian sites. A difficulty with preparing for an extraterrestrial mission is the inability to test instruments and sampling techniques under identical conditions as the final target. Analog research involves identifying terrestrial locations with some (often harsh) conditions comparable to those observed extraterrestrially, and tests prospective techniques at these locations to inform future missions [7-9]. While analog research involves testing that assumes terrestrial biology, potential extraterrestrial life likely evolved differently and may leverage unique means of data storage and metabolism. The FELDSPAR project investigates extraterrestrial analogs to identify environmental and geochemical correlations with terrestrial biology that may help define the qualities that make a sample habitable and conducive to life [10-13]. Iceland’s lava fields are considered Mars analogs due to their glacial and volcanic history, similar surface mineralogy, extreme temperatures and environmental conditions, and relative isolation resulting in limited anthropogenic contamination [14-16]. One such lava field, Dyngjusandur, has been visited annually by the FELDSPAR team from 2016 – 2019 for in situ spectral analysis and sample return for analysis at the University of Akureyri and the Georgia Institute of Technology. Dyngjusandur is located in the Central Highlands of Iceland, south of Lake Askja, and features plains of unconsolidated basaltic tephra that has largely been reduced to a fine, black sand [17-21]. Larger chunks of lava are relatively uncommon and widely distributed across Dyngjusandur, resulting in wide expanses (> 1 km2) of visually homogenous sediment. Southern glacial activity results in flooding near the sampling sites, and the glaciers also provide katabatic winds causing sandstorms that frequently redistribute the surface layers of sediment [17].

The 2017 FELDSPAR expedition to Dyngjusandur was designed for comparison with the 2016 campaign while adapting techniques from the Mars 2020 rover to determine their efficacy for identifying biosignatures [13]. In the field, full sampling sites were mapped using aerial photography, and then specific sampling locations were photographed at approximately Mastcam-Z height [4]. Sampling sites were structured such that the influence of sampling distance could be tested for each sample at multiple scales with two points of comparison. Samples were then analyzed with portable visible near infrared and x-ray fluorescence spectrometers before being returned to the lab for analysis of adenosine triphosphate (ATP) as a measure of bioactivity and double stranded DNA (dsDNA) as a measure of bulk biomass. The combination of ATP and dsDNA provide complementary results, with ATP requiring active metabolism for production, while dsDNA is more robust to degradation and thus can be harvested from living or dead organisms. These biological factors were then compared with sample moisture and grain size, and clustered with neighboring samples to evaluate the influence of sampling distance on biosignature variability. With two years of Dyngjusandur data analyzed, changes in these biological and environmental factors can be monitored temporally, and trends can be determined as the sampling site evolves from year to year.

This work characterizes the 2017 Dyngjusandur sampling site and considers the correlations between bioactivity and biomass proxies of ATP and dsDNA content with environmental and spatial factors. Bulk dsDNA was measured as an estimate of biomass, while ATP was measured as an estimate of bioactivity, and both were compared with gravimetric moisture content and grain size distribution to uncover potential habitability trends. Shifts in these parameters were also monitored at a series of spatial scales to determine the variability of the Dyngjusandur Mars analog and provide insight to improve sampling efficiency. Finally, the 2017 data was compared with the data from the 2016 expedition, highlighting site trends over time.

3.3 Methods – Dyngjusandur Sampling & Analysis

3.3.1 Sampling: Nested Triangular Grids & In Field Assays

Sediment samples were recovered from plains at Dyngjusandur, Iceland in July 2017. Three sampling sites were selected approximately 4 km southwest of the 2016 Dyngjusandur sampling sites, and directly south of Lake Askja. The 2017 Dyngjusandur sampling site was divided into three subsites at the corners of a 1 km equilateral triangle, henceforth referred to as D1-D3. The subsites were located at the following coordinates: D1 at 64.93^{o}N, 16.72^{o}W, D2 at 64.94^{o}N, 16.71^{o}W, and D3 at 64.93^{o}N, 16.69^{o}W. These subsite locations were selected for the mix of visually homogenous and visually heterogenous sediment compositions they possessed, with D1 being largely free of larger lava stones, and thus more homogenous and most comparable to the 2016 sampling sites, D2 composed of larger lava stones dispersed at greater frequency across the surface, and D3 representing a combination of the two paradigms. Procedural similarity was maintained with the 2016 expedition through the use of a nested triangle schematic for sample excavation. Subsites were composed of 100 m equilateral triangles, the corners of which were composed of 10 m equilateral triangles, and additional triangular groupings were continued at sampling distances of 1 m and 0.1 m (Figure 3-1). Groupings were manipulated using individual sample barcodes, allowing samples to be compared at different spatial scales during downstream processing. Site groupings were marked with vibrant tarps and flags in the field for identification during aerial photography and site mapping using a DJI Inspire 1 Quadcopter.

After site mapping, sampling sites were prepared for in field spectroscopic analysis. The top 1 cm of sediment was scraped from the sample area with a sterilized trowel prior to analysis with a portable visible near infrared (VNIR) ASD spectrometer and a portable x-ray fluorescence spectrometer. Spectroscopic analysis and the relevance of the spectroscopic data with respect to the characteristic factors addressed here is being prepared for a sister publication. Following mineralogical analysis, 50 mL conical tubes were filled with sediment, labeled with their respective sample barcodes, and bagged for return to the field lab at the University of Akureyri. Sampling was performed in an attempt to prevent anthropogenic contamination, with researchers wearing gloves, facemasks, non-linting disposable sleeves, and working downwind of the sampling area when possible.

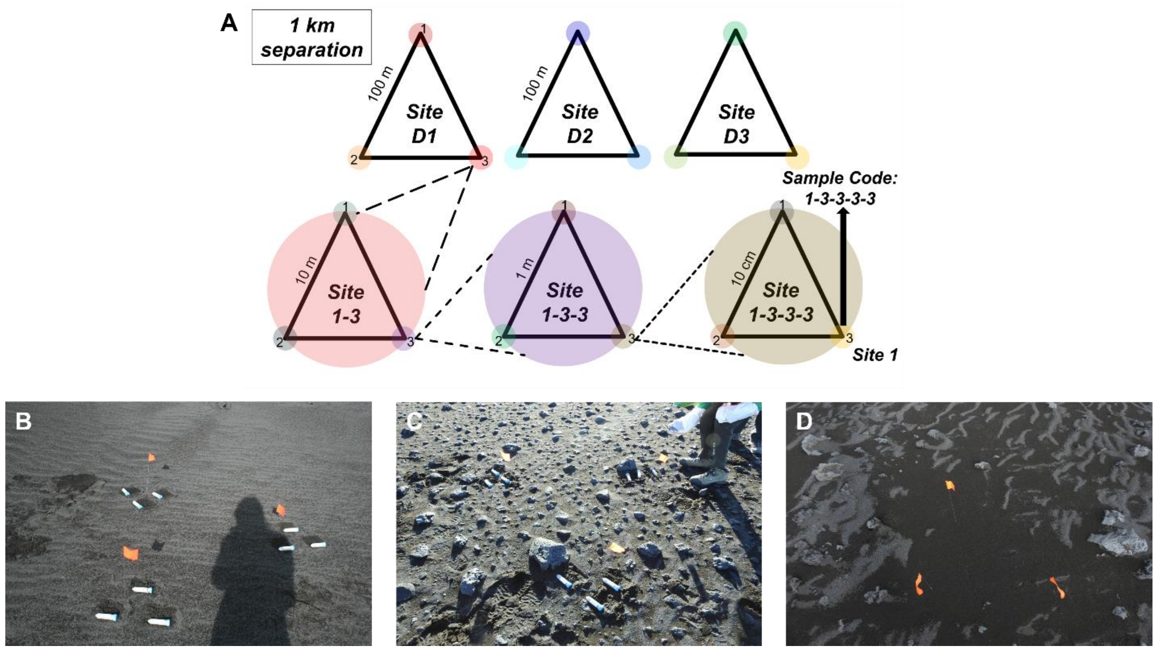

Figure 3-1 – Dyngjusandur, Iceland: 2017 Site Overview. *A) Schematic of Nested Equilateral Triangles: A 1 km equilateral triangle was mapped as a sampling site. The corners of the 1 km triangle were composed of 100 m equilateral triangles. The corners of each subsequent triangle are also composed of equilateral triangles of 10 m, 1 m, and 0.1 m sizes. The corners of each 0.1 m triangle were sampled and assigned a barcode for spatial identification and statistical analysis. B) A 1 m triangle at subsite D1. C) A 1 m triangle at subsite D2. D) A 1 m triangle at subsite D3.*

Upon return to the University of Akureyri, samples were aliquoted for field lab ATP analysis, and the parent samples were maintained in lab freezers until shipped to Georgia Tech. At Georgia Tech, samples were held at -80 ^{o}C until further analysis.

3.3.2 Characterization Factors

3.3.2.1 <u>Environmental Factors (Moisture Content & Grain Size Fractions)</u>

Gravimetric moisture content (mass of moisture / mass of dry sediment) and grain size fraction composition were determined for each collected sample. Samples were defrosted in a sterilized space and then aliquoted in triplicate into labelled, massed vials.

For each 100 m subsite (D1-3), a full 10 m triangle was analyzed in full (DX-1) while the remaining two 10 m triangles (DX-2 & DX-3) at each subsite only considered a single sample from each 0.1 m grouping. Sample vials were covered in foil to prevent sample loss or contamination and placed in an incubator oven at 100 oC for 24 hours. Once dried, the sample mass was measured to determine the composition of mass comprised of moisture. Dried samples were then subjected to dry sieving to determine grain size composition. Four grain size fractions were measured: mass of sediment larger than 2000 μm, between 850-2000 μm, between 425-850 μm, and less than 425 μm. The mass of each fraction was measured and compared with the total dry mass to determine the percent composition of each sample.

3.3.2.2 Biological Factors (ATP & dsDNA Content)

Adenosine triphosphate (ATP) was quantified at the University of Akureyri immediately following sample collection using the ATP Bioluminescence Assay Kit HSII (Roche Diagnostics LTD, Basel, Switzerland) and procedures were followed to the manufacturer specifications. Samples were prepared in 1 mL aliquots in triplicate, and suspended in Tris-EDTA buffer (100 mM, 4 mM EDTA) prior to cell lysis in a boiling water bath for 2 min. After cell lysis, luciferase reagent was added to each sample, and luminescence was quantified with a HY-LiTE 2 luminometer (Merck, VWR International LTD, Radnor, PA) and compared against kit standards.

Once samples were returned to Georgia Tech, double stranded DNA (dsDNA) was quantified for each sample using a Qubit dsDNA High Sensitivity Assay (Thermo Fisher, Waltham, MA). Sediment samples were aliquoted in triplicate, and DNA was extracted from them using a DNeasy PowerLyzer PowerSoil Kit (Qiagen, Hilden, Germany). Similarly to the extractions performed on the 2016 samples, a low-biomass protocol was required for the PowerLyzer kit to produce a quantifiable amount of dsDNA [22]. Purified DNA samples were quantified against Qubit standards using a Qubit fluorimeter.

3.3.2.3 Statistical Analysis of Characteristic Factors

Statistical analyses and data processing were performed using R studio, and tests were chosen to mirror those performed for the 2016 analysis [13]. Spatial influences were identified by using a series of pairwise T and U tests to compare the characteristic factors (gravimetric moisture, ATP, and dsDNA) at each spatial grouping [10]. During this analysis, samples were compared within their parent triangles. For instance, the 1 m grouping compared the characteristic factors of each daughter 0.1 m triangle resulting in significant or insignificant P-values based on a 95% confidence interval. P-values were adjusted with a Bonferroni correction, and the percentage of significant comparisons was determined by comparing the number of significant comparisons to the total number of comparisons [23]. This process was performed at each spatial grouping (100 m, 10 m, and 1 m) at each subsite.

Characteristic factors were also analyzed using Spearman's rank correlation coefficients to generate correlation matrices. Correlations were determined between gravimetric moisture, ATP, dsDNA, and grain size fractions, and both positive and negative correlations with p-values less than 0.1 were plotted.

3.4 Results

3.4.1 Analysis of Characterization Factors Across Subsites

Using a series of nested triangles to establish sampling locations enabled efficient grouping of samples at different spatial distributions. Starting with a 1 km equilateral triangle, three subsite 100 m equilateral triangles were established at each apex (D1-D3). Each subsite is composed of additional triangles separated by 10 m, 1 m, and 0.1 m, and evaluating these subsites with respect to the triangular groupings provided insight into the distribution of biomass and bioactivity at each spatial grouping. For ease of interpretation, characterization factors have been grouped within each subsite at the 10 m level for plotting, however pairwise comparisons were performed at each spatial level.

3.4.2 dsDNA Content

Considerable variation was observed when quantifying dsDNA at each subsite (Figure 3-2). Both subsites D1 and D3 appeared to have similar distributions of bulk DNA, with average values of 9.6 ng/g dsDNA per gram sediment and 11.7 ng/g dsDNA per gram sediment respectively. For both D1 and D3 boxplot whiskers were relatively small within each daughter 10 m triangle, representing a degree of sample homogeneity at these locations. Subsite D2, however, was vastly different from its counterparts when directly compared and within site. At D2, the average dsDNA was 72.9 ng/g dsDNA per gram sediment, and the whiskers for each subgrouping are large, suggesting significant sample heterogeneity. Outlier points for the groupings at D2 range as high as 300 ng/g dsDNA per gram sediment, while the most DNA rich samples observed at D1 and D3 barely contained 50 ng/g dsDNA per gram sediment.

Pairwise T-Tests and U-Tests were performed at each grouping within each subsite to account for parametric and nonparametric distributions, however similar outcomes were observed for both tests for each characteristic factor (Table 1). These tests suggest that dsDNA content is relatively homogenous at 1 m groupings, with 0% significant comparisons across all subsites at this scale. At the 10 m grouping, D1 and D2 have 11% significant comparisons respectively based on pairwise t-tests, while D3 has 22%. The greatest disparity in dsDNA content was observed at the 100 m scale, where D1 showed 0% significant t-test comparisons, while D2 had 33%, and D3 had 67%, however these percentages are limited by the number of comparisons for each subsite (3 total, 1 for each pair of 10 m triangles at each subsite). The 1 km scale saw 33% significantly different comparisons when comparing the three 100 m triangles.

3.4.3 ATP Content

When quantifying ATP as a measure of metabolic activity, variations in quantity by site existed without extreme disparity between subsites compared to dsDNA content (Figure 3-3). Average ATP content at D1 was $2.6x10^{-10}$, at D2 was $4.2\ x10^{-10}$, and at D3 was $4.0x10^{-10}$. As with dsDNA, the boxplot whiskers were largest for D2, extending both above and below the minimum and maximum ATP measures observed at sites D1 and D3. The wide range of ATP measures obtained at D2 suggests a greater degree of heterogeneity within each sample, while the tighter clustering at D1 with few outlier points suggests homogeneity at each corner of the parent 10 m triangles.

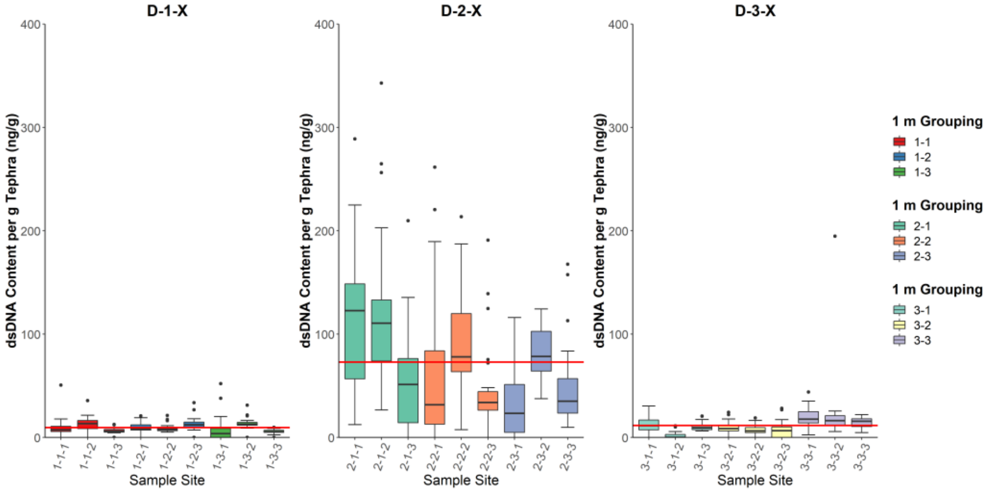

Figure 3-2 – dsDNA Quantification. *dsDNA content was collected for each sample and grouped according to subsite (D1-3) and then grouped by 10 m triangle (D1-X – D3-X). Legend colors represent each 10 m triangle, with three boxplots per color to represent the daughter 1 m triangles (measurements within each 1 m triangle were grouped for display). Red lines on each plot represent the average dsDNA content per site. Site averages were: D1 – 9.6 ng/g, D2 – 72.9 ng/g, D3 – 11.7 ng/g.*

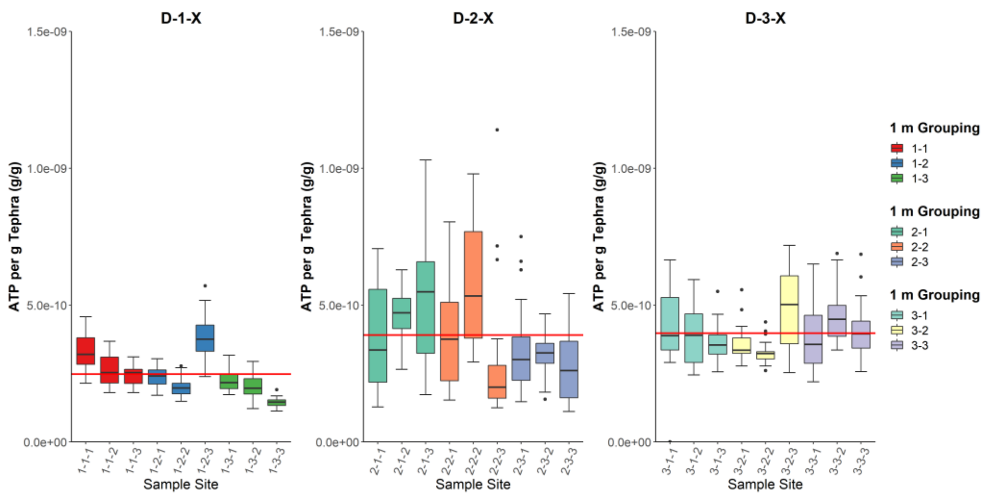

Figure 3-3 – ATP Quantification. *ATP content was collected for each sample and grouped according to subsite (D1-3) and then grouped by 10 m triangle (D1-X – D3-X). Legend colors represent each 10 m triangle, with three boxplots per color to represent the daughter 1 m triangles (measurements within each 1 m triangle were grouped for display). Red lines on each plot represent the average dsDNA content per site. Site averages were: D1 – 2.6x10-10 g/g, D2 – 4.2 x10-10 g/g, D3 – 4.0 x10-10 g/g.*

Considering pairwise T-Tests and U-Tests to determine statistical differences between samples revealed similar trends for ATP as dsDNA (Table 1). Both tests yielded parallel outcomes, starting with 4% or fewer statistically significant differences observed at the 1 m scale. At the 10 m grouping, ATP varied considerably at subsite D1 with 78% significantly different comparisons, while D2 and D3 each displayed 11% significantly different comparisons. While all three subsites shared 11% significantly different comparisons for dsDNA at the 10 m grouping, D1 displayed the greatest volume of significant comparisons for ATP. The tight clustering of the ATP data for D1 may have influenced the number of significant outcomes when comparing different spatial groupings, resulting in areas of consistent bioactivity that varied across the subsite as a whole. Like with dsDNA, the 100 m grouping saw a spread of significantly different comparisons ranging from 0-67%, while the 1 km grouping showed 67% significantly different comparisons when comparing the three 100 m triangles.

Table 3-1. Influence of Spatial Distribution on Characteristic Factors Using Two Quantitative Tests

	Pairwise T-Test			Pairwise Mann-Whitney-U			
	Site 1			***Site 1***			
Separation	**100 m**	**10 m**	**1 m**	**100 m**	**10 m**	**1 m**	
DNA Content	0%	11%	0%	0%	22%	0%	*Significant Pairwise Comparisons*
ATP	67%	78%	0%	67%	67%	0%	
% Moisture	33%	11%	0%	33%	22%	0%	
	Site 2			***Site 2***			
Separation	**100 m**	**10 m**	**1 m**	**100 m**	**10 m**	**1 m**	
DNA Content	33%	11%	0%	33%	22%	0%	*Significant Pairwise Comparisons*
ATP	33%	11%	4%	33%	11%	0%	
% Moisture	0%	22%	0%	0%	22%	0%	
	Site 3			***Site 3***			
Separation	**100 m**	**10 m**	**1 m**	**100 m**	**10 m**	**1 m**	
DNA Content	67%	22%	0%	67%	22%	0%	*Significant Pairwise Comparisons*
ATP	0%	11%	0%	0%	0%	0%	
% Moisture	0%	33%	0%	33%	22%	0%	
	Combined Site			***Combined Site***			
DNA Content	***1 km***		*33%*	***1 km***		*0%*	*Significant Pairwise Comparisons*
ATP			*67%*			*33%*	
% Moisture			*100%*			*100%*	

**Table 3-1 represents the percentage of different comparisons at each spatial scale. Statistically significant comparisons were $0.05 \geq p$. The percentage of statistically significant comparisons at each scale was determined by comparing the number of significant comparisons within each grouping to the total number of comparisons performed for each grouping.*

3.4.4 Gravimetric Moisture Content

In comparison to the biomass and bioactivity characteristic factors (dsDNA and ATP), moisture content is an environmental factor that shows consistency across all three subsites (Figure 3-4). Average moisture contents were 10.3% for D1, 7.4% for D2, and 8.9% for D3. Despite the average moisture content for all three subsites being within 3% of each other, tight clustering at each subsite show fluctuations in moisture across the 10 m parent triangles, indicating that samples taken 10 m apart can vary in moisture by as much as 2-3%.

Gravimetric moisture content was subjected to the pairwise testing used for dsDNA and ATP analyses, and the percentage of significant comparisons by spatial grouping appeared highest at the 10 m scale (Table 1). For moisture, 0% significant differences were observed at the 1 m scale and increased to 22% and 33% for D2 and D3 respectively at the 10 m scale. Subsite D1 experienced 11% significantly different comparisons at the 1 m scale for moisture content. At the 100 m grouping, the limited number of comparisons saw some differences averaged out with a lower percentage of significant comparisons for D2 and D3 (0%), and a slightly higher percentage of differences for D1 (33%, representing two significant comparisons of three). However, despite the decline in significant comparisons at the 100 m grouping, the 1 km grouping comparing the three 100 m triangles found 100% significant comparisons, implying that all three triangles have significantly different moisture contents.

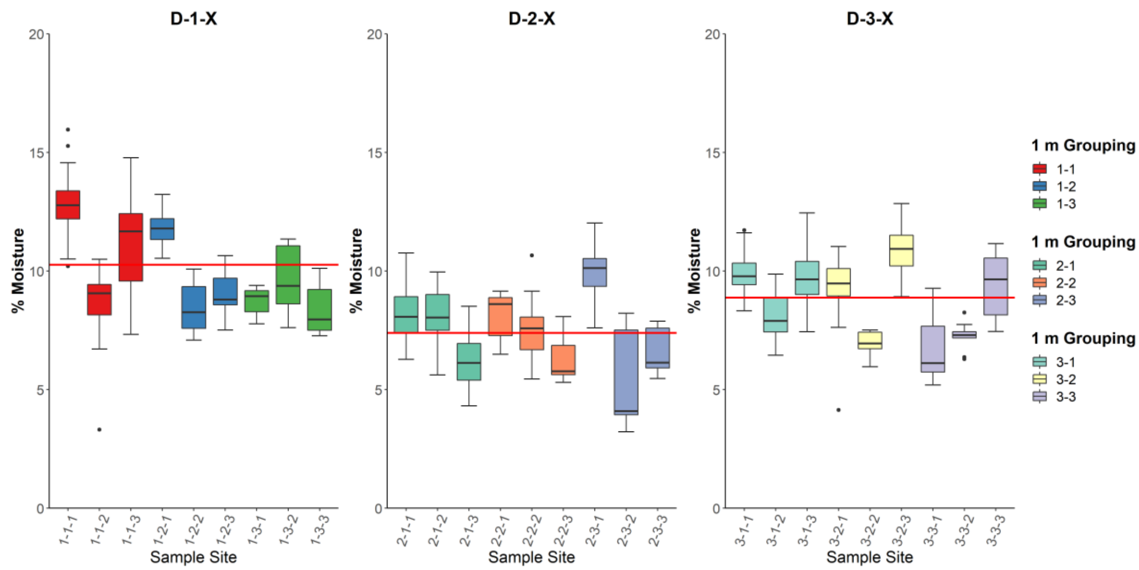

Figure 3-4 – Gravimetric Moisture Quantification. *Moisture content was collected for each sample and grouped according to subsite (D1-3) and then grouped by 10 m triangle (D1-X – D3-X). Legend colors represent each 10 m triangle, with three boxplots per color to represent the daughter 1 m triangles (measurements within each 1 m triangle were grouped for display). Red lines on each plot represent the average dsDNA content per site. Site averages were: D1 – 10.3%, D2 – 7.4%, D3 – 8.9%.*

3.4.5 Grain Size Fractions

Four grain size fractions were obtained for each sample, and the percentage of each fraction relative to the total sample mass was determined (Figure 5). Across all three subsites, grain size composition of each sample was consistent with a few notable discrepancies. The bulk of each sample, roughly 75%, was composed of fine sediment with a grain size less than 425 µm. The two mid-sized fractions compose the majority of the remaining sample, with the fraction between 425-850 µm making up 15-25% of each sample and the fraction between 850-2000 µm making up 10-20% of each sample. The largest grain size fraction, greater than 2000 µm, composed the least amount of most samples, barely reaching 5% of the samples at D1 and D3. Subsite D2 exhibited a unique sediment distribution with regard to the largest sediment fraction, seeing a greater percentage of large sediment in each sample (as much as 10%).

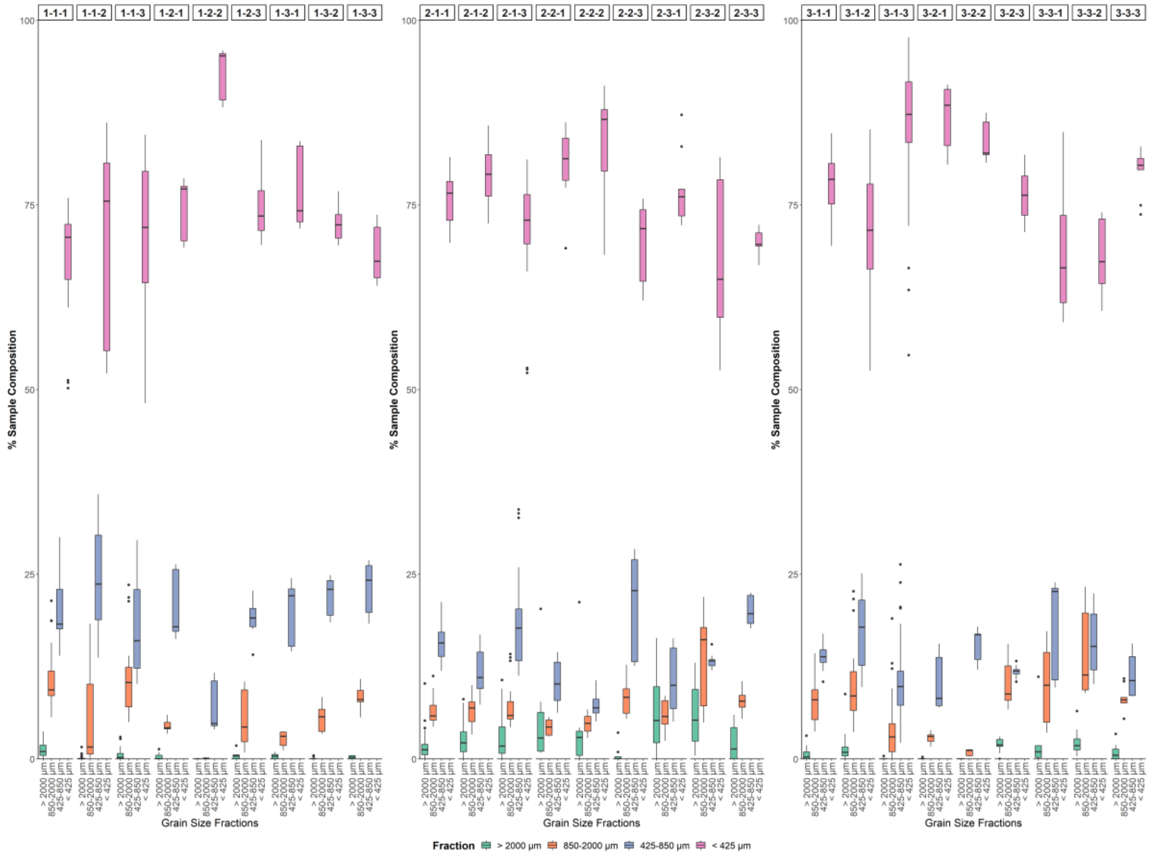

Figure 3-5 *– Grain Size Fractions. Sample composition with respect to grain size was determined via dry sieving. Percent composition of each fraction was determined by comparing moisture mass against total dry sample mass. Samples were grouped by subsite (D1-3), 10 m triangle (D1-X – D3-X), and finally 1 m triangle (D1-X-Y – D3-X-Y). The grain size fraction greater than 2000 μm is presented in green, the fraction between 850-2000 μm is presented in orange, the fraction between 425-850 μm is presented in violet, and the fraction less than 425 μm is presented in pink.*

3.4.6 *Correlation Matrices*

Correlation matrices were prepared to identify relationships among the characteristic factors (Figure 3-6). Across all three subsites, several correlation trends are observed. The finest sediment size (< 425 µm) is strongly inversely correlated with mid-sized fractions (425-850 µm & 850-2000 µm). Moreover, the mid-sized fractions are strongly positively correlated, and ATP is weakly positively correlated with the largest sediment fraction (> 2000 µm) at each subsite. Gravimetric moisture content was also shown to have a significant negative correlation with the 425-850 µm grain size fraction.

Beyond the trends apparent for all three subsites, a few notable correlations are shared by some of the subsites. A positive correlation was observed for sites D1 and D3 between the two largest sediment fractions, while D2 and D3 shared positive correlations between the finest sediment and moisture. Subsites D2 and D3 also share a weak negative correlation between the sediment fraction 425-850 µm and ATP. Both D1 and D3 demonstrate no correlations between dsDNA and other characteristic factors, however D2 is unique in this regard having strong positive correlations between dsDNA content and ATP, and dsDNA and the finest sediment size. Subsite D2 also showed a strong negative correlation between dsDNA content and the grain size fraction from 425-850 µm.

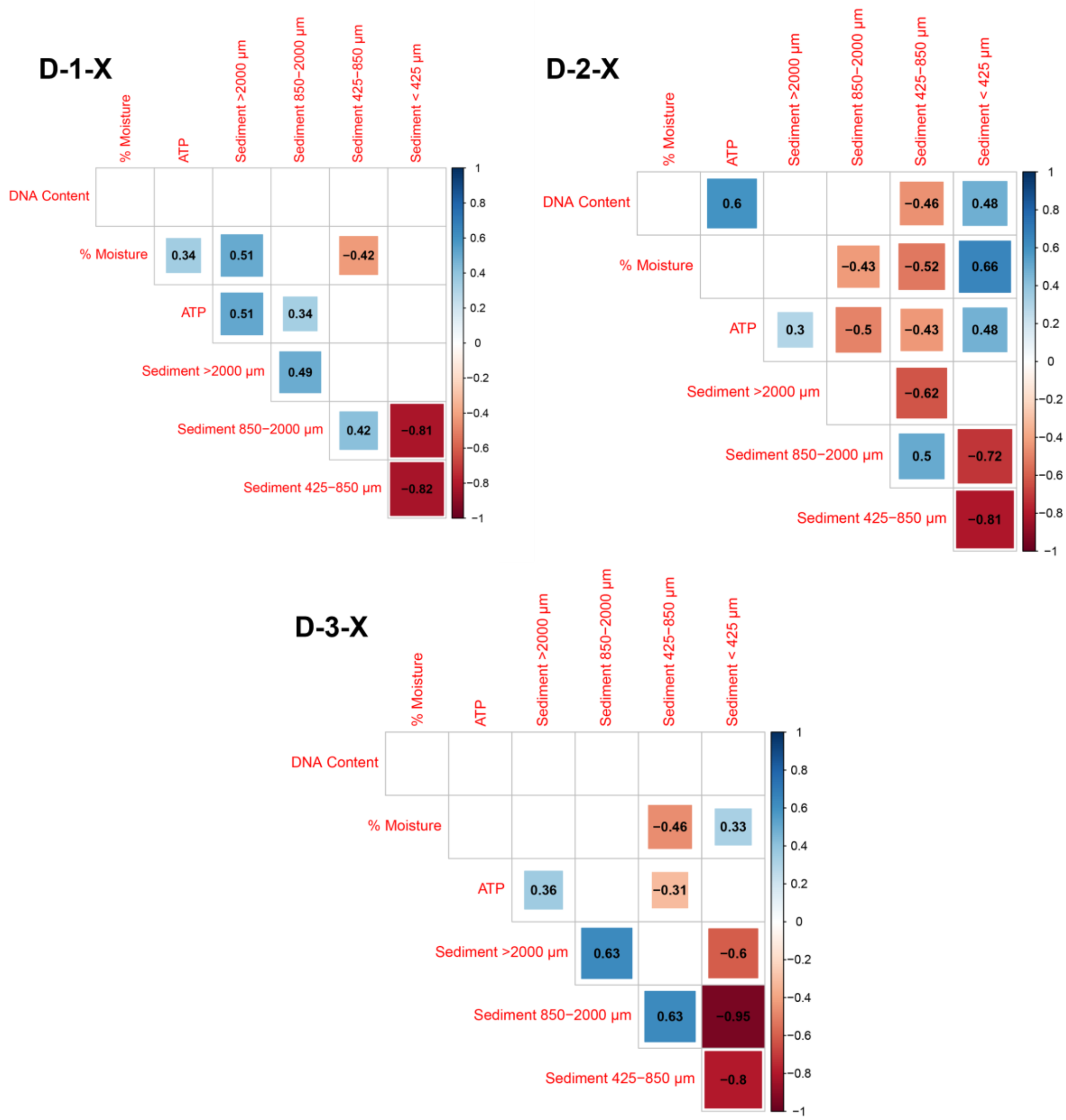

Figure 3-6 – Correlation Matrices All Subsites. *Correlations were determined between each characteristic factor at each subsite using Spearman's rank correlation coefficients. Significant comparisons were determined based on a 90% confidence interval, and correlation coefficients were overlayed on significant comparisons. Blank squares represent insignificant correlations.*

3.5 Discussion

3.5.1 Spatial Variation & Environmental Influences

Much like previous FELDSPAR expeditions, the 2017 Dyngjusandur campaign was concerned with identifying the influence of spatial scale on Mars analog sampling. Qualitative inspection of the characteristic factors in boxplot form identified variability across and within subsites, and pairwise comparisons provided a quantitative perspective on these observations. Leveraging the results of pairwise testing provided insight into the spatial groupings responsible for the most variability, potentially allowing for more efficient sample site characterization and the collection of fewer samples per site.

Across the three sampling subsites in 2017, several trends were observed when considering the variability of characteristic factors with respect to spatial scale. One of the most apparent trends is the lack of significantly different results at the 1 m scale, with significant differences representing a maximum of 4% of the possible comparisons tested. This suggests a high degree of homogeneity in samples with close proximity to each other and implies that replicate samples may not be a necessity when characterizing a larger sampling site with a limited number of sampling containers. When comparing samples separated by 10 m, however, a higher percentage of significant results were observed for each characteristic factor at each subsite. The dsDNA content across subsites had 11-22% significantly different comparisons, ATP content ranged from 11-78%, and gravimetric moisture content ranged from 11-33%. From these results, dsDNA appears to be the most consistent across 10 m of separation, while moisture had a slightly larger range of outcomes. The ATP content at the 10 m grouping demonstrated a large volume of significant comparisons at subsite D1 (78%), suggesting subsite D1 may have experienced more recent surface disruption. The 10 m grouping at D1 is particularly interesting due to the relatively few significantly different comparisons observed for dsDNA. While the ATP assay yielded a wider range of significant comparisons across subsites, the reliance of ATP on active metabolism means that fluctuations can result from areas of high or low bioactivity. Conversely, the dsDNA assay measured bulk biomass, and given the high stability of DNA, areas of declining metabolic activity can be surveyed to determine historic biopotential.

The limited number of comparisons available obscures evaluation of the pairwise comparisons at the 100 m grouping. Three common outcomes at the 100 m scale are 67% significant comparisons, representing two of three significant comparisons: only one pair of triangles was considered statistically similar. Another common outcome is 0% significant comparisons, suggesting that the variability observed at the 10 m and 1 m groupings is averaged out when comparing the characteristic factors from sites separated by 100 m. Finally, several sites displayed 33% significantly different comparisons, showing one out of three comparisons was significantly different. No variable or subsite displayed 100% significantly different comparisons at the 100 m level. Even though the small sample size makes evaluating the 100 m grouping challenging, the outcome trends across subsites suggest that sampling with 100 m separation will likely produce unique samples, although additional sampling within each site is required at each location to fully characterize the variability of bioactivity and biomass at the site.

3.5.2 Patterns with the 2016 Dyngjusandur Expedition

An interesting point of comparison to the 2017 results are the characteristic factors measured for the 2016 Dyngjusandur FELDSPAR expedition [13]. For the 2016 data set, bacterial amplicons were measured as a characteristic factor, but this factor was replaced by the ATP assay in subsequent field campaigns. However, while a direct measure of bioactivity is not comparable between the 2016 and 2017 data sets, gravimetric moisture content, dsDNA, and grain size can all be compared, and Mars analog trends can be uncovered as the sampling site matures.

The samples collected in 2016 were from sites about 4 km northeast of the 2017 sampling sites [13]. Despite the distance between the sampling sites, qualitative observation designated the sites as visually and morphologically comparable. The one exception to the site parallels observed from year to year was 2017 D2, which had a relatively high density of surficial large lava rocks dispersed across the sampling area. On average, the 2016 sampling sites had greater densities of biomass than 2017, with the 2016 subsites (D16-1 & D16-2) having 33 (±15 SD) and 42 (±17 SD) ng dsDNA / g tephra and the 2017 subsites having 9.6 (±7.3 SD), 73 (±60 SD), and 12 (±4 SD) ng dsDNA / g tephra for D1-3 respectively (Figure 7). While biomass was, on average, greater in 2016 in comparison to D1 and D3, the standard deviations were larger suggesting less homogeneity at each site. The heterogeneity observed at 2017 D2 also appears to play a major role in biomass variability. Notably, the average biomass at D2 is much higher than all other sampling sites, and the standard deviation is equally large, pointing towards the widest range of dsDNA measures. Furthermore, D2 was the only site in 2017 to demonstrate a positive correlation between ATP and dsDNA suggesting that a larger portion of the biomass recovered at D2 originates from living microorganisms. The stochasticity observed at D2 likely supports the importance of the overall site heterogeneity, specifically increased large sediment and lava quantity. Grain size has shown to have a prominent impact on Mars analog biomass and bioactivity, and the frequent, large chunks of lava may provide the native microorganisms protection from extreme environmental conditions, access to important nutrients, or the surface area conducive to community networking and symbiosis. The impact of environmental conditions is especially apparent given the aeolian resurfacing experienced by the Dyngjusandur sampling sites. The sampling sites selected for the 2016 and 2017 expeditions fall in the middle of the Dyngjusandur wind patterns provided by Sara et al 2017, and the sandstorms observed by the FELDSPAR team during sampling campaigns support the idea that the Dyngjusandur microbial communities are frequently disturbed, distressed, and redistributed at the surface level. This was tested in 2016 with a depth profile that uncovered larger quantities of dsDNA at deeper sampling depths [13]. Given the known aeolian impacts at Dyngjusandur, a sampling site like D2 with larger stony formations likely forms pockets of bioactivity that are allowed to mature undisturbed. Such a paradigm would result in protected areas of high biomass measures concurrently with ATP production, while other unprotected locations might be home to biomass measures more similar to the other Dyngjusandur subsites analyzed.

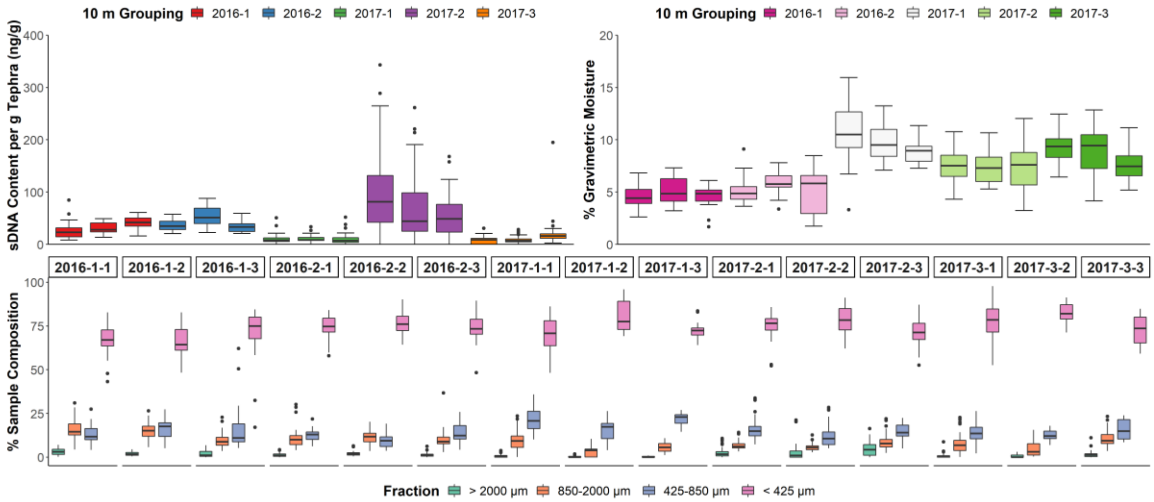

Figure 3-7 – Characteristic Factors at Dyngjusandur from 2016-2017. *Data from FELDSPAR expeditions to Dyngjusandur in 2016 and 2017. A) dsDNA grouped at the 100 m level for each subsite in 2016 and 2017. B) Gravimetric moisture content grouped at the 100 m level for each subsite in 2016 and 2017. C) Grain size composition of samples from 2016 and 2017 grouped at the 100 m level.*

Unlike dsDNA, gravimetric moisture content was relatively consistent from year to year and varied similarly from site to site. In 2016, average gravimetric moisture content was 5% (±2% SD) for D16-1 and 5% (±3% SD) for D16-2, and in 2017 the average gravimetric moisture content was 10% (±2% SD) for D1, 7% (±2% SD) for D2, and 9% (±2 SD) (Figure 3-7). Even though, on average, Dyngjusandur was slightly more hydrated in 2017, similar standard deviations were observed for each subsite implying sample homogeneity was consistent over time. This is also true when considering the outcomes of pairwise comparisons. In 2016, at the 10 m grouping, D16-1 had 44% significantly different comparisons and D16-2 had 33% significantly different comparisons, while the subsites in 2017 ranged from 11-33% significantly different comparisons. This shows that at 10 m of separation, Dyngjusandur samples have tight moisture content groupings at 1 m that result in significantly different comparisons despite fluctuations of only 1-2%.

Correlations between other characteristic factors and moisture were also similar from year to year. Generally, moisture appeared most correlated with grain size fractions, showing positive correlation with the finest grain size fraction, and strong negative correlations with the grain size fractions between 425-850 μm and 850-2000 μm in 2016. These correlations are also observed in 2017, with D2 sharing all three, D1 sharing the 425-850 μm, and D3 sharing the negative correlation with the 425-850 μm fraction and the positive correlation with the finer fraction. The one existing disparity between 2016 and 2017 moisture was a weak positive correlation between dsDNA content and moisture in 2016. No correlations were observed in 2017 between moisture and biological measures, however the necessity of water for terrestrial life implies a need for a baseline level of hydration, and the lack of correlations uncovered here imply a diminished impact on biomass or bioactivity at higher or lower moisture levels.

Sediment grain size has proven to be a key characteristic factor influencing biomass and bioactivity in 2016 and 2017. In 2016 grain size < 425 μm displayed positive correlation with dsDNA content, while in 2017 weak positive correlations were observed between ATP and the grain size fractions > 2000 μm, and for D2 positive correlation was observed with the grain size fraction < 425 μm. Negative correlations were observed between dsDNA and the 425-850 μm and 850-2000 μm grain size fractions in 2016, and the 850-2000 μm grain size fraction and ATP at D2 and D3 in 2017. Consistent positive correlations between ATP and the largest grain size in 2017 may suggest that the larger chunks of sediment provide competitive advantages for organisms, or that larger sediment is not considerably influenced by aeolian action. Despite ATP positively correlating with the largest grain size, no correlation was observed between large sediment and dsDNA, highlighting the influence of large grain size on living organisms only. Interestingly, the correlations observed in 2017 provide additional support for the influence of aeolian action in sculpting the surface of the Dyngjusandur plains. For D1 and D3 no correlations are observed between characteristic factors and dsDNA, while positive correlations were only observed for ATP and the largest sediment size. Subsite D2, however, demonstrated positive correlations between ATP and dsDNA and the smallest sediment size. The lack of correlations observed at sites D1 and D3 between these characteristic factors could be attributed to the aeolian action at the site having great influence over fine sediment. Given that all three subsites in 2017 have similar grain size distributions, and that D2 demonstrates correlations between its biological measures and the finest grain size, the unique site heterogeneity at D2 may provide the protection necessary to limit aeolian action in certain areas, allowing microorganisms to thrive in pockets of the finest grain size undisturbed.

Beyond characteristic factors, clear similarities exist in the influence of spatial scale between 2016 and 2017. In 2016, almost no significant differences in pairwise comparisons were found at the 1 m scale, and in 2017 a similar lack of significant differences at the 1 m scale was observed. Notably, the 10 m grouping in 2017 also showed a similar percentage of significant comparisons in comparison to its 2016 counterpart, suggesting that characteristic factor variability may not change considerably from year to year. However, the high variability of ATP at 2017 subsite D1 in contrast to the low variability of dsDNA may suggest that 2017 sites experienced significant turnover in comparison to its counterparts. Furthermore, pairwise comparisons of dsDNA content in 2017 produced slightly fewer significantly different comparisons than in 2016, and lower average biomass was observed for unprotected 2017 subsites D1 and D3. These qualities could suggest that the microbial communities in 2016 were more settled as a result of less frequent or less recent aeolian disruption, leading to more distinct microbial communities. Thus, if recent aeolian activity is suspected at a potential extraterrestrial sampling location, increased sampling frequency may be necessary to capture the variability introduced at smaller scales.

3.5.3 Astrobiological Implications

Many of the trends uncovered during the 2016 Dyngjusandur field campaign, and at sister FELDSPAR analog sites, regarding spatial scale and sample environment were supported by the 2017 sample set. This additional evidence in support of Mars analog trends helps to bolster our understanding of extraterrestrial sampling conditions and informs the considerations that must be made when composing a sampling plan for future missions. While monetary and space limitations may restrict the number of samples that can be included recovered during extraterrestrial missions, this research aims to improve sampling procedure to maximize scientific return.

The results of the 2016 Dyngjusandur expedition had several implications for extraterrestrial sampling. Sampling at 1 m scales and lower was considered to have limited upside given the lack of statistically significant comparisons observed. In contrast, the 10 m spatial grouping had the greatest density of significant comparisons, more accurately capturing the overall site variability. The 100 m spatial grouping saw much of the finer scale variability averaged out, implying the need for additional sampling at smaller spatial scales to fully characterize the site. These results were largely replicated at the 2017 sites where small spatial groupings yielded few differences, while the large groupings omitted important site details. Especially at potential sampling targets with frequent aeolian disruption, more closely grouped samples should be considered to account for increased heterogeneity.

In addition to similarities between 2016 and 2017 with regard to spatial groupings, these two expeditions also demonstrated the importance of sample grain size as a predictive factor for biosignatures. In 2016, a positive correlation was observed between the finest grain size fraction tested and dsDNA, while dsDNA demonstrated negative correlations with the mid-sized fractions (425-850 µm & 850-2000 µm). In 2017, correlations between dsDNA and these grain size fractions were observed at subsite D2, and all three subsites saw ATP correlated with sediment >2000 µm. The increased significantly different comparisons at smaller spatial scales in 2017 implies increased or recent aeolian activity, which may have disturbed the finest sediment size and obscured potential biosignature correlations. This hypothesis is supported by the unique activity observed at D2, which saw positive correlations between the finest sample sizes and dsDNA and ATP when additional wind protection was offered. While not directly related, gravimetric moisture content was also positively correlated with the finest sediment size in 2016, and also negatively correlated with the mid-sized fractions. For sites D2 and D3 in 2017, similar moisture correlations were observed, suggesting that the finest sediment size may be best suited for water retention to support life. In both 2016 and 2017 moisture was shown to display limited correlations with biosignatures, implying that hydration may need to reach a baseline threshold to support life, but additional moisture fluctuations beyond the baseline do not encourage additional growth.

The characteristic factors studied in this work were intended to determine the influence of spatial scale and environmental factors on biosignature quantity. While future extraterrestrial missions may not have the luxury of identifying terrestrial biology, these results aim to showcase trends in habitability that may be replicated by extraterrestrial organisms under similar stresses. Continued analysis of the FELDSPAR team's catalogue of expedition samples will bolster these results and provide additional insights into the habitable conditions of a Mars analog plain. Ultimately, future sampling missions can consider the lessons offered from the Dyngjusandur expeditions to optimize sampling return and sampling efficiency.

3.6 Citations

1. Mustard, J., et al., Report of the Mars 2020 Science Definition Team. 2013.

2. Allwood, A.C., et al., PIXL: Planetary Instrument for X-Ray Lithochemistry. Space Science Reviews, 2020. 216(8): p. 132.

3. Beegle, L., et al., Scanning Habitable Environments with Raman and Luminescence for Organics and Chemicals (SHERLOC) on Mars 2020. Abstracts of Papers of the American Chemical Society, 2019. 257: p. 2.

4. Hayes, A.G., et al., Pre-Flight Calibration of the Mars 2020 Rover Mastcam Zoom (Mastcam-Z) Multispectral, Stereoscopic Imager. Space Science Reviews, 2021. 217(2): p. 95.

5. Perez-Izquierdo, J., et al., The Thermal Infrared Sensor (TIRS) of the Mars Environmental Dynamics Analyzer (MEDA) instrument onboard Mars 2020, a general description and performance analysis. Measurement, 2018. 122: p. 432-442.

6. Wiens, R.C., et al., The SuperCam Instrument Suite on the NASA Mars 2020 Rover: Body Unit and Combined System Tests. Space Science Reviews, 2021. 217(1): p. 87.

7. Lammer, H., et al., What makes a planet habitable? Astronomy and Astrophysics Review, 2009. 17(2): p. 181-249.

8. Moissl-Eichinger, C., C.S. Cockell, and P. Rettberg, Venturing into new realms? Microorganisms in space. Fems Microbiology Reviews, 2016. 40(5): p. 722-737.

9. Preston, L.J. and L.R. Dartnell, Planetary habitability: lessons learned from terrestrial analogues. International Journal of Astrobiology, 2014. 13(1): p. 81-98.

10. Gentry, D.M., et al., Correlations Between Life-Detection Techniques and Implications for Sampling Site Selection in Planetary Analog Missions. Astrobiology, 2017. 17(10): p. 1009-1021.

11. Amador, E.S., et al., Synchronous in-field application of life-detection techniques in planetary analog missions. Planetary and Space Science, 2015. 106: p. 1-10.

12. Rader, E., et al., Preferably Plinian and Pumaceous: Implications of Microbial Activity in Modern Volcanic Deposits at Askja Volcano, Iceland, and Relevancy for Mars Exploration. Acs Earth and Space Chemistry, 2020. 4(9): p. 1500-1514.

13. Sutton, S.M.S., A. C.; Hanna, A. M.; Tan, G. K.; Gentry, D. M.; Cable, M. L.; Rader, E.; Cullen, D.; Geppert, W.; Stockton, A. M.; FELDSPAR Team, Microbial Population and Distribution at Dyngjusandur, Iceland a Mars Analog Alluvial Plain. 2021.

14. Bathgate, E.J., et al., Raman, FTIR and XRD study of Icelandic tephra minerals: implications for Mars. Journal of Raman Spectroscopy, 2015. 46(10): p. 846-855.

15. Kargel, J.S. and R.G. Strom, ANCIENT GLACIATION ON MARS. Geology, 1992. 20(1): p. 3-7.

16. Thordarson, T. and A. Hoskuldsson, Postglacial volcanism in Iceland. Jokull, 2008. 58: p. 197-228.

17. Baratoux, D., et al., Volcanic sands of Iceland - Diverse origins of aeolian sand deposits revealed at Dyngjusandur and Lambahraun. Earth Surface Processes and Landforms, 2011. 36(13): p. 1789-1808.

18. Sara, M.J., Dyngjusandur sand sheet, Iceland, as a depositional analog to the Stimson Fm. in Gale Crater, Mars. p. xii, 145 pages.

19. Arnalds, O., P. Dagsson-Waldhauserova, and H. Olafsson, The Icelandic volcanic aeolian environment: Processes and impacts — A review. Aeolian Research, 2016. 20: p. 176-195.

20. Baker, V.R., et al., ANCIENT OCEANS, ICE SHEETS AND THE HYDROLOGICAL CYCLE ON MARS. Nature, 1991. 352(6336): p. 589-594.

21. Hartmann, W.K. and G. Neukum, Cratering chronology and the evolution of Mars. Space Science Reviews, 2001. 96(1-4): p. 165-194.

22. Hale, L. and D. Crowley, DNA extraction methodology for biochar-amended sand and clay. Biology and Fertility of Soils, 2015. 51.

23. Dunn, O.J., MULTIPLE COMPARISONS AMONG MEANS. Journal of the American Statistical Association, 1961. 56(293): p. 52-&.

CHAPTER 4. LESSONS OF SAMPLING & SAMPLE HABITABILITY AT THE DYNGJUSANDUR, ICELAND, MARS ANALOG FROM 2016-2018

Adapted with permission from: “Lessons of Sampling & Sample Habitability at the Dyngjusandur, Iceland, Mars Analog from 2016-2018” Submitted to Astrobiology Spring 2022 © Mary Ann Liebert, Inc.

4.1 Abstract

From 2016 to 2018, the FELDSPAR team visited the Dyngjusandur, Iceland, Mars analog plains to characterize the importance of spatial separation and abiotic measurements for extraterrestrial sampling protocols and the predictivity of biosignatures. The FELDSPAR team has approached analog sampling with the goal of emulating the protocols and instruments available on board the Mars 2020 Perseverance Rover so as to inform future missions and optimize science return. The Dyngjusandur plains are primarily comprised of fine basaltic tephra, ideal for investigating biological variability at visually homogenous sampling sites. In 2018, the Dyngjusandur sampling site was selected to overlap one from 2017, enabling for year-to-year comparisons of patterns in biosignature variability and habitability. Samples were collected using a schematic of nested triangles established during previous field campaigns, designed to allow for statistical comparisons between samples at multiple spatial scales. As with prior expeditions, characteristic factors analyzed for each sample included: ATP, dsDNA, gravimetric moisture content, and grain size composition. Data from 2016-2018 was analyzed to identify shifts in these

characteristic factors over time and the dependance of their relationships on spatial groupings and environmental factors. Aeolian action was found to be a primary source of biosignature variability at Dyngjusandur, with biomass content increasing at sampling sites with environmental protection from the wind. Grain size fractions were also influential for bioactivity and biomass with both ATP and dsDNA positively correlating with larger sediment grains. Samples collected with 10 m of separation were most likely to be significantly different, while samples separated by 1 m were found to be statistically similar. Samples collected at 100 m of separation were often significantly different, however more comparisons are necessary to characterize the variability of biosignatures at larger scales. This work provides additional evidence to influence our interpretation of the 2016 and 2017 Dyngjusandur data, and the patterns uncovered over three years of study serve as a starting point for characterization of the Mars analog.

4.2 Introduction

With the Mars 2020 Perseverance Rover landing in February 2021, a renaissance in Astrobiological interest has occurred. Previous missions to Mars and recent remote sensing work of its surface geochemistry have provided evidence for water on Mars, an essential characteristic of life as we know it, and the Perseverance Rover was designed with the intention of characterizing the Martian environmental conditions, geochemistry, and signs of potential biosignatures [1, 2]. The instruments on board the rover measure environmental characteristics, geochemistry, and subsurface structures (SuperCAM, PIXL, SHERLOC, MEDA, and RIMFAX), and conduct site and sample photography (Mastcam-Z) [3-8]. Based on these analyses, the rover also will cache samples for future recovery and return for future analysis, carrying 43 sampling containers, and a stated goal of collecting a minimum of 20 samples [9]. The limited sampling capacity highlights the importance of informed sample selection when attempting to return samples with the highest possible science return, and also highlights the importance of understanding how to predict the best samples for return based on these techniques. With these concerns in mind, the Field Exploration and Life Detection Sampling for Planetary and Astrobiology Research (FELDSPAR) team has visited Icelandic Mars analog locations annually since 2013, emulating the protocols performed by the Perseverance Rover to determine the most effective sampling approach for returning habitable samples [10-15].

The vast amount of time and money required for NASA's flagship missions represent a tremendous investment that must be addressed with careful planning. Space and weight limitations on rovers and landers requires that instruments must be selected with practicality in mind, and gold standards of the analytical chemistry world, such as mass spectrometry, must undergo significant innovation before they are applicable for extraterrestrial missions. Limited consumables and sometimes mission duration make sampling limited, which highlights the need for careful sample selection. These constraints make analog research a critical step for informing future missions, providing researchers the opportunity to characterize the sampling conditions at locations similar, in some ways, to prospective Martian targets [16-20]. An ideal analog location should include many of the variables that sculpt the target environment, and Icelandic lava fields are home to many notable characteristics that have similarities to our understanding of the Martian surface. In particular, the sandy plains of basaltic tephra of Dyngjusandur, Iceland, have been revisited from 2016-2019 by the FELDSPAR team for their glacio-volcanic history, remoteness from anthropogenic activity, frequent dust storms, limited available nutrients and moisture, and harsh climate. Previous geochemical analysis at the Dyngjusandur surface also revealed similarities between Dyngjusandur basalts and Martian basalts, presenting parallels in the high percentages of Fe_2O_3 and MgO [21-25]. In addition to these qualities, the plains of Dyngjusandur were typically relatively visually and morphologically homogenous, with fine sediment dominating the surface composition. While larger chunks of lava were infrequently dispersed at most Dyngjusandur plains, primarily heterogenous sampling locations were also visited as a point of comparison. Most research performed at Dyngjusandur has been geological in nature, however biochemical assays present the opportunity to directly map the distribution of bulk biosignatures under the paradigms of the Mars analog. Even though terrestrial biosignature measurements are not necessarily indicative of how life may have manifested on Mars, further understanding of the qualities that make a sample habitable could reveal abiotic measurements predictive for identifying sample candidates most conducive to life as we know it.

In 2018, the FELDSPAR team returned to Dyngjusandur for their third visit [14, 15]. Previous field campaigns in 2016 and 2017 helped to standardize the experimental approach employed in 2018, and the 2018 sampling site was selected to overlap with 2017 subsite 3, enabling direct comparisons over the course of a year. All expeditions to Dyngjusandur have attempted to emulate the protocols of the 2020 Perseverance Rover, from photography to spectroscopy. Sites were mapped using aerial quadcopter imaging, and higher resolution photos of each site were taken prior to sampling. Near infrared (NIR) and x-ray fluorescence (XRF) spectra were collected in situ for each sample, and sediment was collected from each site and returned to the lab for analyses of biomass (double stranded DNA) and bioactivity (adenosine triphosphate). Sampling sites were structured using a schematic of nested triangles, providing each sample two points of comparison, and allowing for groupings to monitor how biosignature quantity shifts spatially. In addition, the moisture content of each sample was determined as well as the grain size composition to determine the effects of these sample characteristics on biosignature distribution.

This work addresses the results from the FELDSPAR 2018 Dyngjusandur expedition, and the trends uncovered from three years of Dyngjusandur sampling. Biosignature and environmental values were compared at multiple spatial groupings to characterize the variability of each factor and assess potential correlations. Trends observed in the 2018 sample set were compared with those uncovered in 2016 and 2017, allowing for observations regarding aeolian disruption and comparisons of site paradigms. Ultimately, this work aims to outline lessons learned from this temporal study, attempting to characterize the Dyngjusandur analog to inform sampling plans on future extraterrestrial, and terrestrial, missions.

4.3 Methods – Sampling, Assays, & Analysis

4.3.1 Site Selection, Mapping, and In Situ Analysis

The FELDSPAR team returned to the Dyngjusandur plain in June 2018, approximately one year following the 2017 expedition [15, 26]. A single sampling site was mapped in 2018, centered at the same location as Subsite 3 in 2017, and southwest of the sampling sites in 2016 [15, 26]. Year-to-year GPS coordinates for the Dyngjusandur sampling sites are given in Table 1. As with previous Dyngjusandur campaigns, the 2018 sampling site was structured as a 100 m equilateral triangle, with nested equilateral triangles at each apex at a series of smaller spatial scales ranging from 10 m to 0.1 m (Figure 1). Qualitatively, the 2018 sampling site appeared to change little from 2017, with the sampling sites being visually and morphologically similar. Large lava rocks were uncommonly dispersed at the 2018 sampling site, with the uppermost layers of sediment composed primarily of a fine black sand. The 2018 site was mapped and photographed using a DJI Inspire 1 Quadcopter, and sampling locations were identified with tarps and flags to denote spatial groupings of interest.

Following initial mapping and site photography, the top 1 cm of sediment was removed from the surface of each sampling location and analyzed with a portable visible near infrared (VNIR) ASD spectrometer and x-ray fluorescence spectrometer. Like the spectroscopic data from previous years, the 2018 spectral measurements will be analyzed alongside biological measurements in a sister manuscript to determine geochemical influences that may be the most predictive of habitability at Mars analog locations. Once spectral analysis was completed, 50 mL conical tubes were filled with sediment from each sampling site and each sample was assigned a barcode for downstream sample identification and processing. Samples were gathered in an a manner to limit anthropogenic contamination. Field researchers were equipped with gloves, masks, and non-linting arm sleeves, and considerations were made to ensure samples were gathered downwind of the other sites. The collected samples were returned to the University of Akureyri for ATP quantification and storage. At the end of the field campaign, samples were shipped to the Georgia Institute of Technology and maintained at -80 ^{o}C for additional investigation.

Table 4-1. Dyngjusandur Expedition GPS Coordinates 2016-2018

Campaign Season	Subsite 1	Subsite 2	Subsite 3
2016	*64.95^{o}N, 16.62^{o}W*	*64.95^{o}N, 16.64^{o}W*	
2017	*64.93^{o}N, 16.72^{o}W*	*64.94^{o}N, 16.71^{o}W*	*64.93^{o}N, 16.69^{o}W*
2018	*64.93^{o}N, 16.69^{o}W*		

*Coordinates represent the center point of each 100 m triangle.

4.3.2 Characteristic Sample Factors

4.3.2.1 Environmental Factors (Moisture Content & Grain Size Fractions)

At Georgia Tech, samples were aliquoted in triplicate into glass vials under sterile conditions. Sample vials were loosely covered with foil to allow moisture to escape while preventing cross contamination during heating and were placed in an oven at 100 ^oC for 24 hours. After drying, sediment mass was measured, and compared with the amount of moisture lost to obtain gravimetric moisture content (mass of moisture / mass of dry sediment). Each dried sample was then separated into four fractions by dry sieving. Fractions captured include large sediment bigger than 2000 µm, mid-sized sediment between 850-2000 µm and between 425-850 µm, and fine sediment less than 425 µm. The mass of each sample fraction was compared with total sample mass to determine the percent composition of each fraction.

4.3.2.2 Biological Factors (Biomass & Bioactivity)

Two biological assays were performed to quantify biomass and bioactivity respectively. Bioactivity measurements were collected immediately at the University of Akureyri following sample collection using adenosine triphosphate (ATP) as an indicator as previously described [14, 15]. Briefly, samples were aliquoted in triplicate into 1 mL centrifuge tubes, and ATP was quantified using the Roche HSII ATP Bioluminescence Assay Kit (Roche Diagnostics LTD, Basel, Switzerland) following the manufacturer specifications. Samples were suspended in Tris-EDTA buffer (100 mM, 4 mM EDTA) and then cells were lysed in a boiling water bath for 2 minutes. Luciferase reagent was added to each sample, and a HY-LiTE 2 luminometer (Merck, International LTD, Radnor, PA) was used to quantify ATP with respect to kit standards.

Given its relative stability, double stranded DNA (dsDNA) content was determined upon return to Georgia Tech as a measure of bulk biomass again, as previously described [14, 15]. Aliquoted samples were prepared in triplicate and dsDNA was extracted from each using a DNeasy PowerLyzer PowerSoil Kit (Qiagen, Hilden, Germany) with protocol adjustments for low biomass samples [27]. Extracts were quantified using a Qubit dsDNA High Sensitivity Assay and a Qubit fluorimeter (Thermo Fisher, Waltham, MA) against kit standards.

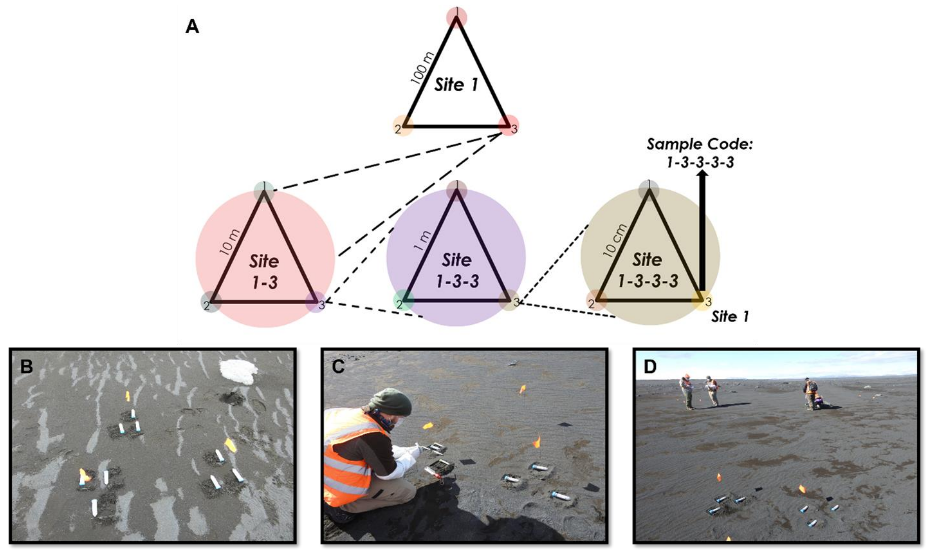

Figure 4-1 – Dyngjusandur 2018 Expedition. *A) Sampling Site Schematic: the 2018 sampling site was structured as a series of nested equilateral triangles. A single 100 m triangle was mapped, the corners of which were composed of 10 m equilateral triangles. Each corner of the 10 m triangles was composed of 1 m triangles, continuing with more refined groupings to a scale of 0.1 m. A barcode was generated for each sample for spatial identification. B) 2017 Subsite 3: subsite 3 in 2017 shares the same GPS coordinates as the sampling site in 2018. C) 2018 Sampling Site: samples being exhumed and placed in conical tubes. Qualitatively similar to the same site in 2017. D) 2018 Sampling Site Full: the greater 2018 sampling site was primarily visually and morphologically homogenous. Larger chunks of lava were infrequently dispersed.*

4.3.2.3 Statistical Analysis

Statistical analysis and plotting were performed in R studio. Like the previous FELDSPAR work at Dyngjusandur, a series of pairwise tests were leveraged to determine the frequency of statistically significant variation in each characteristic factor at each spatial scale [11, 13-15]. Both pairwise T-Tests and pairwise U-Tests were performed to account for normal and non-normal distributions based on a 95% confidence interval, and samples were grouped depending on the spatial scale of interest [10, 11]. P-values for each comparison were adjusted with Bonferroni corrections [28]. At the 1 m scale, daughter 10 cm triangles at each apex were compared against each other considering each characteristic factor. The number of significant comparisons at each scale was compared against the total number of comparisons to determine the percentage of statistically significant differences between groupings of 100 m, 10 m, and 1 m, were analyzed.

In addition to pairwise comparisons, correlations were determined between the characteristic factors using Spearman's rank correlation coefficients. Correlation matrices were generated displaying positive or negative correlations when the respective p-value was less than 0.1.

4.4 Results

4.4.1 Confluence of Environmental & Biological Factors

Of the FELDSPAR expeditions to Dyngjusandur, the 2018 field campaign considered the smallest sampling site, composed of a single 100 m equilateral triangle. Previous Dyngjusandur sites were composed of two 100 m triangles in 2016 and three 100 m triangles in 2017 and these previous sampling locations were separated by about 4 km. The 2018 sampling site it uniquely positioned for close comparison with 2017 subsite 3, allowing for clearer interpretation of temporal trends. Samples were recovered with spatial groupings of 10 m, 1 m, and 0.1 m, and, for ease of interpretation, 2018 characteristic factors are grouped at the 1 m scale when presented as 10 m subsites.

4.4.2 Biomass & Bioactivity

Biomass and bioactivity were estimated for each sample using dsDNA and ATP as indicators. On average, 22.7 (±26 standard deviation) ng dsDNA / g sediment was recovered from each sample, while average ATP was $2.1\text{x}10^{-10}$ ($\pm 1.9\text{x}10^{-10}$ sd) g ATP / g sediment per sample. As the large standard deviation values suggest, both biomass and bioactivity were highly variable, and their respective boxplots showed a large number of densely populated samples particularly at the second 10 m triangle (Figure 4-2).

Pairwise T-Tests and U-Tests were performed on dsDNA and ATP at spatial groupings of 100 m, 10 m, and 1 m (Table 4-2). While the two tests showed slight variations in the number of significant differences observed for each grouping, the same general trend was observed for each. At 1 m of separation, 0% of comparisons were significantly different for both ATP and dsDNA. A large increase in significant differences was observed when grouping these characteristic factors at the 10 m level. ATP displayed 22% significant differences while dsDNA displayed 11% significant differences in comparisons between groupings at the 10 m level based on pairwise T-Tests and U-Tests. The 100 m grouping continued to show a large percentage of significant differences comparisons, with the pairwise T-Tests showing 67% significant differences for dsDNA and 67% for ATP. While the U-Tests still suggested high variability at the 100 m scale, an uptick in significant differences was not observed from 10 m to 100 m as both dsDNA and ATP maintained 33% significant differences.

4.4.3 Environmental Factors

The gravimetric moisture content and grain size composition was determined for each sample to characterize the habitat and identify potential influences on dsDNA and ATP (Figure 2). Across the full site, 7.3% (±3% sd) moisture was the average moisture surveyed. Grain size compositions were distributed such that the bulk of each sample was composed of the finest sediment, with sediment smaller less than 425 µm composing an average of 72% (±10% sd) of each sample. The mid-sized sediment fractions were also abundant, with sediment between 425-850 µm representing an average of 16% (±7.2% sd) of each sample and sediment between 850-2000 µm representing an average of 7.5% (± 4% sd). In contrast to the biological factors, moisture content experienced less variability within each sample as indicated by each boxplot only encompassing a moisture range of about 5%. Grain size was most variable when considering the two most abundant fractions (< 425 µm and 425-850 µm). The finest sediment fraction composed 60-80% of a sample, and the interquartile range of the fraction between 425-850 µm usually fell within 10-25% of a sample. The largest two grain size fractions consistently represented less than 10% of a sample with tight interquartile ranges, however these two fractions also experienced more outliers.

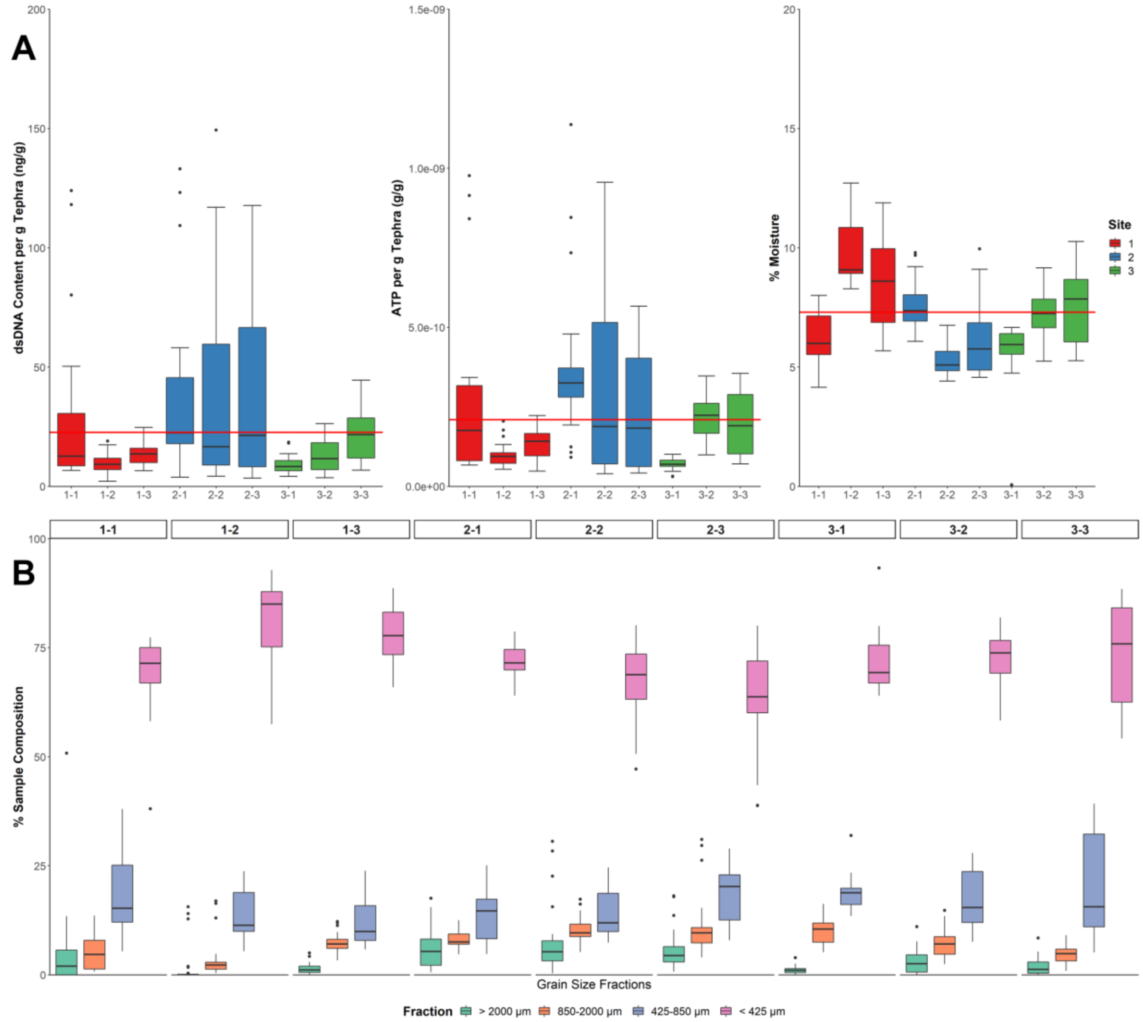

Figure 4-2 – 2018 Dyngjusandur Characteristic Factors. *A) dsDNA Content (ng / g sediment), ATP content (g / g sediment), and Gravimetric Moisture Content (g moisture / g dry sediment) with 1 m groupings. Colors represent each parent 10 m triangle. B) % Grain Size Fractions: > 2000 µm, 850-2000 µm, 425-850 µm, and < 425 µm. Samples are grouped at the 1 m level, and colors are representative of each fraction.*

Moisture content was also evaluated by pairwise testing and followed similar trends as the biological factors (Table 2). No significant differences were observed when comparing samples at the 1 m grouping, and a dramatic increase was observed at the 10 m grouping (33% for pairwise T-Test, 33% for pairwise U-Test). Unlike the other characteristic factors, a further increase in significant differences was not observed at the

100 m grouping, with 33% different comparisons based on pairwise T-Tests and 33% different comparisons based on pairwise U-Tests.

Table 4-2. Pairwise Testing of Characteristic Factors

	Pairwise T-Test			**Pairwise Mann-Whitney-U**			
	2018			***2018***			
Separation	**100 m**	**10 m**	**1 m**	**100 m**	**10 m**	**1 m**	
DNA Content	67%	11%	0%	33%	11%	0%	*Significant Pairwise Comparisons*
ATP	67%	22%	4%	33%	22%	0%	
% Moisture	33%	33%	0%	33%	33%	0%	

**Separation indicates the grouping considered within the nested triangular schematic. Statistically significant comparisons were determined based on a 95% confidence interval. At each grouping, the number of significant comparisons was compared to the total number of comparisons to determine the percentage of significant tests.*

4.4.4 Correlation Testing

Correlation coefficients and p-values were determined for each pair of characteristic factors and used to generate a correlation matrix to aid in identifying potential relationships (Figure 3). Biological factors (dsDNA & ATP) followed nearly identical trends. Both dsDNA and ATP were strongly positively correlated with each other, and they were both also strongly correlated with the largest sediment size (> 2000 µm). The biological factors also shared the same weak negative correlation with the grain size fraction ranging from 425-850 µm. Moisture was not correlated with either biological factor, but it experienced negative correlations with the mid-sized sediment fractions (425-850 µm & 850-2000 µm) and a strong positive correlation with the finest sediment size. Generally, the sediment fractions were negatively correlated with two exceptions. First, the largest sediment size and the next largest size (850-2000 µm) were positively correlated, and second, the two mid-sized fractions shared no correlation. The finest sediment fraction showed increasingly strong negative correlations starting with the largest sediment size and decreasing in size sequentially.

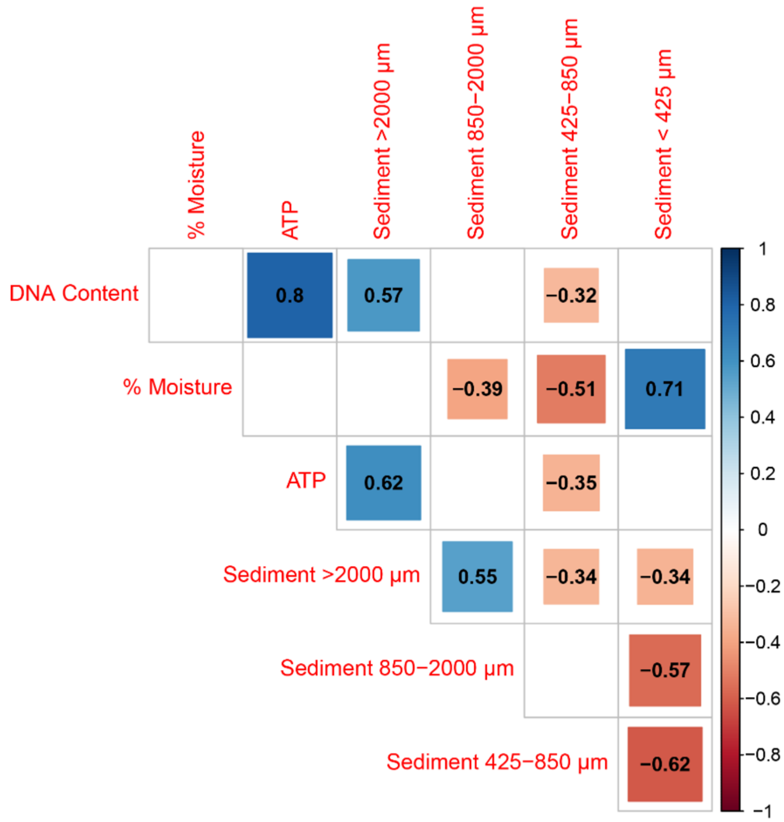

Figure 4-3 – Dyngjusandur 2018 Correlation Matrix. *Correlations were determined between characteristic factors using Spearman's rank correlation coefficients (overlayed on the matrix). Positive correlations are in blue, while negative correlations are displayed in red. Significant correlations were determined based on a 90% confidence interval, and insignificant correlations were left blank.*

4.5 Discussion

4.5.1 Trends at Dyngjusandur from 2017 to 2018

One of the most fascinating qualities of the 2018 Dyngjusandur sampling site is its close proximity to 2017 subsite 3. Both sites share the same central GPS coordinates, and the 2018 site is rotated such that the vertices of the 2018 100 m equilateral triangle fall near the edges of the 2017 100 m triangle (Figure 4A). While a key characteristic of 2017 subsite 3 was its visual homogeneity across the entire sampling site, the 2018 sampling site had a greater density of large lava chunks dispersed at the second 10 m triangle (18-1-2). Previous FELDSPAR work at Dyngjusandur 2017 subsite 2 has shown large lava chunks to be an indicator of biological variability, potentially indicating that larger sediment provides habitation advantages for microorganisms under extreme stress conditions [15]. This hypothesis is particularly relevant given the frequent sandstorms experienced by the Dyngjusandur plains causing continual resurfacing of the top levels of sediment. In 2017, subsites 1 & 3 were lacking in significant wind protection, while subsite 2 contained large lava chunks in abundance, and when interrogated, subsite 2 was found to have the samples with the greatest biomass content and also the greatest range of dsDNA measurements [15]. Thus, while the characteristic factors tested in 2018 display sitewide averages similar to those observed in 2017, the unique distribution of site 18-1-2 was worth additional consideration (Figure 5). For both dsDNA and ATP, the box and whisker plots for 18-1-2 displayed a much wider range of outcomes in comparison to its sister 10 m triangles (18-1-1 & 18-1-3). Several outlier values for 18-1-1 reached similar maximum thresholds of dsDNA and ATP when compared to 18-1-2, however excluding outliers reveals a much smaller range of measurements for 18-1-1.

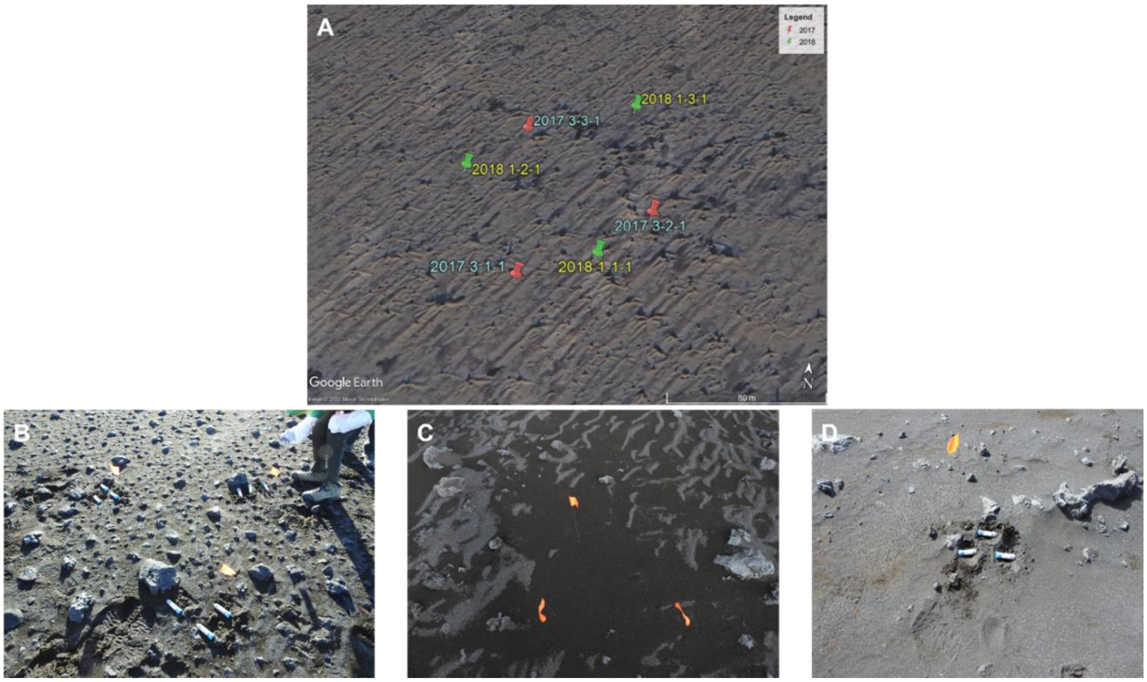

Figure 4-4 – 2017 vs. 2018: Spatial Separation & Visual Comparison. *A) 2017 and 2018 Sampling Sites: a visual representation of the proximity between the 2017 and 2018 sampling sites. B) 2017 Subsite 2: in field photography of a 1 m triangle sampling site from 2017 subsite 2. Large chunks of lava were abundant. C) 2017 Subsite 3: in field photography of a 1 m triangle sampling site from 2017 subsite 3. Large chunks of lava were infrequent and surrounding the sampling sites. D) 2018 Site 18-1-2: in field photography of a 1 m triangle sampling site from the second 10 m triangle in 2018. Large lava chunks were frequent, and nearly in contact with the sampling area.*

Revisiting the site photography from the 2018 expedition, visual similarities were uncovered between 18-1-1 and 18-1-3 and subsite 3 from 2017. Larger basaltic stones often surrounded these sampling sites but did not infringe on the sampling area (Figure 4C). In contrast, 18-1-2 was found to be nestled amongst the larger rocks, with samples nearly in contact with the rocks in some cases (Figure 4D). Given the similar biosignature distributions observed at 2017 subsite 2 and 18-1-2 and the proximity of each site to large lava, this work provides additional evidence to support the hypothesis that aeolian action can limit the habitability of non-sheltered sediment plains.

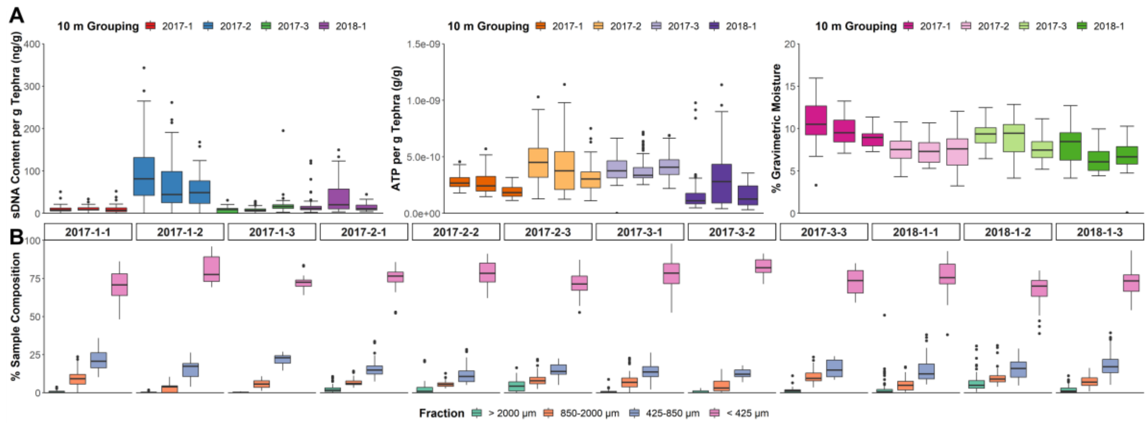

Figure 4-5 – 2017 vs. 2018 Characteristic Factors. *A) dsDNA content per g Tephra (ng/g), ATP content per g Tephra (g/g), and percent gravimetric moisture content per sample. Sites are displayed with 10 m groupings, and colors representative of each grouping. B) % Grain Size Fractions: > 2000 µm, 850-2000 µm, 425-850 µm, and < 425 µm. Samples are grouped at the 10 m scale, and each color is representative of a different fraction.*

Analysis of the 2017 sample set also revealed a distinct set of correlations between characteristic factors for each 100 m triangle. While only a single 100 m correlation matrix was possible in 2018, correlations were observed that mirrored the data from the previous year. In 2017, subsites 1 and 3 showed no dsDNA correlations, while subsite 2 showed a strong positive correlation between ATP and dsDNA. The lack of correlation between ATP and dsDNA at subsites 1 and 3 was attributed to the susceptibility of these locations to aeolian disruption, suggesting a significant portion of the uncovered dsDNA content originated from non-metabolizing organisms. Conversely, the strong positive correlation of ATP and dsDNA at subsite 2 was attributed to wind protection offered by frequent lava rocks, implying that dsDNA was potentially primarily recovered from metabolizing organisms. At all three sites, ATP was positively correlated with the largest sediment fraction, suggesting this fraction may provide some wind protection in otherwise barren plains.

The 2018 sampling site represented a unique confluence of the site profiles studied in 2017, with a greater mix of lava across the sampling areas. Sitewide, correlations were uncovered in the 2018 data that matched many of the trends observed at 2017 subsite 2 (Figure 3). In the 2018 set, a strong correlation was observed between dsDNA and ATP, likely resulting from the congruent spikes in dsDNA and ATP content at 18-1-2. As observed in 2017, the 2018 site also had a positive correlation between ATP and the largest sediment size, but unlike the sites in 2017, dsDNA was also positively correlated with the largest sediment size. Despite the scarcity of large sediment among the fine sediment prevalent at Dyngjusandur, when present it continued to represent a haven for organisms. Larger sediment may provide greater surface area for community networking, ideal porosity for organism habitation, or it may rebuff some wind activity allowing the microbiome to mature undisturbed, making it ideal for colonization in comparison to the finer sediment in the majority. The 2018 correlations also showed parallels to 2017 subsite 2 with its strong positive correlation between fine sediment and moisture, and inverse correlations between the finest sediment fraction and the larger sediment fractions. However, a clear disparity was observed between the correlations at these sites, as 2017 subsite 2 showed positive correlations between the biosignatures at the finest sediment fraction, while no correlations were observed with these factors in 2018 or at 2017 subsites 1 and 3. Visual inspection suggests that the 2017 site was home to a greater density and abundance of large stones than all other sites surveyed, potentially providing enough shelter to protect even the finest sediment from aeolian disruption. While the 2018 site had more large lava rocks than its 2017 counterpart, it may be dispersed infrequently enough that it does not afford the same degree of protection to finer sediment, or the less protected sites 18-1-1 and 18-1-3 are obscuring the effects of environmental shelter primarily observed at 18-1-2.

Pairwise comparisons have been a means of comparing biosignature variability with respect to spatial scale for all previous Dyngjusandur sample sets. Determining the percentage of significantly different comparisons at each spatial scale helps define the distance between sample sites where visually homogenous samples are likely to deviate in biosignature content. The 2018 sample set displayed nearly identical trends to those identified in 2017, and both pairwise T-Tests and pairwise U-Tests followed similar patterns with slight variations in the abundances of significant comparisons. At the 1 m scale, fewer than 5% of comparisons were considered significantly different in the characteristic factors tested (dsDNA, ATP, and percent gravimetric moisture). At 10 m of separation, samples displayed a dramatic increase in variability, ranging from 11-78% significantly different comparisons in 2017, and 11-33% significant comparisons in 2018 based on pairwise T-Tests. The percentage of significantly different comparisons increased again at sample separation of 100 m, with the percentage of significantly different comparisons ranging from 0-67% in 2017 and 33-67% in 2018. On average, the 10 m scale represented the smallest scale tested with the greatest chance to recover unique samples.

4.5.2 Dyngjusandur Harmony: 2016-2018 Lessons Learned at the Mars Analog

4.5.2.1 2016 Site Introduction & Dyngjusandur Temporal Overviw

The 2016 expedition was the first time the FELDSPAR team visited the Dyngjusandur plains, and two 100 m nested triangular sites separated by 1 km were established [14]. These sites were situated approximately 4 km northeast of the 2017 and 2018 Dyngjusandur sampling sites, however site homogeneity and sediment morphological similarity were considered for each field campaign. Dyngjusandur experiences frequent sandstorms originating from southern katabatic winds, and wind patterns established in previous work suggest the FELDSPAR 2017 and 2018 sampling sites to be located in the central area of wind activity [21]. In contrast, the 2016 site falls further downwind, potentially exposing it to different levels of aeolian interaction.

Similar characteristic factors have been gathered from year to year at Dyngjusandur to allow for consistency during analysis. Measures recorded across all three years include gravimetric moisture, dsDNA content, and grain size fractions. In 2016, bacteria-specific qPCR primers were used to determine the amount of DNA recovered from bacterial organisms, however this assay was replaced with ATP bioluminescence to uncover metabolic activity in 2017 and 2018. The 2016 data set also included 16S amplicon sequencing results revealing the most prevalent phyla across one of the 100 m sampling sites, and a small depth profile series to directly test the relationship between biomass abundance and aeolian resurfacing.

4.5.2.2 Sampling & Spatial Distribution

An ongoing area of focus for all three years of Dyngjusandur expeditions has been determining the most efficient way to sample at a Mars analog location to characterize the site while achieving the greatest science return. To approach this issue, the nested triangular sampling scheme was employed and used across all three years at Dyngjusandur, and its barcoded system was invaluable for identifying site trends and highlighting spatial groupings with high variability. Leveraging this system enabled pairwise comparisons of biological characteristic factors and moisture to identify the frequency of statistically significant measurements. Generally, samples recovered from small spatial intervals were more likely to be considered statistically similar, with few significantly different comparisons across all sites and all characteristic factors at the 1 m grouping. For all three years, 10 m of separation between samples consistently resulted in statistically significant differences, despite site differences spatially and morphologically. In 2016, the 10 m scale yielded a range of 22-44% significant comparisons, 2017 had a range of 11-78%, and 2018 had a range of 11-33%. Moving beyond the 10 m scale, the 100 m scale yielded both a large percentage of significantly different comparisons and also instances of no significant differences. However, the comparisons at the 100 m scale only considered three comparisons per subsite, one pair for each set of 10 m triangles, so variability may be masked by the limited number of outcomes. The 2017 expedition represented the only opportunity to compare the characteristic factors of multiple 100 m triangles, and the T-Test found 67% significant differences (2 out of 3) when considering ATP, and 100% significant differences (3 out of 3) when ccomparing gravimetric moisture. Comparisons of dsDNA at 1 km of separation yielded 33% significant comparisons (1 out of 3) based on T-Test, while U-Test found the dsDNA statistically similar across all three subsites.

The results of these pairwise tests revealed several trends. Interestingly, both the biological factors and moisture appeared to show similar percentages of significant differences at each scale and the number seemed to increase similarly as spatial scales increased. These observations, and the high degree of similarity maintained across three years, suggest that 10 m of distance between samples provides a "sweet spot" for finer scale sampling, allowing for more comprehensive site characterization without oversampling at smaller, less variable scales. Sampling at distances of 100 m or greater may produce unique communities, but the extent of characteristic factor variability between sampling locations may be lost.

4.5.2.3 Consequences of Aeolian Action

An intrinsic element of the Dyngjusandur sampling sites has been continual resurfacing by aeolian action. Previous depth profiling analysis in 2016 revealed higher biomass levels several centimeters below the surface of the sampling area, implying the stabilization of the microbial community when sheltered from the wind. The impact of these winds was observed again in 2017 at subsite 2, where high densities of biomass were identified and attributed to shelter provided by frequently dispersed large lava rocks. The environmental shelter observed at 2017 subsite 2 appeared to encourage pockets of habitability, as indicated by the vast range of biomass measures encompassed by the 10 m grouping. Additional evidence was uncovered in 2018 that provided support for the hypothesis of localized areas of habitability, as the second 10 m triangle in 2018 fell amongst large stones and displayed a dsDNA distribution that mirrored the one observed in 2017 (Figure 4-6). Of note, the 2016 sampling sites displayed the highest average biomass content with relatively small standard deviations, and as a combined site, dsDNA content displayed a significant positive correlation with the finest sediment size. This is particularly relevant as the only other site displaying a positive correlation between the finest grain size fraction and biomass was 2017 subsite 2, however, the correlation observed in 2017 was attributed to wind protection while the 2016 sites were unprotected. Thus, the 2016 site may have experienced less turnover resulting in fewer significant pairwise comparisons and greater stability of the finest sediment fraction.

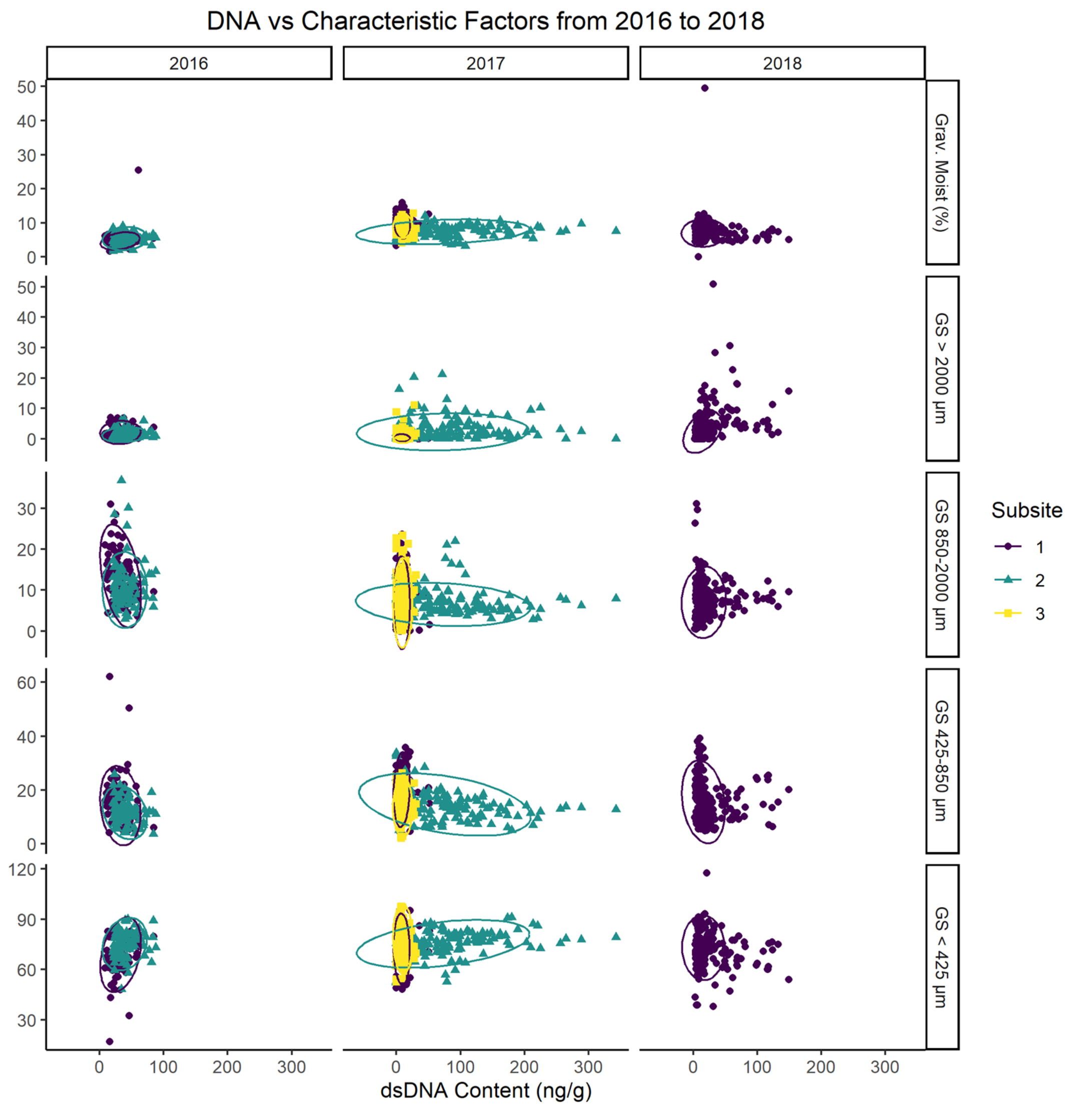

Figure 4-6 – Distributions of DNA Content Over Time. *For each year of data, dsDNA was plotted against each other characteristic factor: gravimetric moisture and grain size fractions. ATP was excluded from this figure given its lack of collection in 2016. Each color represents a 100 m triangle (subsite), and ellipses were plotted to encompass trends of significance**.***

4.5.2.4 Characteristic Factor Relationships

Each year, characteristic factors were measured and compared against each other with different spatial groupings to identify biological and environmental trends relevant over the course of three years. Of primary interest were the correlations related to biomass and bioactivity, informing future extraterrestrial missions of the impacts of grain size distribution and moisture on habitability (Figure 4-6). Biomass (dsDNA) was found to display few correlations, showing a single weak correlation with moisture in 2016, strong positive correlations with ATP for 2017 subsite 2 and 2018, and positive correlations with the finest sediment fraction (< 425 μm) in 2016 and at 2017 subsite 2. While biomass lacked consistent correlations from site to site, ATP displayed a single positive correlation with the largest sediment size at each site. These patterns make several implications about habitability at this Mars analog. In 2017 and 2018, correlations were only observed for dsDNA when the sampling site was afforded environmental protection from wind disruption. Given the lack of protection at the 2016 sites, and the biomass correlations uncovered, aeolian action may have been more infrequent in 2016 allowing for more established communities in finer sediment. This hypothesis is further supported by the positive correlations between ATP and the largest sediment size, and a lack of correlations between ATP and the finest sediment (Figure 4-7). ATP represents the presence of active metabolism and degrades at ambient conditions, suggesting that positive correlations observed with ATP and grain size likely represent the localization of living organisms to specific grain size fractions. Furthermore, positive correlations between DNA and ATP were only observed when environmental protection was available, and positive correlation between ATP and the finest sediment size at 2017 subsite 2 imply that the additional protection allowed for expanded colonization of the sampling area.

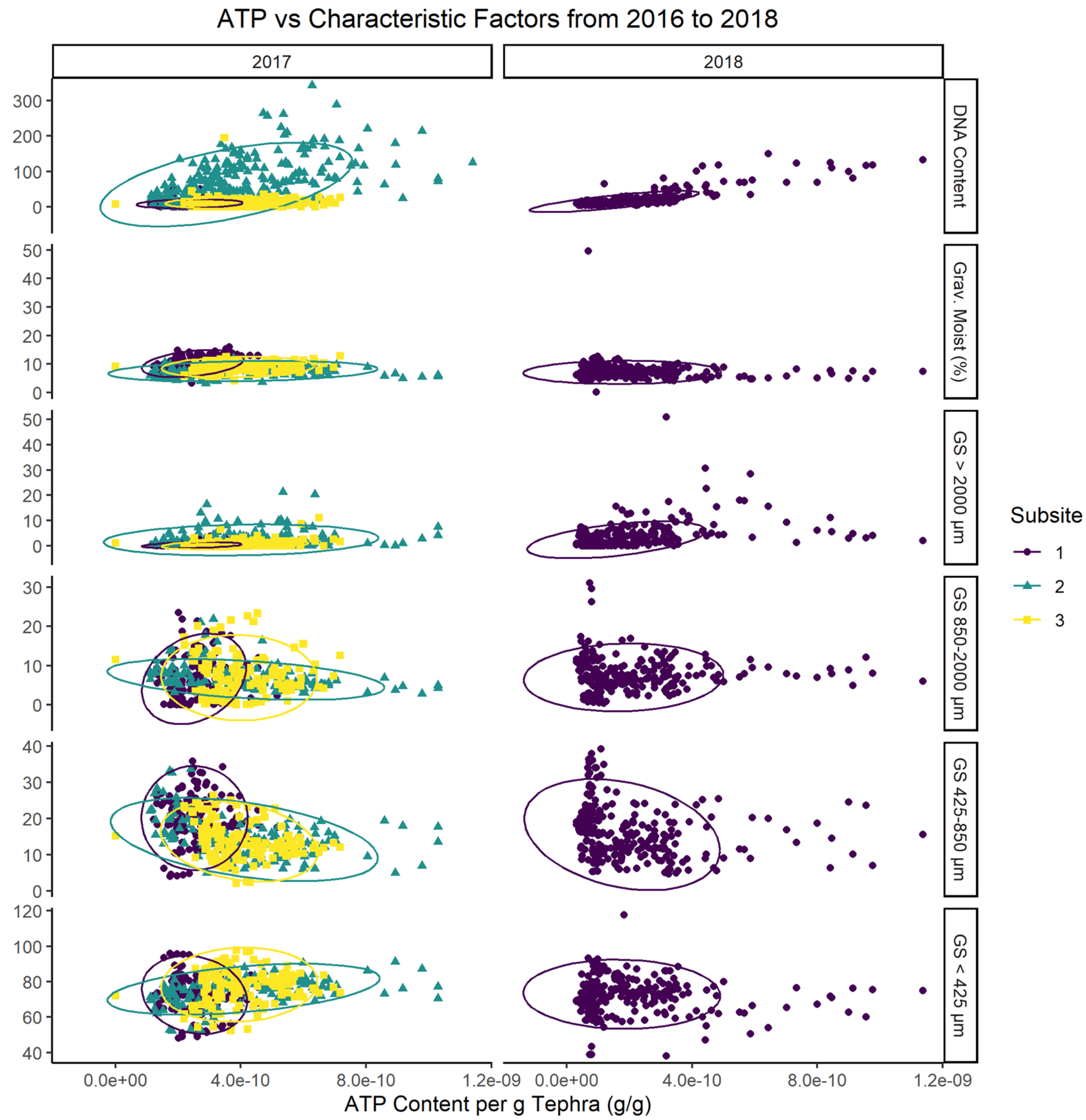

Figure 4-7 – Distributions of ATP Content Over Time. *For each year of data, ATP was plotted against each other characteristic factor: dsDNA, gravimetric moisture, and grain size fractions. Each color represents a 100 m triangle (subsite), and ellipses were plotted to encompass trends of significance.*

Measures of biomass and bioactivity often correlated with different grain size fractions, however correlations with moisture were rare, and the moisture correlations observed were weak. Moisture is a known requirement for terrestrial life, making its lack of biological correlations noteworthy. Despite a lack of meaningful correlations, moisture appeared to be an important quality of the Dyngjusandur sites, as consistent levels of moisture were observed across all three years. Gravimetric moisture ranged from approximately 5-15% at all sites, and while statistically significant spatial groupings were identified for moisture, the vast majority of samples fell within the relatively small range of moisture measures. Thus, consistent low levels of moisture appear to be an important quality for life at Dyngjusandur, however small fluctuations in moisture do not seem to increase or decrease the habitability of a sample.

4.5.3 Implications for Astrobiology

This work aims to inform future extraterrestrial missions through the characterization of habitable conditions at a Mars analog lava field shaped by glacial and aeolian activities. Through three years of study, analysis of the Dyngjusandur plains has provided key environmental data related to biosignature distribution to influence sample planning for missions to similar targets. While this work has focused on terrestrial biosignatures, dsDNA and ATP, as indicators of microbial distribution, extraterrestrial life may use different methods of information storage and metabolism. For this reason, the campaigns to Dyngjusandur have focused on identifying abiotic influences that may be indicative of sample habitability. Here, we show the influence of grain size fractions at an aeolian plain, and suggest how organisms may localize in these fractions with respect to environmental stresses. Furthermore, this work also highlights the importance of heterogeneity at a prospective sampling site for providing additional shelter from weathering, implying the potential for denser microbial colonization. Lastly, shifts in characteristic factor variability with respect to distinct spatial groupings showed consistent trends over time, suggesting that taking samples too closely together (1 m or less) is unlikely produce statistically unique samples. Sampling at large distances (100 m or more) will likely result in unique samples; however they are not likely to rigorously characterize the target location. Collection of a small set of samples at intervals of approximately 10 m represented an ideal medium for uncovering biological and moisture shifts across a larger sampling area. Thus, when preparing a sampling plan for future extraterrestrial missions, these results can help tailor a sampling scheme to fit intended science goals, providing flexibility depending on the level of site characterization required.

This work represents a starting point for future analysis at Dyngjusandur. Spectroscopic data from the Dyngjusandur expeditions will help uncover trends between the characteristic factors explored here and the mineralogical composition of each sample. Additionally, sequencing of samples from 2017 and 2018 would enable analysis of community changes over time, while performing these experiments at another analog location sculpted by different environmental factors may result in different correlations of interest and different trends in characteristic factor variability with spatial scale. Ultimately, continued sampling research at Dyngjusandur and other Mars analogs will inform our understanding of sample habitability, enabling future extraterrestrial missions to optimize their sample return depending on the qualities of their target.

4.6 Citations

1. Ojha, L., et al., Spectral evidence for hydrated salts in recurring slope lineae on Mars. Nat Geosci, 2015. 8: p. 829.

2. Martín-Torres, F.J., et al., Transient liquid water and water activity at Gale Crater on Mars. Nat Geosci, 2015. 8: p. 357.

3. Wiens, R.C., S. Maurice, and F.R. Perez, The SuperCam Remote Sensing Instrument Suite for the Mars 2020 Rover: A Preview. Spectroscopy, 2017. 32(5): p. 50-55.

4. Allwood, A.C., et al., PIXL: Planetary Instrument for X-Ray Lithochemistry. Space Science Reviews, 2020. 216(8): p. 132.

5. Beegle, L., et al., Scanning Habitable Environments with Raman and Luminescence for Organics and Chemicals (SHERLOC) on Mars 2020. Abstracts of Papers of the American Chemical Society, 2019. 257: p. 2.

6. Perez-Izquierdo, J., et al., The Thermal Infrared Sensor (TIRS) of the Mars Environmental Dynamics Analyzer (MEDA) instrument onboard Mars 2020, a general description and performance analysis. Measurement, 2018. 122: p. 432-442.

7. Hayes, A.G., et al., Pre-Flight Calibration of the Mars 2020 Rover Mastcam Zoom (Mastcam-Z) Multispectral, Stereoscopic Imager. Space Science Reviews, 2021. 217(2): p. 95.

8. Hamran, S.E., et al., Radar Imager for Mars' Subsurface Experiment-RIMFAX. Space Science Reviews, 2020. 216(8).

9. Mustard, J., et al., Report of the Mars 2020 Science Definition Team. 2013.

10. Amador, E.S., et al., Synchronous in-field application of life-detection techniques in planetary analog missions. Planetary and Space Science, 2015. 106: p. 1-10.

11. Gentry, D.M., et al., Correlations Between Life-Detection Techniques and Implications for Sampling Site Selection in Planetary Analog Missions. Astrobiology, 2017. 17(10): p. 1009-1021.

12. Rader, E., et al., Preferably Plinian and Pumaceous: Implications of Microbial Activity in Modern Volcanic Deposits at Askja Volcano, Iceland, and Relevancy for Mars Exploration. Acs Earth and Space Chemistry, 2020. 4(9): p. 1500-1514.

13. Tan, G., et al., Spatial Variation in Results of Biosignatures Analyses of Apparently Homogenous Samples from Mars Analog Environments in Iceland. Acs Earth and Space Chemistry, 2021.

14. Sutton, S.M.S., A. C.; Hanna, A. M.; Tan, G. K.; Gentry, D. M.; Cable, M. L.; Rader, E.; Cullen, D.; Geppert, W.; Stockton, A. M.; FELDSPAR Team, Microbial Population and Distribution at Dyngjusandur, Iceland a Mars Analog Alluvial Plain. 2021.

15. Sutton, S.V.H., S. R.; Tan, G. K.; Patel, A.; Hanna, A. M.; Simspon, A. C.; Gentry, D. M.; Cable, M. L.; Rader, E.; Cullen, D.; Geppert, W.; Stockton, A. M.; FELDSPAR

Team, Biosignature Distribution & Characterization of the Dyngjusandur, Iceland Mars Analog Plain from 2016-2017. Submitted to Astrobiology, 2022.

16. Lammer, H., et al., What makes a planet habitable? Astronomy and Astrophysics Review, 2009. 17(2): p. 181-249.

17. Moissl-Eichinger, C., C.S. Cockell, and P. Rettberg, Venturing into new realms? Microorganisms in space. Fems Microbiology Reviews, 2016. 40(5): p. 722-737.

18. Preston, L.J. and L.R. Dartnell, Planetary habitability: lessons learned from terrestrial analogues. International Journal of Astrobiology, 2014. 13(1): p. 81-98.

19. Bathgate, E.J., et al., Raman, FTIR and XRD study of Icelandic tephra minerals: implications for Mars. Journal of Raman Spectroscopy, 2015. 46(10): p. 846-855.

20. Hays, L.E., et al., Biosignature Preservation and Detection in Mars Analog Environments. Astrobiology, 2017. 17(4): p. 363-400.

21. Sara, M.J., Dyngjusandur sand sheet, Iceland, as a depositional analog to the Stimson Fm. in Gale Crater, Mars. 2017. p. xii, 145 pages.

22. Baratoux, D., et al., Volcanic sands of Iceland - Diverse origins of aeolian sand deposits revealed at Dyngjusandur and Lambahraun. Earth Surface Processes and Landforms, 2011. 36(13): p. 1789-1808.

23. Mangold, N., et al., Segregation of olivine grains in volcanic sands in Iceland and implications for Mars. Earth and Planetary Science Letters, 2011. 310(3-4): p. 233-243.

24. Arnalds, O., P. Dagsson-Waldhauserova, and H. Olafsson, The Icelandic volcanic aeolian environment: Processes and impacts — A review. Aeolian Research, 2016. 20: p. 176-195.

25. Baker, V.R., et al., ANCIENT OCEANS, ICE SHEETS AND THE HYDROLOGICAL CYCLE ON MARS. Nature, 1991. 352(6336): p. 589-594.

26. Cable, M.L., et al., Geochemical and Spectral Characterization of Icelandic Lava Flow-Fields and Glaciovolcanic Sandur, and their Relevance as Mars Analog Environments. JGR Planets, 2022.

27. Hale, L. and D. Crowley, DNA extraction methodology for biochar-amended sand and clay. Biology and Fertility of Soils, 2015. 51.

28. Dunn, O.J., MULTIPLE COMPARISONS AMONG MEANS. Journal of the American Statistical Association, 1961. 56(293): p. 52-&.

CHAPTER 5. CONCLUSIONS & FUTURE WORK

Three years of study at the Dyngjusandur Mars analog has resulted in habitability trends that should be considered when planning future extraterrestrial missions to environments experiencing similar stresses. While unique characteristic factor correlations were uncovered each year, consistent patterns were also observed that help to define the site as a whole.

Aeolian action at Dyngjusandur was determined to be one of the most influential factors for habitability. In 2016, the depth profile study showed significantly higher levels of biomass several centimeters below the surface sediment when compared to samples gathered at the surface. This suggested that only the most robust organisms were able to survive the sediment disruption caused by the frequent sandstorms. In 2017, more evidence was added to the observations from 2016, with a uniquely heterogenous sub-site displaying higher levels of biomass content in comparison to its more homogenous counterparts. These results implied that larger lava rocks were providing enhanced protection from the katabatic winds, potentially enabling microbial communities to colonize the upper layers of sediment without disruption. While the 2018 site overlapped with 2017 sub-site 3, additional large lava rocks observed at 2018 sites resulted in a biomass distribution mirroring the one uncovered at 2017 sub-site 2. The biomass distribution trends observed at heterogenous sites in 2017 and 2018 provided additional evidence to suggest that protective structures at Mars analog sites may encourage localized pockets of biological activity that should be targeted during site mapping.

In addition to Aeolian action, grain size was found to be immensely important, with bioactivity displaying strong positive correlations with large grain sizes in 2017 and 2018. Conversely, bioactivity lacked correlations with the finest, and most abundant, grain size, suggesting that the large sediment grains offer qualities that may encourage colonization. While this work does investigate the specific qualities that may enable large sediment to support metabolizing organisms, we can speculate that the additional surface area or the porosity of large sediment may contribute to making these grains more habitable.

For all three years of study, a system of barcodes was employed to determine the distribution of biomass and bioactivity at different spatial scales. Comparing these results from year to year revealed several trends. First, the 10 m spatial grouping always displayed the most variability at small scales (by pairwise T-Tests and U-Tests, 95% confidence interval). Second, the 1 m scale was not variable, never offering more than 4% significantly different comparisons. While variability was observed at the 100 m scale, the limited number of available comparisons make determining the impact of this scale inconclusive. However, the 100 m grouping often displayed few statistically significant comparisons, masking the greater abundance of statistically different comparisons at smaller groupings. Thus, while taking few samples at larger separation may result in unique samples, they are not likely enough to encompass the biological variability of the greater area.

5.1 Suggestions for Future Study

Additional characterization of Mars analog sites is necessary to better inform future extraterrestrial missions, however this work acts as starting point for correlating the biotic and abiotic factors present at these locations. With the data currently accumulated and the samples maintained in the Stockton lab at Georgia Tech, the FELDSPAR expeditions to Dyngjusandur can continue to inform our understanding of these Mars analog locations.

Amplicon sequencing was performed on the 2016 sample set; however a much deeper analysis is possible here. Sequencing could be performed on the 2017 and 2018 samples to determine how the microbial community has adjusted over time, and the communities inhabiting homogenous and heterogenous sampling sites could be compared to determine how aeolian action influences community distribution. Beyond temporal distributions of phyla, a more rigorous analysis of the sequencing data could unveil specifics about the organisms inhabiting Dyngjusandur and kinds of processes they may utilize to survive the relatively harsh conditions. This data could also be compared with sequences from other Mars analogs to determine if ubiquitous community members exist as a result of similar environmental pressures.

Since starting this project, the FELDSPAR team has expressed interest in creating machine learning code to predict sample habitability based on site photos, spectroscopic data, and environmental factors. Such a program would represent a form of agnostic biosignature determination, making it especially applicable for predicting extraterrestrial habitability despite our current lack of understanding how extraterrestrial life might have formed. With more analog data collected, creating and training a machine learning program remains an ever-increasing possibility.

APPENDIX A. High Resolution Figures

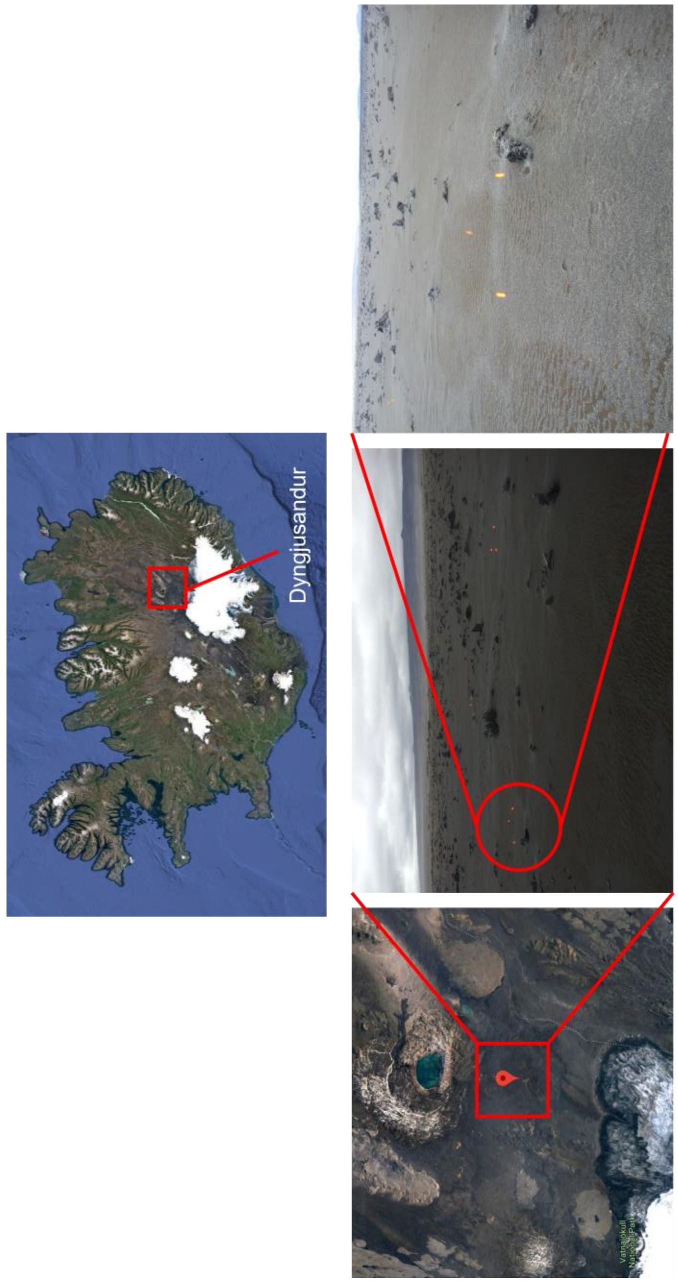

***Figure A1-1** – **The Dyngjusandur Mars Analog**. Dyngjusandur is located in the Central Highlands of Iceland, and is primarily composed of fine, black tephra. Large lava rocks were infrequently dispersed across Dyngjusandur's plains, resulting in an analog that is often dispersed by southern Katabatic winds.*

Figure A2-1 – The Dyngjusandur field site. *Dyngjusandur alluvial plain is located in the central highlands of Iceland, 16 km south of the Askja Caldera. The sand is composed of unconsolidated basaltic tephra, and while portions of the plains are morphologically homogenous, others are distributed with basaltic stone.*

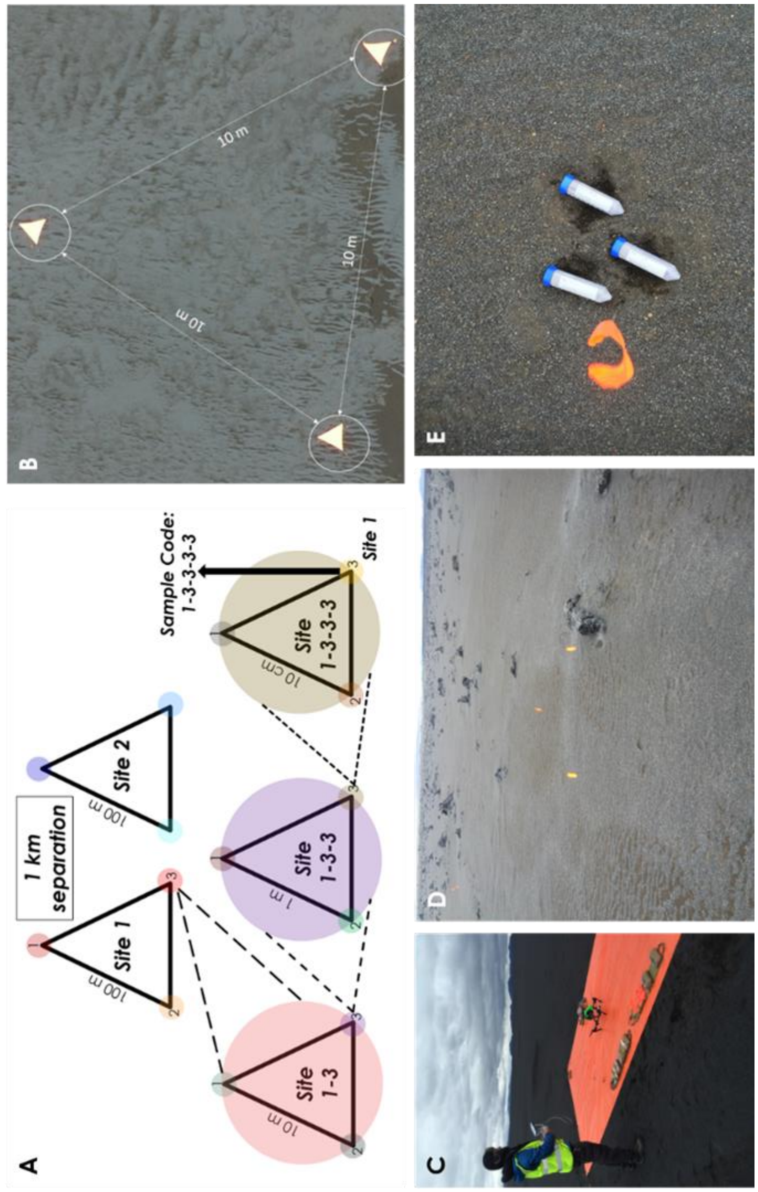

Figure A2-2 – Nested Triangular Grids Sampling System. *Two sampling sites were selected with a separation of 1 km. At each sampling site, a series of nested triangular grids was sampled to determine spatial heterogeneity of bioactivity. (A) The sampling schematic employed at Dyngjusandur. Each site was mapped into equilateral triangles, with the vertices separated by 100 m. The corner of each triangle was then mapped into a smaller triangle, with distributions of 10 m, 1 m, and 0.1 m. A code was generated for each sample based on its placement in the nested triangular grid. (B) A 10 m triangle from Site 1. Orange, triangular tarps with 1 m per side were placed at the corners of each 10 m triangle for visualization. (C) Aerial mapping of each site was obtained using a quadcopter for imaging. (D) The 1 m triangles prior to sample collection and aerial mapping were denoted in field by small orange flags. (E) Triplicate samples at 0.1 m spacing were recovered at the corners of each 1 m triangle after removing the top 1 cm of surface sediment.*

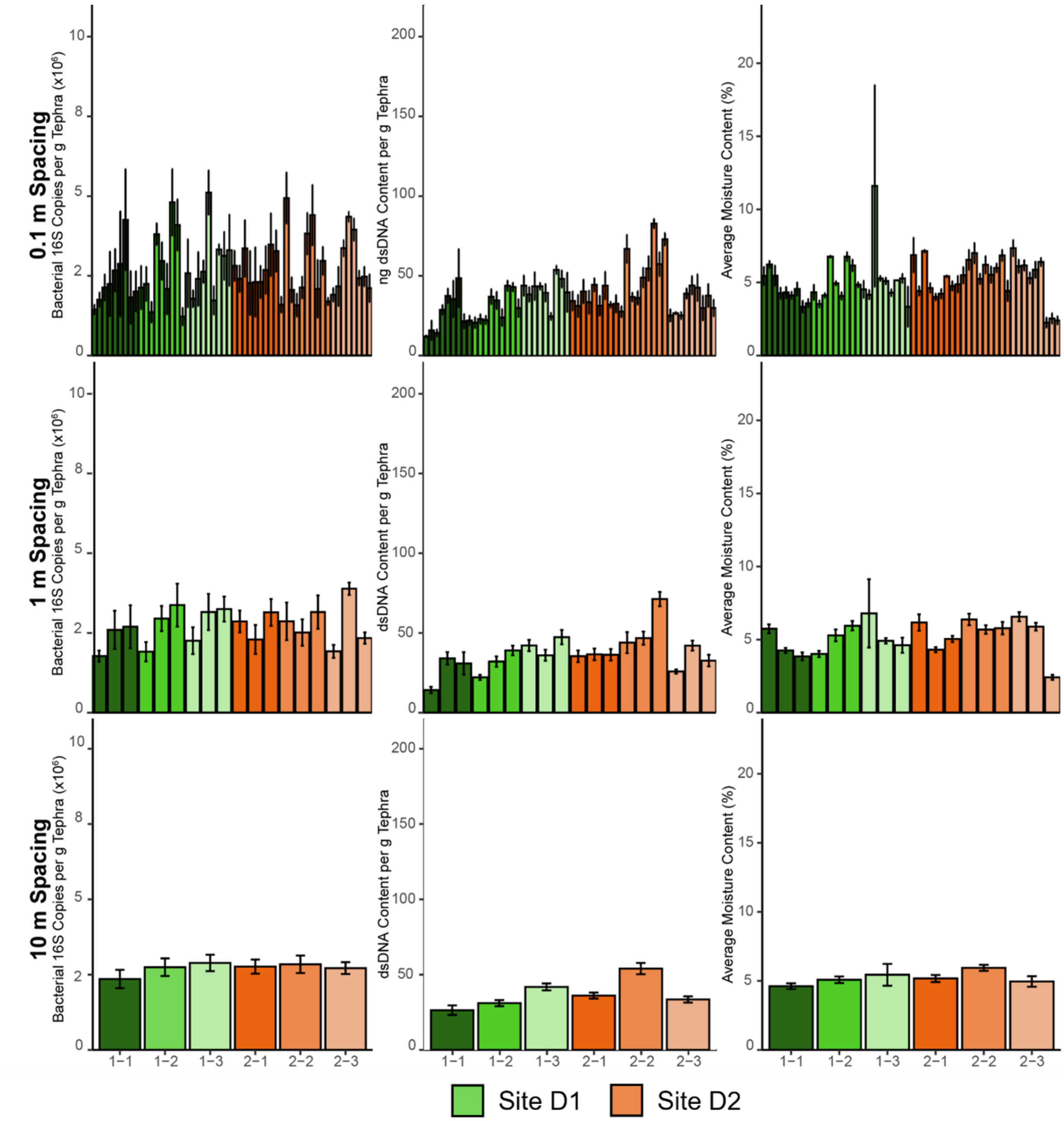

Figure A2-3 – Dyngusandur Characteristic Measurements. *16S copies, dsDNA content, and gravimetric moisture content at spatial distributions of 10 m, 1 m, and 10 cm. Shades of red and blue correspond to their respective x-axis value, denoting the 0.1 m and 1 m triangle. Three sub-samples of each sample at 0.1 m spacing were analyzed, thus error bars represent the heterogeneity of the sample. The measurements at the 0.1 m spacing were combined to yield the data presented for 1 m and 10 m spacing.*

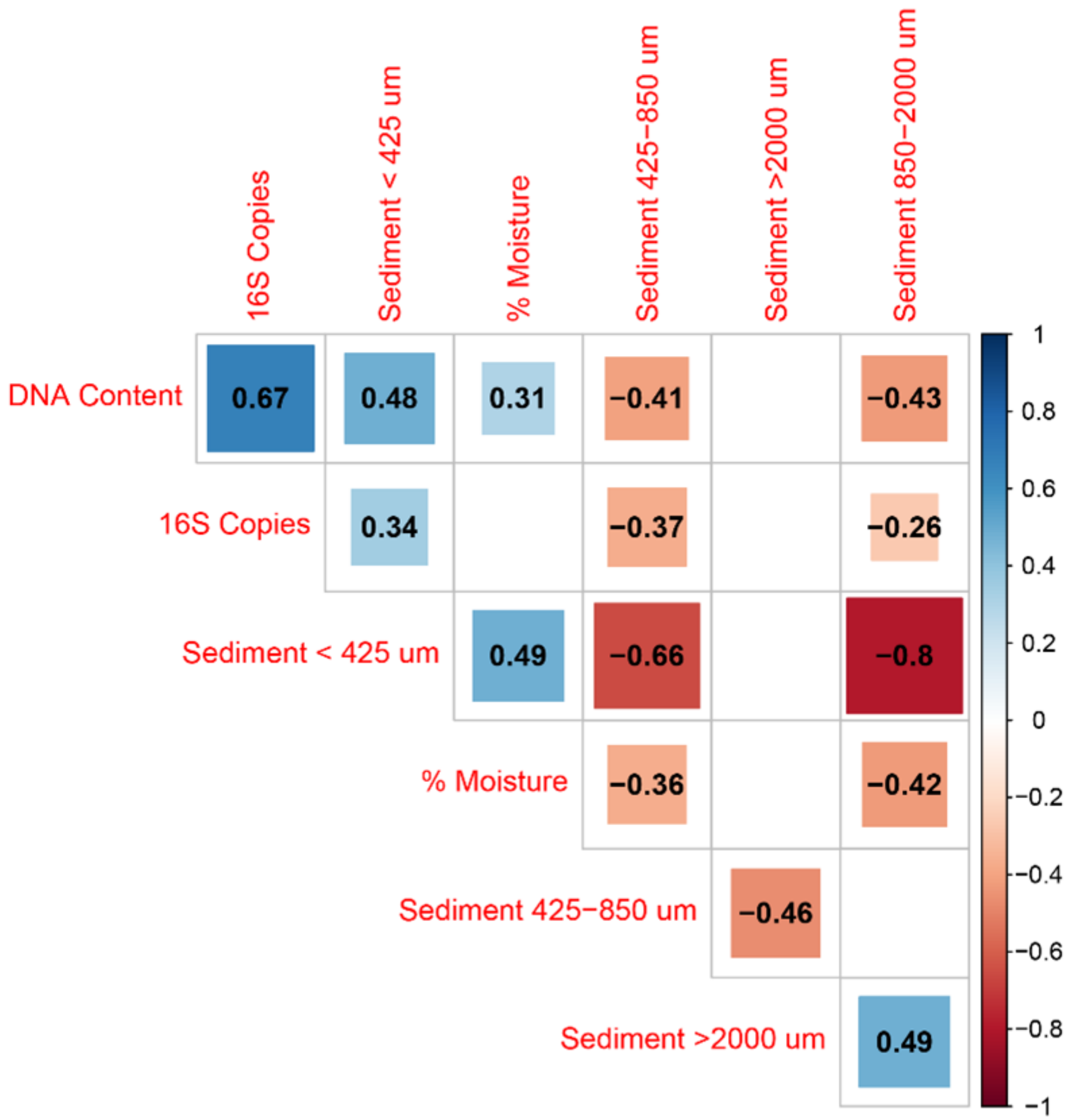

Figure A2-4 – Correlations between bacterial copies, dsDNA Content, moisture content, and grain size. *Blue represents positive correlations, while red represents an inverse correlation. Correlation coefficients are overlayed for significant comparisons. Significant comparisons are based on a 90% confidence interval. Empty boxes represent a lack of significant correlation.*

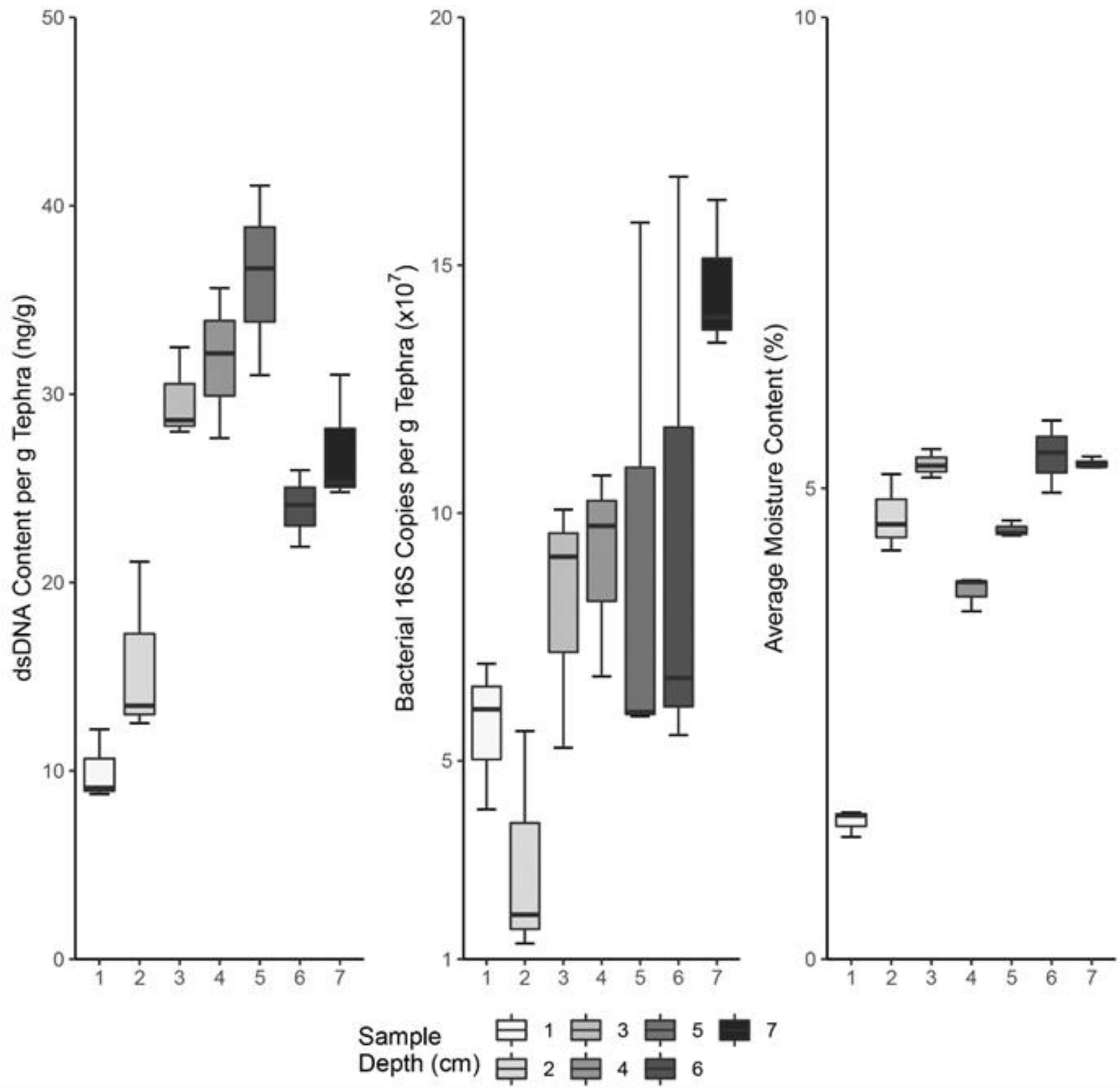

Figure A2-5 – Dyngjusandur Depth Profile Measurements. *DNA content, 16S Copies, and gravimetric moisture content from samples recovered from depths of 1-7 cm. Samples were taken in 1 cm increments. Triplicate sub-samples were analyzed for each data point.*

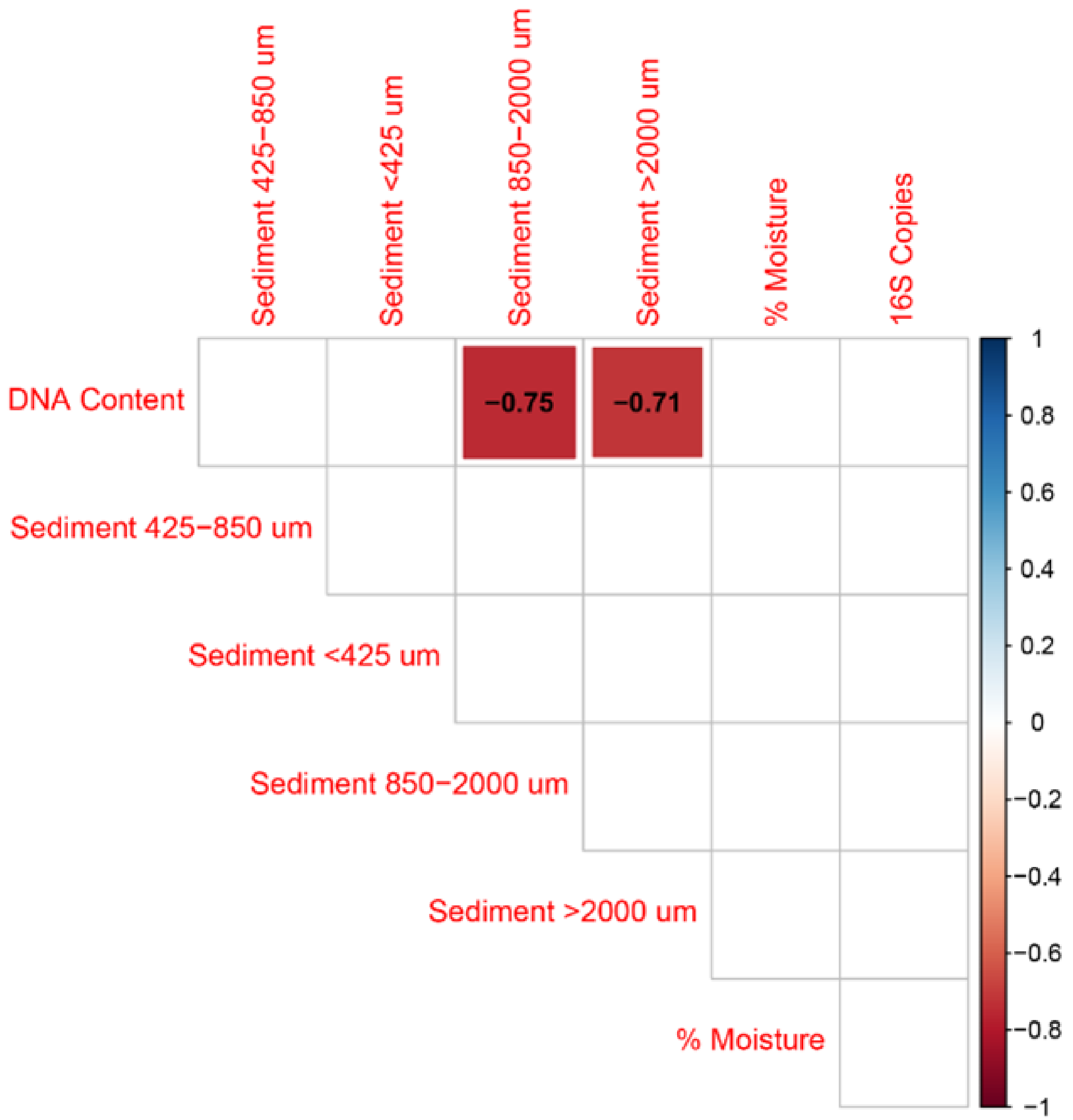

Figure A2-6 – Depth Profile Correlations Between Bacterial Copies, dsDNA Content, Moisture Content, and Grain Size. *Blue represents positive correlations, while red represents inverse correlation. Correlation coefficients are overlayed for significant comparisons. Significant comparisons are based on the 90% confidence interval. Empty boxes represent a lack of significant correlation.*

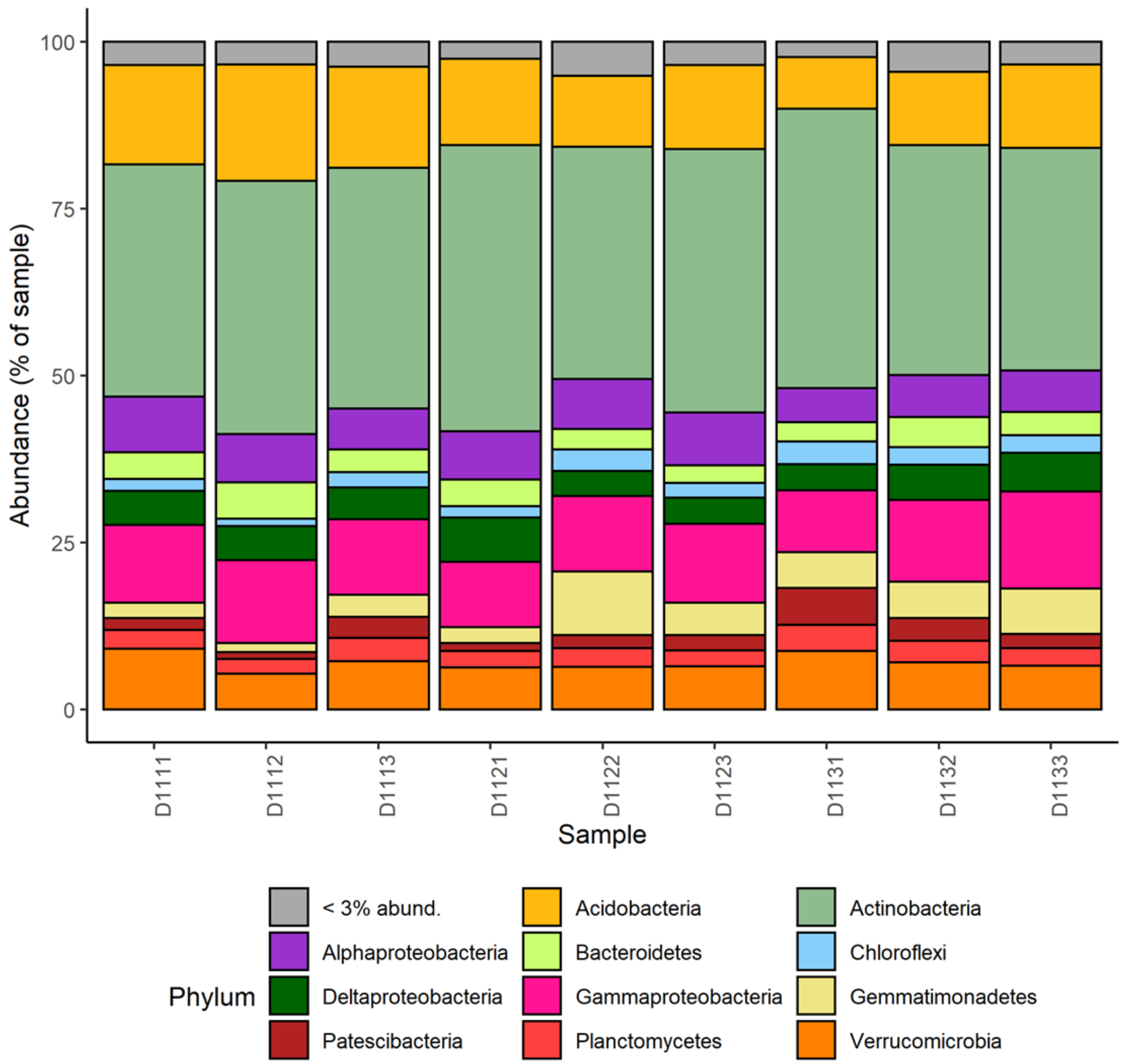

Figure A2-7 – Abundant Sequences in Dyngjusandur Samples. *Sequencing results from one sample from each 1 m triangular grid from Site D1, representing the phyla with greater than 3% abundance. Of the nine most abundant phyla, Actinobacteria, Proteobacteria, and Acidobacteria each accounted for more than 10% of the total population.*

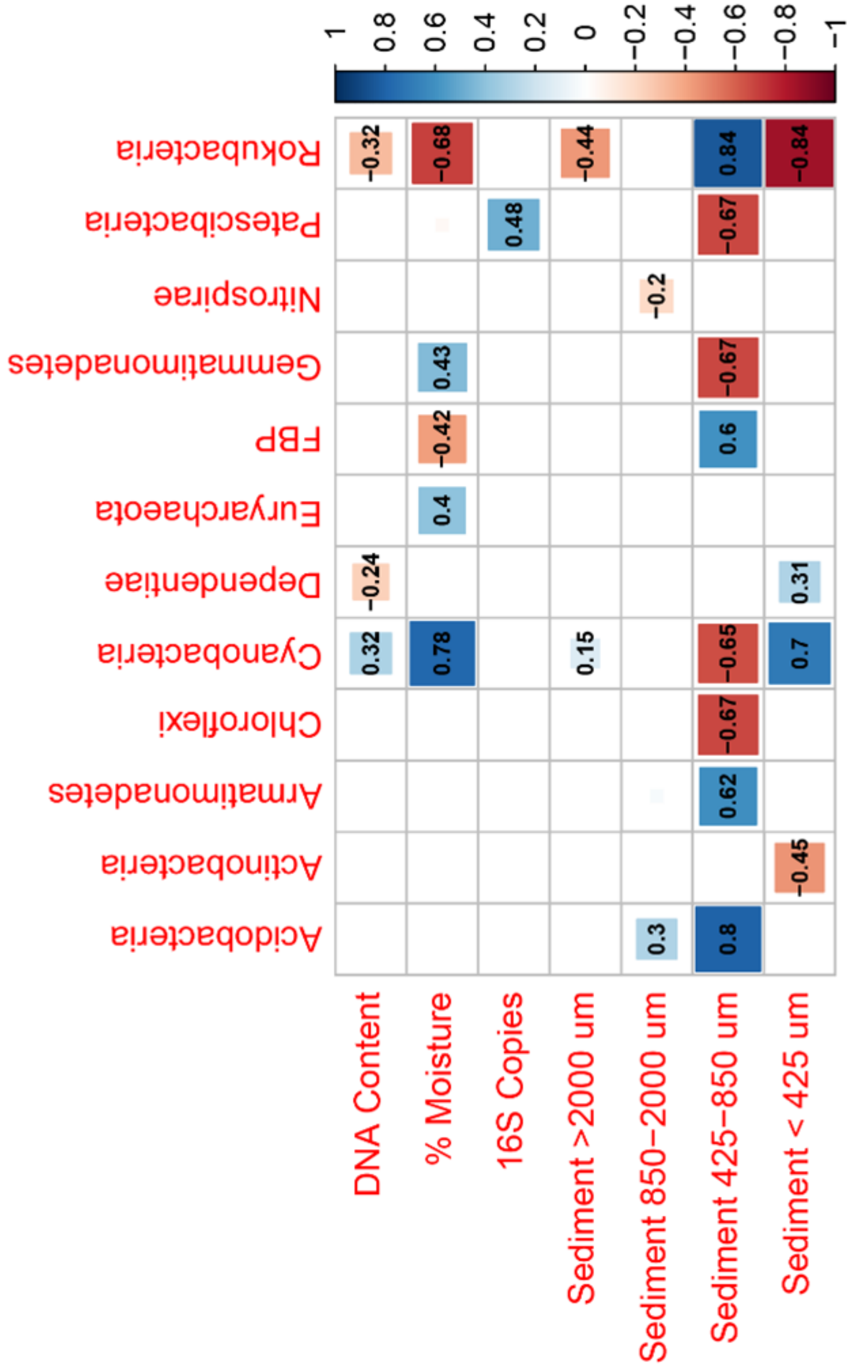

Figure A2-8 – Correlations Between Phyla and Primary Measures. *Phyla demonstrating a significant correlation (p-value less than 0.1) with dsDNA content, bacterial copies, moisture content, or grain size were included in the plot above. Shades of blue represent a positive correlation and shades of red represent a negative correlation. Correlation coefficients are overlayed for significant comparisons. Measurements were performed in triplicate. Empty boxes represent a lack of significant correlation.*

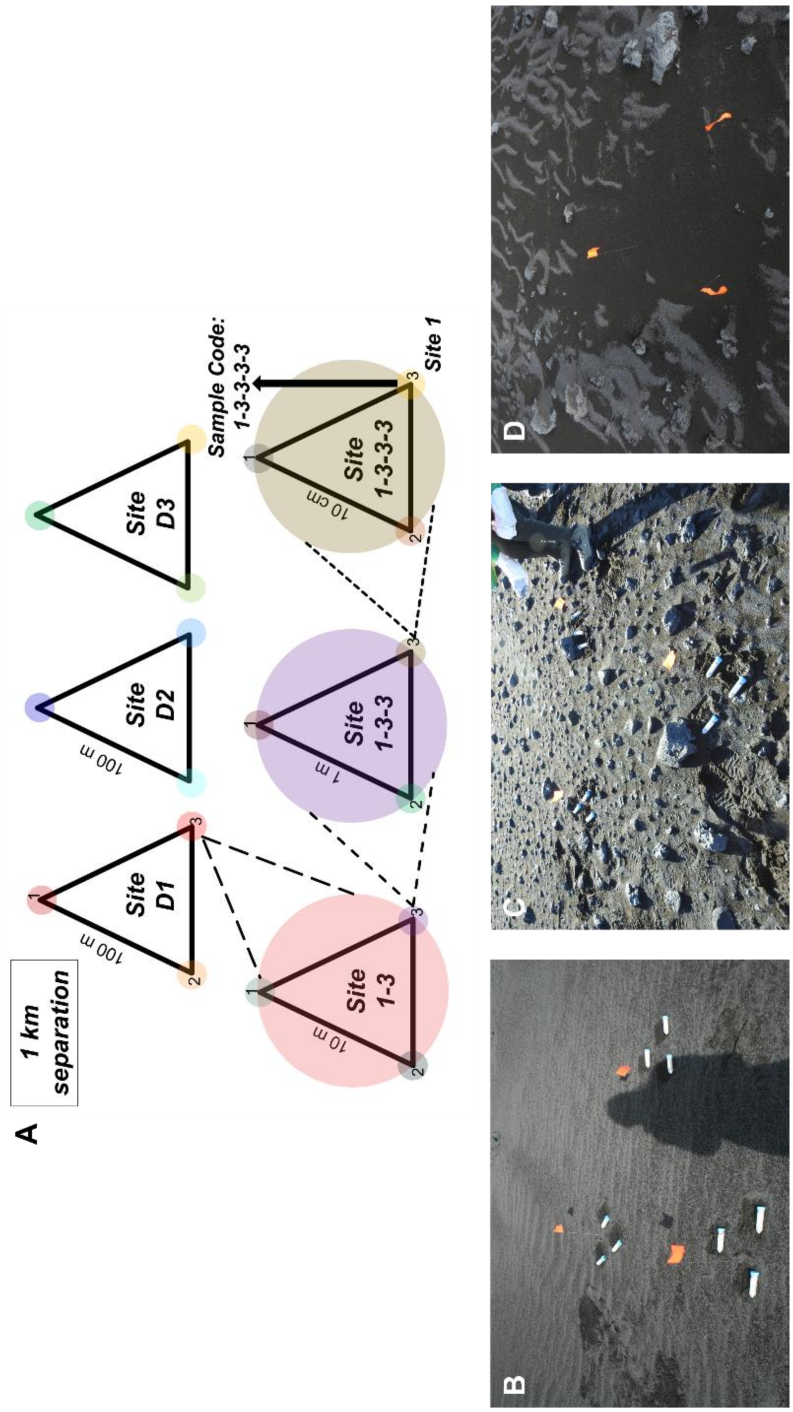

Figure A3-1 – Dyngjusandur, Iceland: 2017 Site Overview. *A) Schematic of Nested Equilateral Triangles: A 1 km equilateral triangle was mapped as a sampling site. The corners of the 1 km triangle were composed of 100 m equilateral triangles. The corners of each subsequent triangle are also composed of equilateral triangles of 10 m, 1 m, and 0.1 m sizes. The corners of each 0.1 m triangle were sampled and assigned a barcode for spatial identification and statistical analysis. B) A 1 m triangle at subsite D1. C) A 1 m triangle at subsite D2. D) A 1 m triangle at subsite D3.*

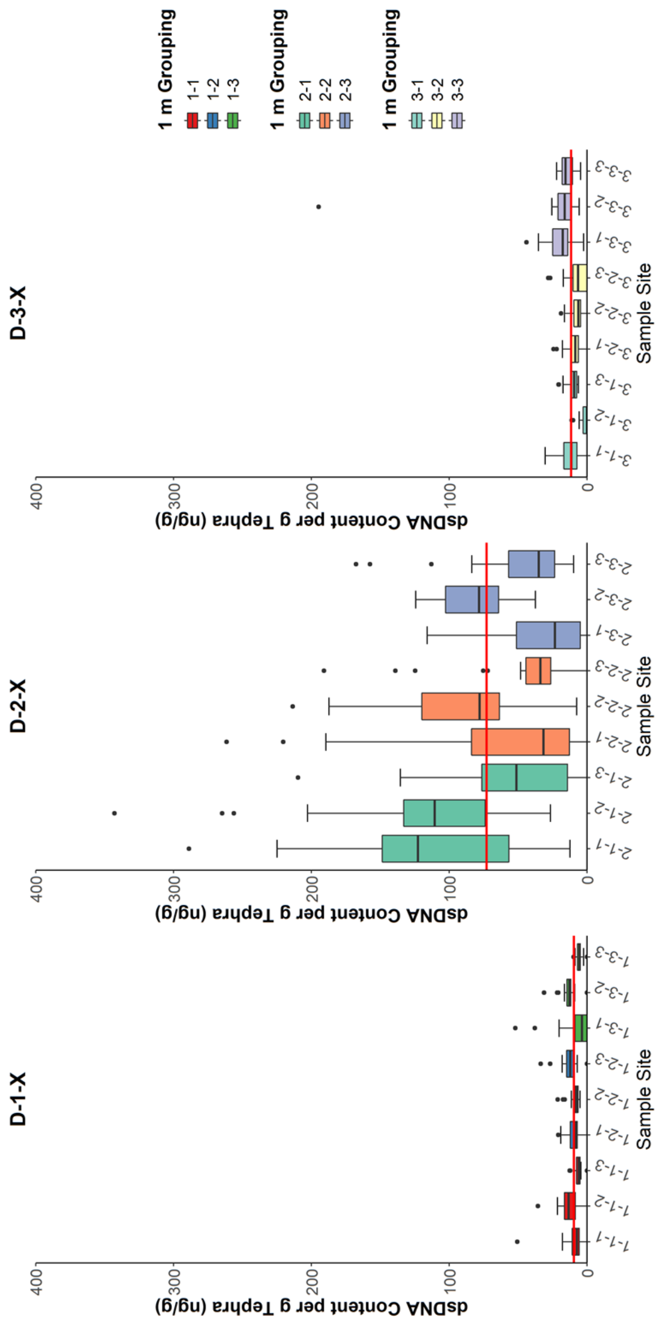

Figure A3-2 – dsDNA Quantification. *dsDNA content was collected for each sample and grouped according to subsite (D1-3) and then grouped by 10 m triangle (D1-X – D3-X). Legend colors represent each 10 m triangle, with three boxplots per color to represent the daughter 1 m triangles (measurements within each 1 m triangle were grouped for display). Red lines on each plot represent the average dsDNA content per site. Site averages were: D1 – 9.6 ng/g, D2 – 72.9 ng/g, D3 – 11.7 ng/g.*

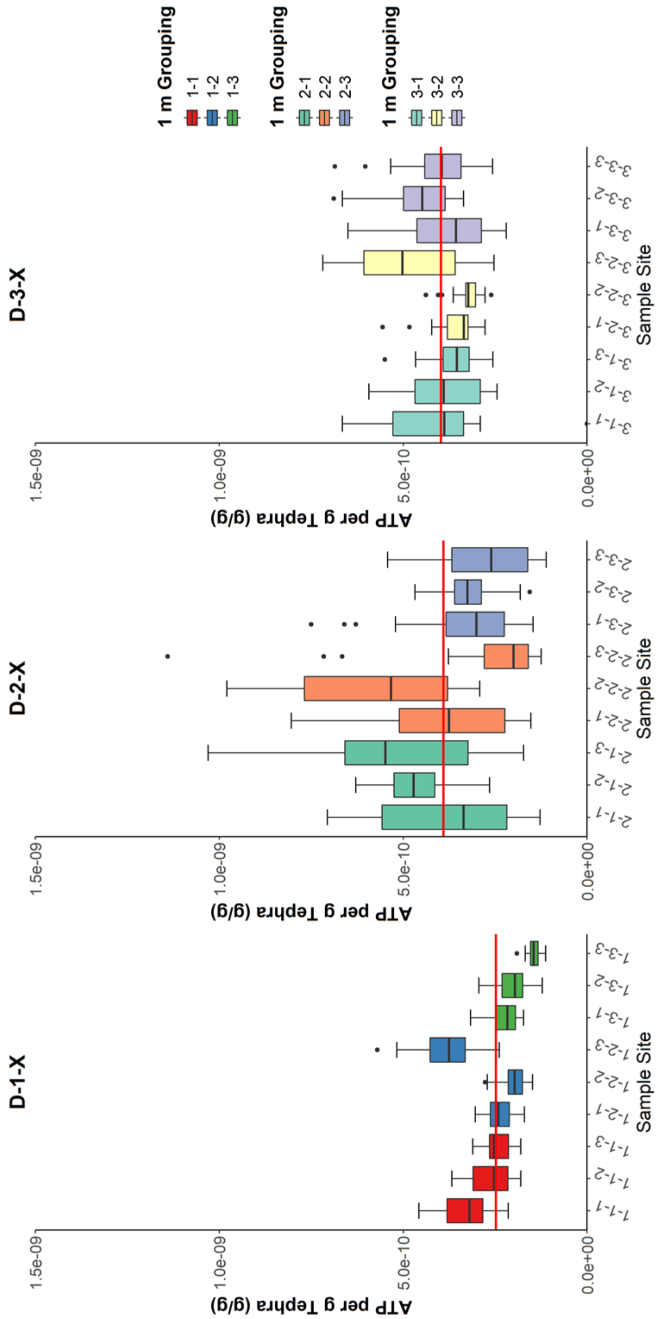

Figure A3-3 – ATP Quantification. *ATP content was collected for each sample and grouped according to subsite (D1-3) and then grouped by 10 m triangle (D1-X – D3-X). Legend colors represent each 10 m triangle, with three boxplots per color to represent the daughter 1 m triangles (measurements within each 1 m triangle were grouped for display). Red lines on each plot represent the average dsDNA content per site. Site averages were: D1 – 2.6x10-10 g/g, D2 – 4.2 x10-10 g/g, D3 – 4.0 x10-10 g/g.*

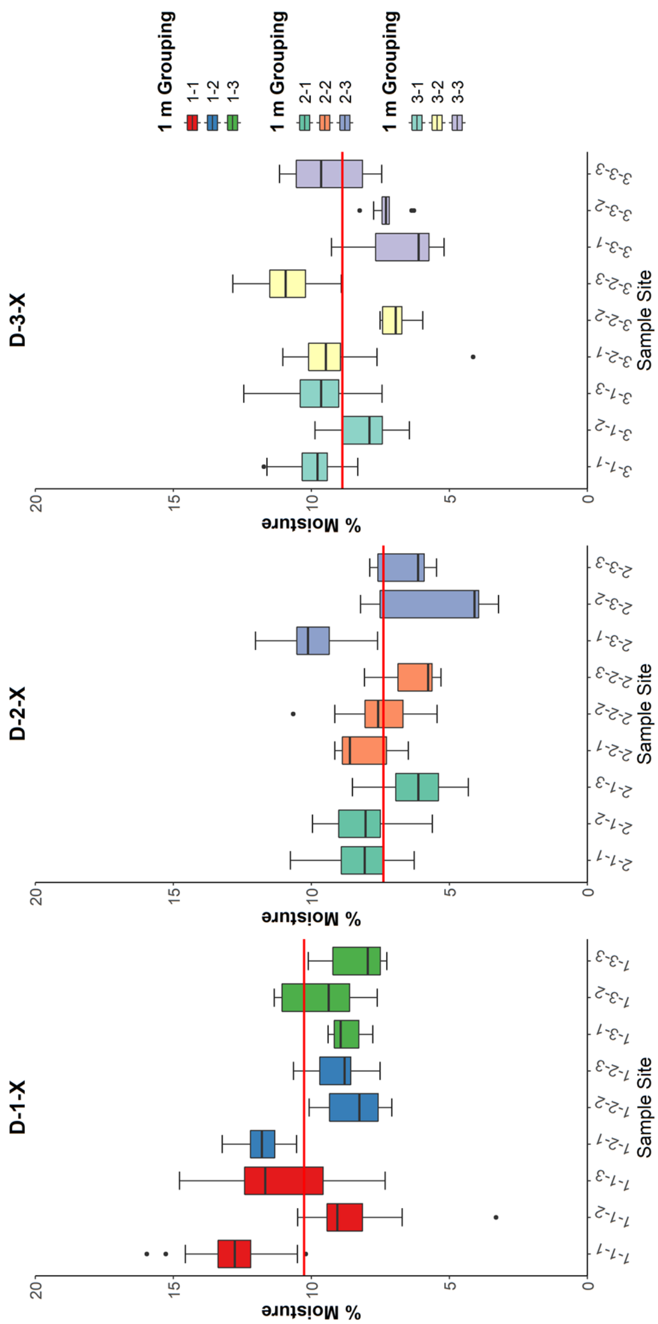

Figure A3-4 – Gravimetric Moisture Quantification. *Moisture content was collected for each sample and grouped according to subsite (D1-3) and then grouped by 10 m triangle (D1-X – D3-X). Legend colors represent each 10 m triangle, with three boxplots per color to represent the daughter 1 m triangles (measurements within each 1 m triangle were grouped for display). Red lines on each plot represent the average dsDNA content per site. Site averages were: D1 – 10.3%, D2 – 7.4%, D3 – 8.9%.*

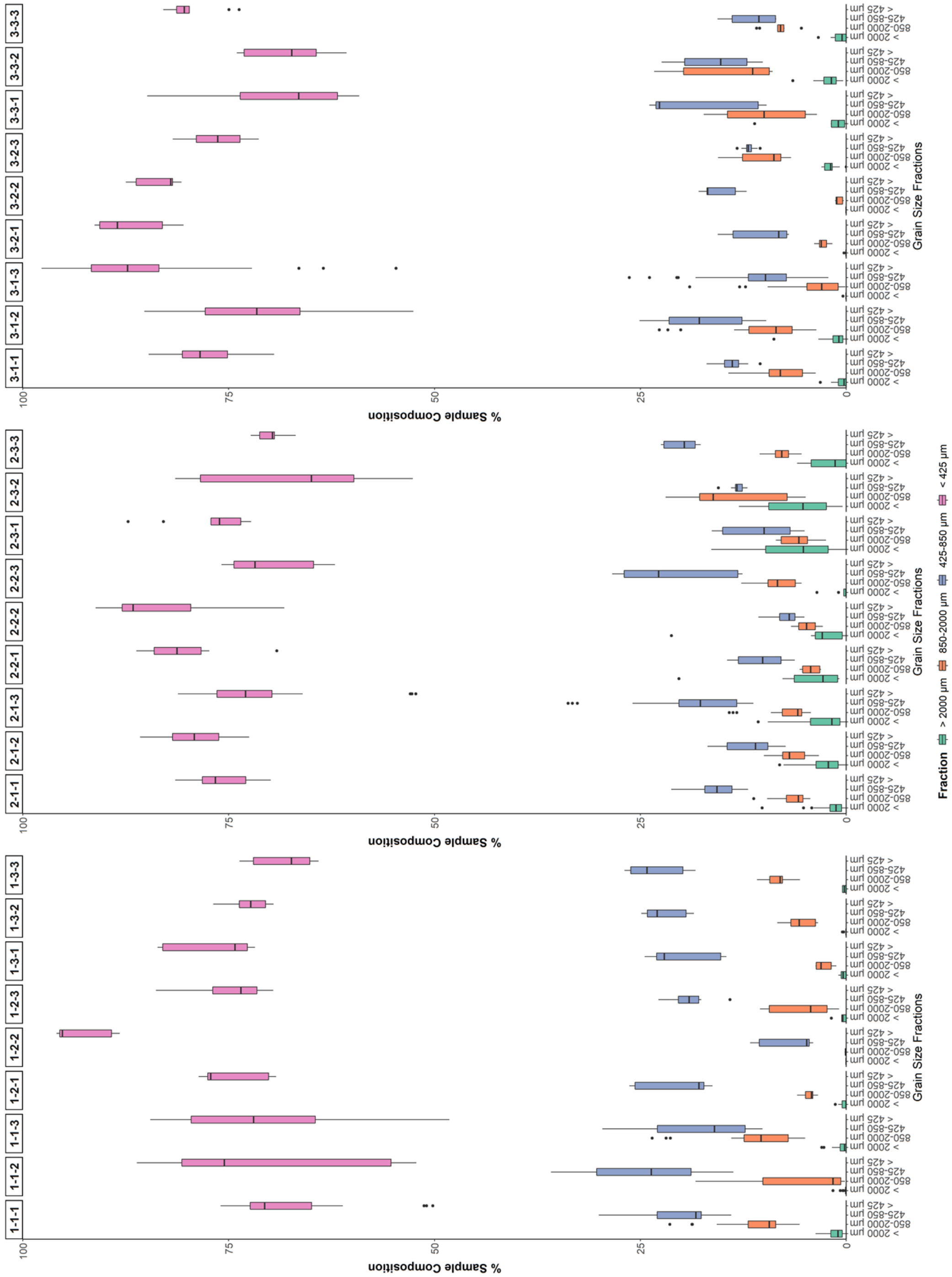

Figure A3-5 – Grain Size Fractions. *Sample composition with respect to grain size was determined via dry sieving. Percent composition of each fraction was determined by comparing moisture mass against total dry sample mass. Samples were grouped by subsite (D1-3), 10 m triangle (D1-X – D3-X), and finally 1 m triangle (D1-X-Y – D3-X-Y). The grain size fraction greater than 2000 µm is presented in green, the fraction between 850-2000 µm is presented in orange, the fraction between 425-850 µm is presented in violet, and the fraction less than 425 µm is presented in pink.*

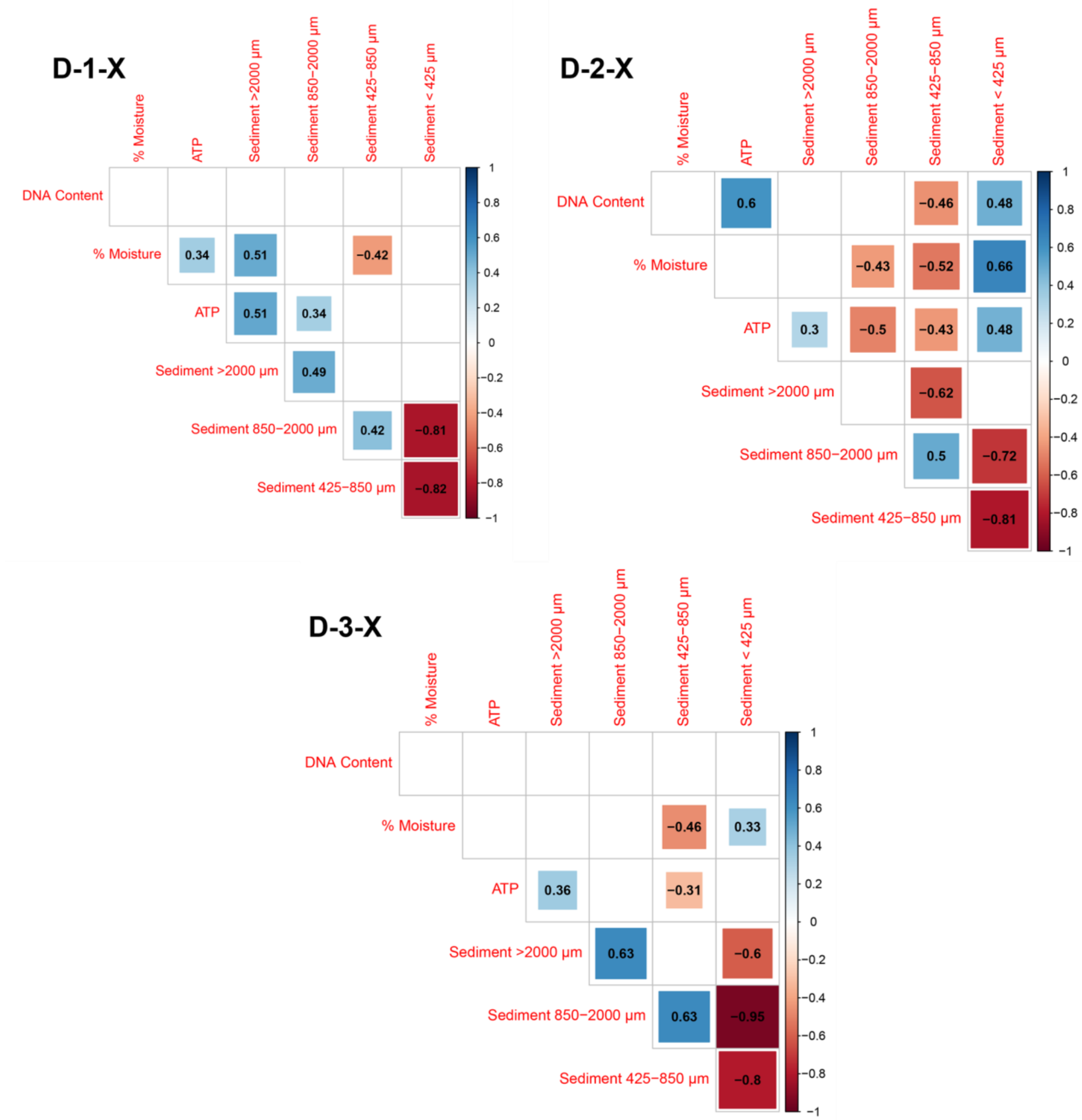

Figure A3-6 – Correlation Matrices All Subsites. *Correlations were determined between each characteristic factor at each subsite using Spearman's rank correlation coefficients. Significant comparisons were determined based on a 90% confidence interval, and correlation coefficients were overlayed on significant comparisons. Blank squares represent insignificant correlations.*

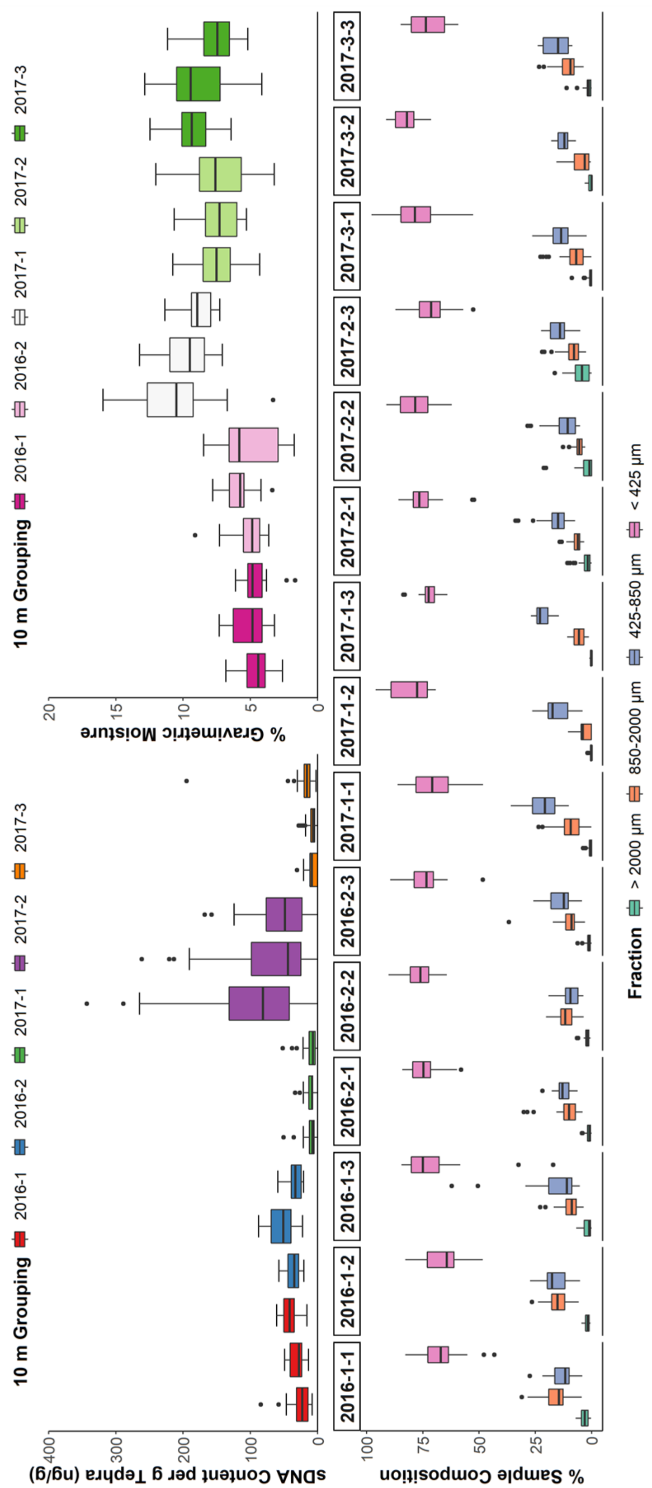

Figure A3-7 – Characteristic Factors at Dyngjusandur from 2016-2017. *Data from FELDSPAR expeditions to Dyngjusandur in 2016 and 2017. A) dsDNA grouped at the 100 m level for each subsite in 2016 and 2017. B) Gravimetric moisture content grouped at the 100 m level for each subsite in 2016 and 2017. C) Grain size composition of samples from 2016 and 2017 grouped at the 100 m level.*

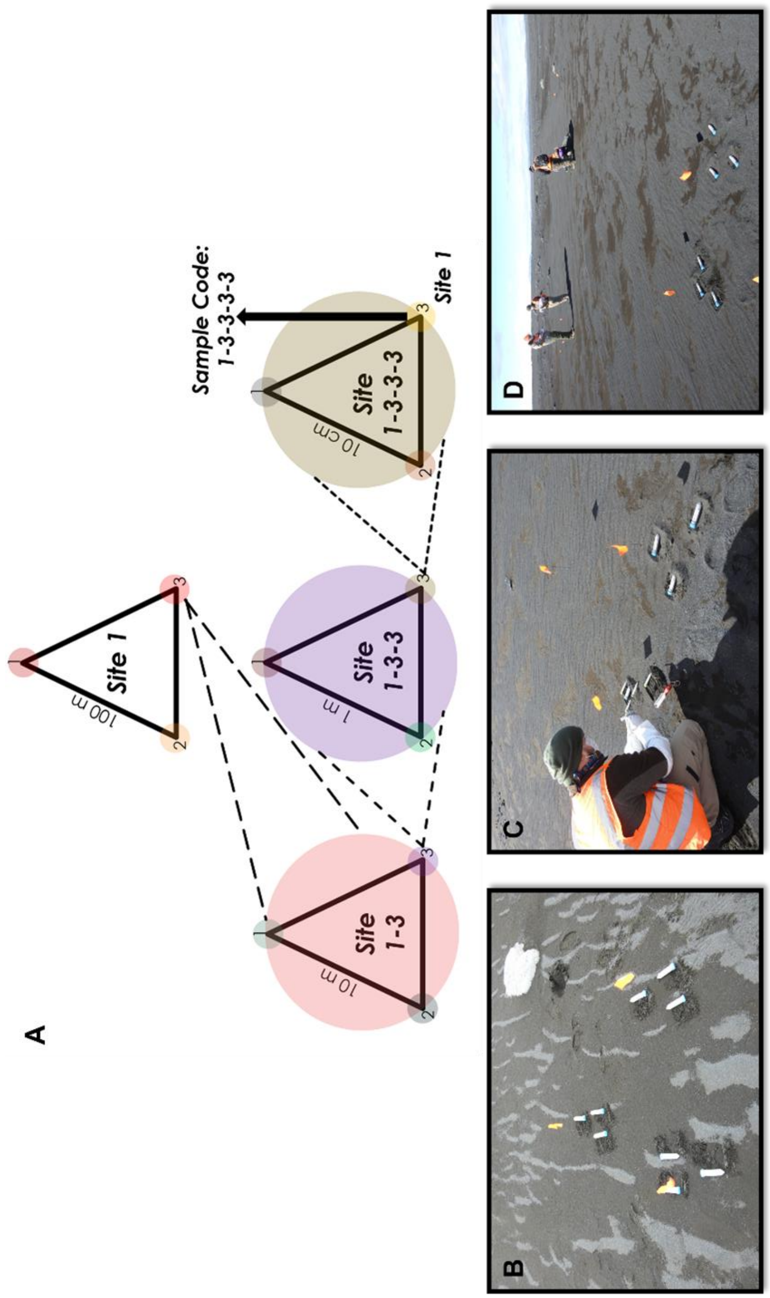

Figure A4-1 – Dyngjusandur 2018 Expedition*. A) Sampling Site Schematic: the 2018 sampling site was structured as a series of nested equilateral triangles. A single 100 m triangle was mapped, the corners of which were composed of 10 m equilateral triangles. Each corner of the 10 m triangles was composed of 1 m triangles, continuing with more refined groupings to a scale of 0.1 m. A barcode was generated for each sample for spatial identification. B) 2017 Subsite 3: subsite 3 in 2017 shares the same GPS coordinates as the sampling site in 2018. C) 2018 Sampling Site: samples being exhumed and placed in conical tubes. Qualitatively similar to the same site in 2017. D) 2018 Sampling Site Full: the greater 2018 sampling site was primarily visually and morphologically homogenous. Larger chunks of lava were infrequently dispersed.*

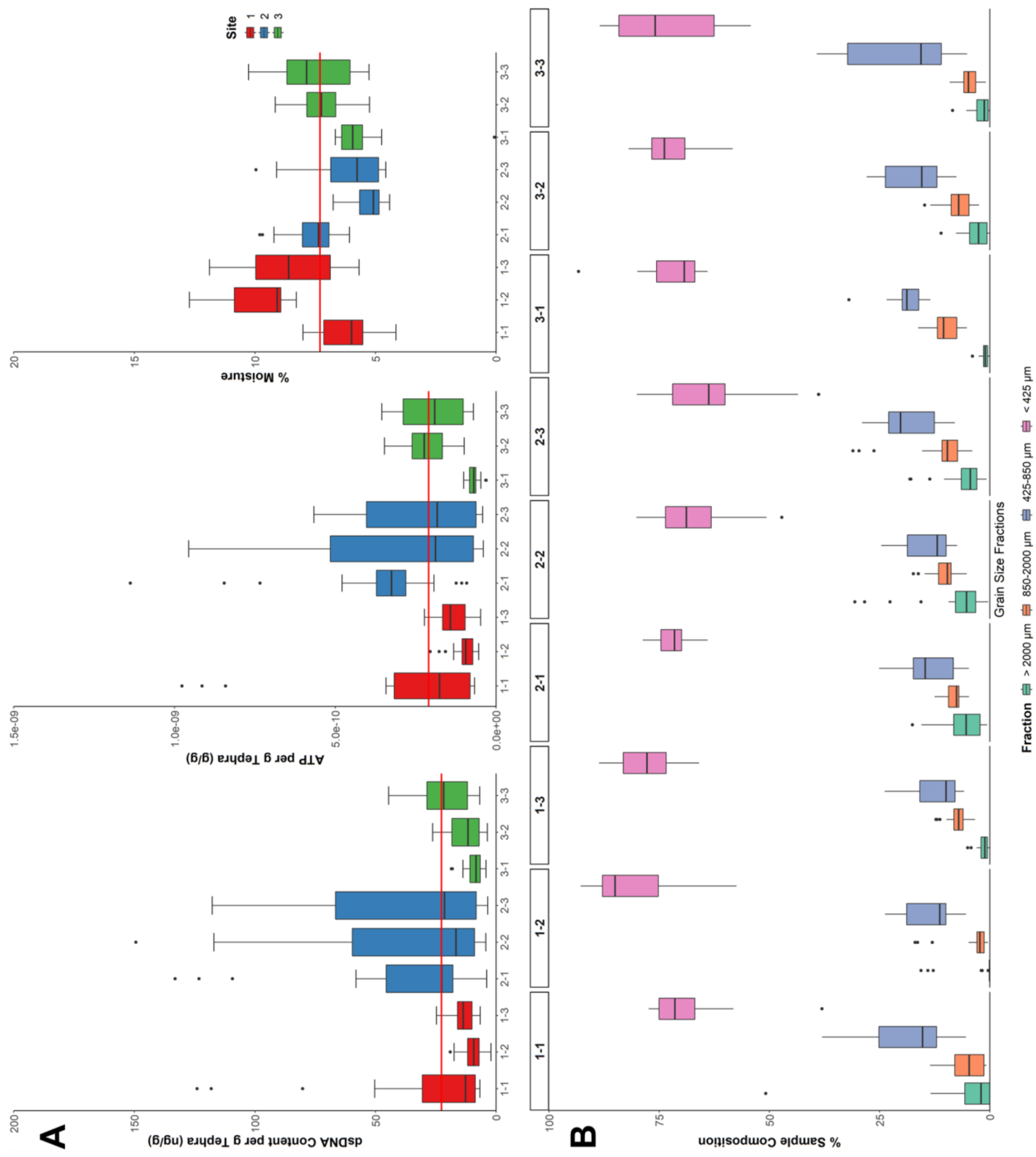

Figure A4-2 – 2018 Dyngjusandur Characteristic Factors. *A) dsDNA Content (ng / g sediment), ATP content (g / g sediment), and Gravimetric Moisture Content (g moisture / g dry sediment) with 1 m groupings. Colors represent each parent 10 m triangle. B) % Grain Size Fractions: > 2000 µm, 850-2000 µm, 425-850 µm, and < 425 µm. Samples are grouped at the 1 m level, and colors are representative of each fraction.*

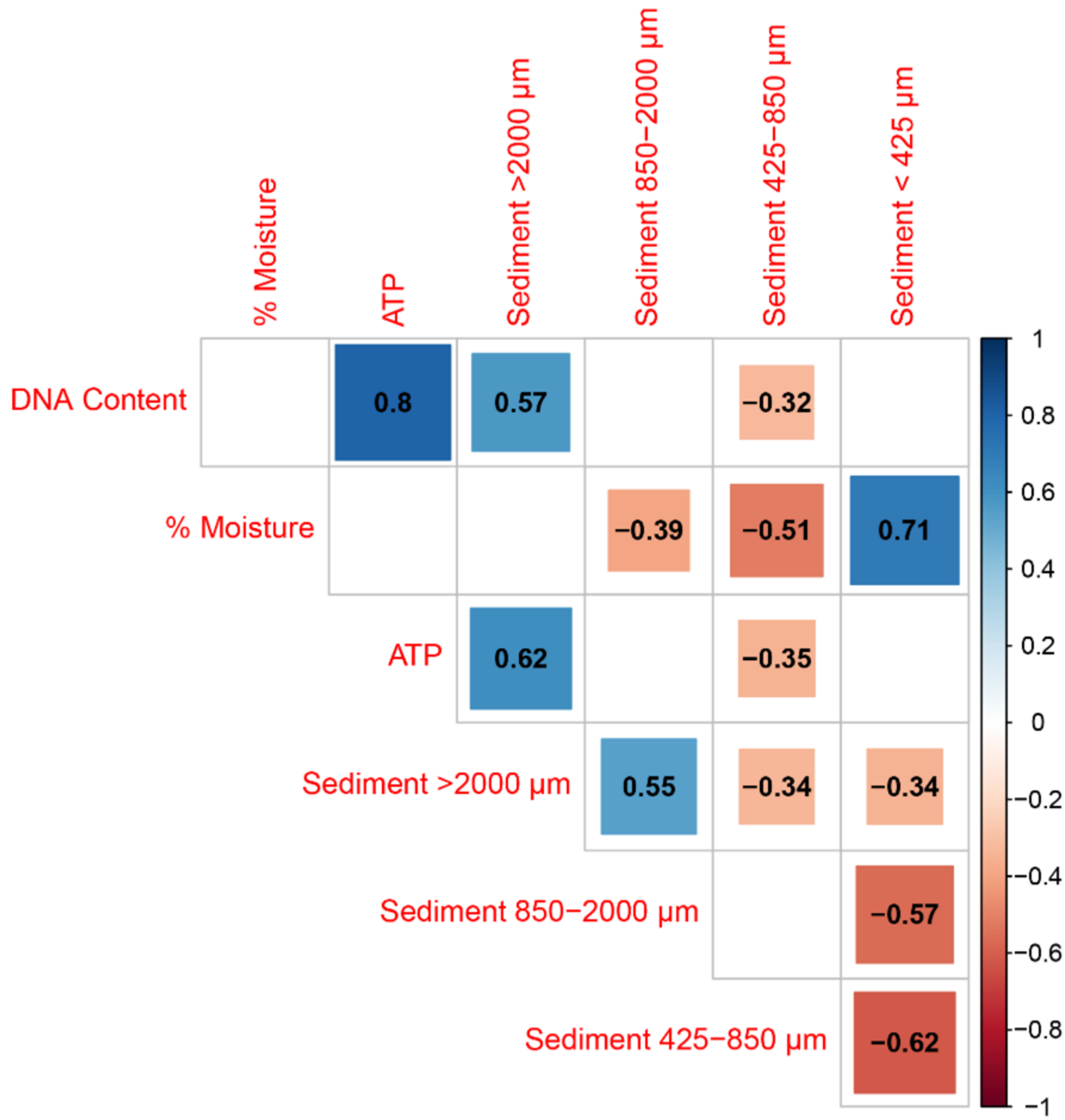

Figure A4-3 – Dyngjusandur 2018 Correlation Matrix. *Correlations were determined between characteristic factors using Spearman's rank correlation coefficients (overlayed on the matrix). Positive correlations are in blue, while negative correlations are displayed in red. Significant correlations were determined based on a 90% confidence interval, and insignificant correlations were left blank.*

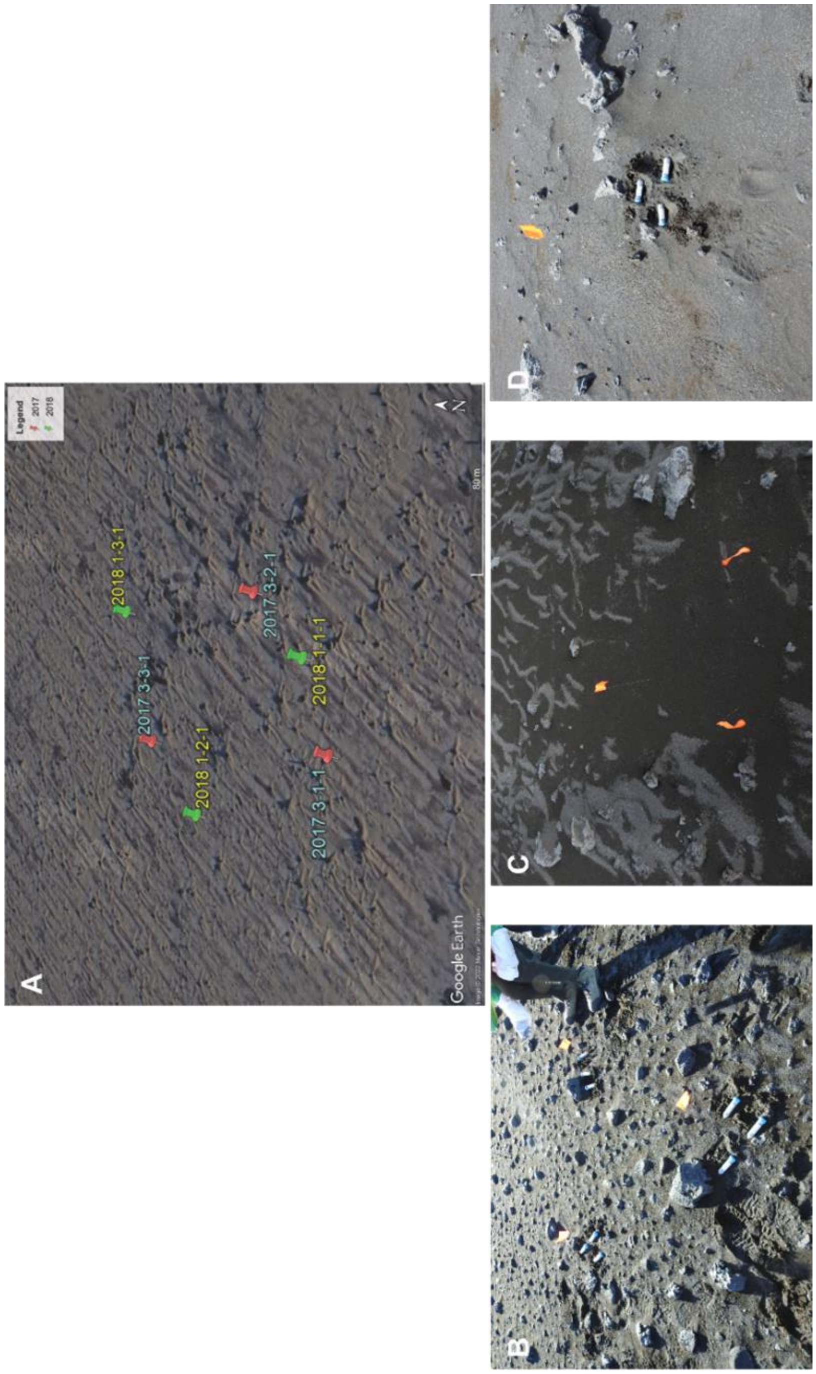

Figure A4-4 – 2017 vs. 2018: Spatial Separation & Visual Comparison. *A) 2017 and 2018 Sampling Sites: a visual representation of the proximity between the 2017 and 2018 sampling sites. B) 2017 Subsite 2: in field photography of a 1 m triangle sampling site from 2017 subsite 2. Large chunks of lava were abundant. C) 2017 Subsite 3: in field photography of a 1 m triangle sampling site from 2017 subsite 3. Large chunks of lava were infrequent and surrounding the sampling sites. D) 2018 Site 18-1-2: in field photography of a 1 m triangle sampling site from the second 10 m triangle in 2018. Large lava chunks were frequent, and nearly in contact with the sampling area.*

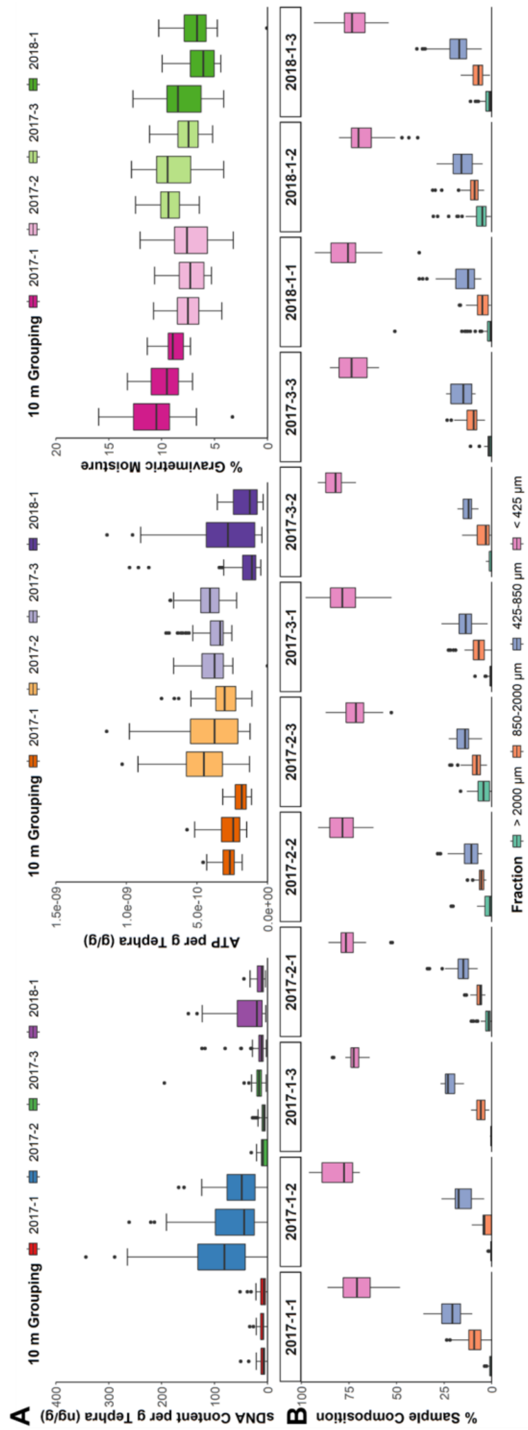

Figure A4-5 – 2017 vs. 2018 Characteristic Factors. *A) dsDNA content per g Tephra (ng/g), ATP content per g Tephra (g/g), and percent gravimetric moisture content per sample. Sites are displayed with 10 m groupings, and colors representative of each grouping. B) % Grain Size Fractions: > 2000 µm, 850-2000 µm, 425-850 µm, and < 425 µm. Samples are grouped at the 10 m scale, and each color is representative of a different fraction.*

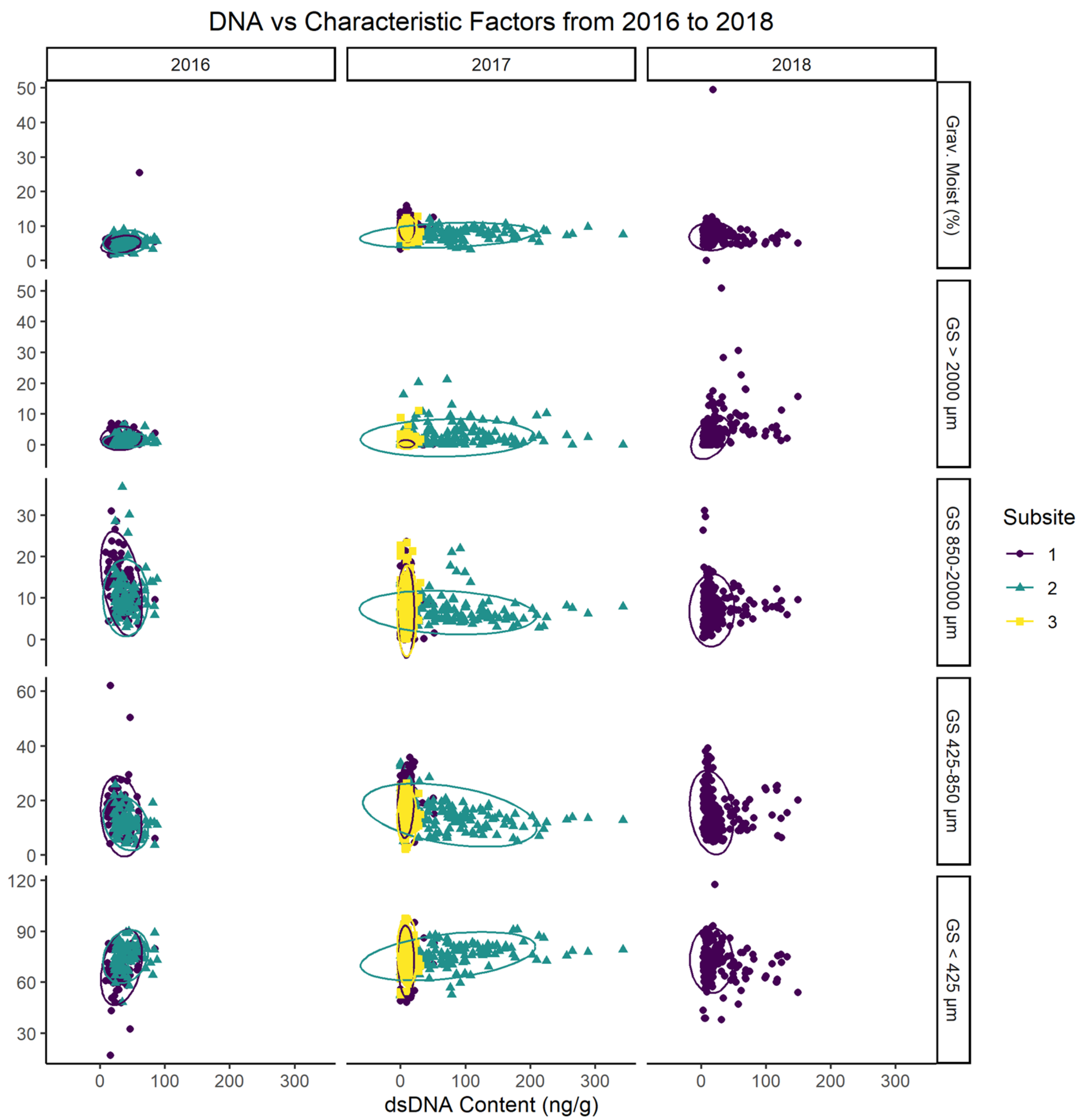

Figure A4-6 – Distributions of DNA Content Over Time*. For each year of data, dsDNA was plotted against each other characteristic factor: gravimetric moisture and grain size fractions. ATP was excluded from this figure given its lack of collection in 2016. Each color represents a 100 m triangle (subsite), and ellipses were plotted to encompass trends of significance.*

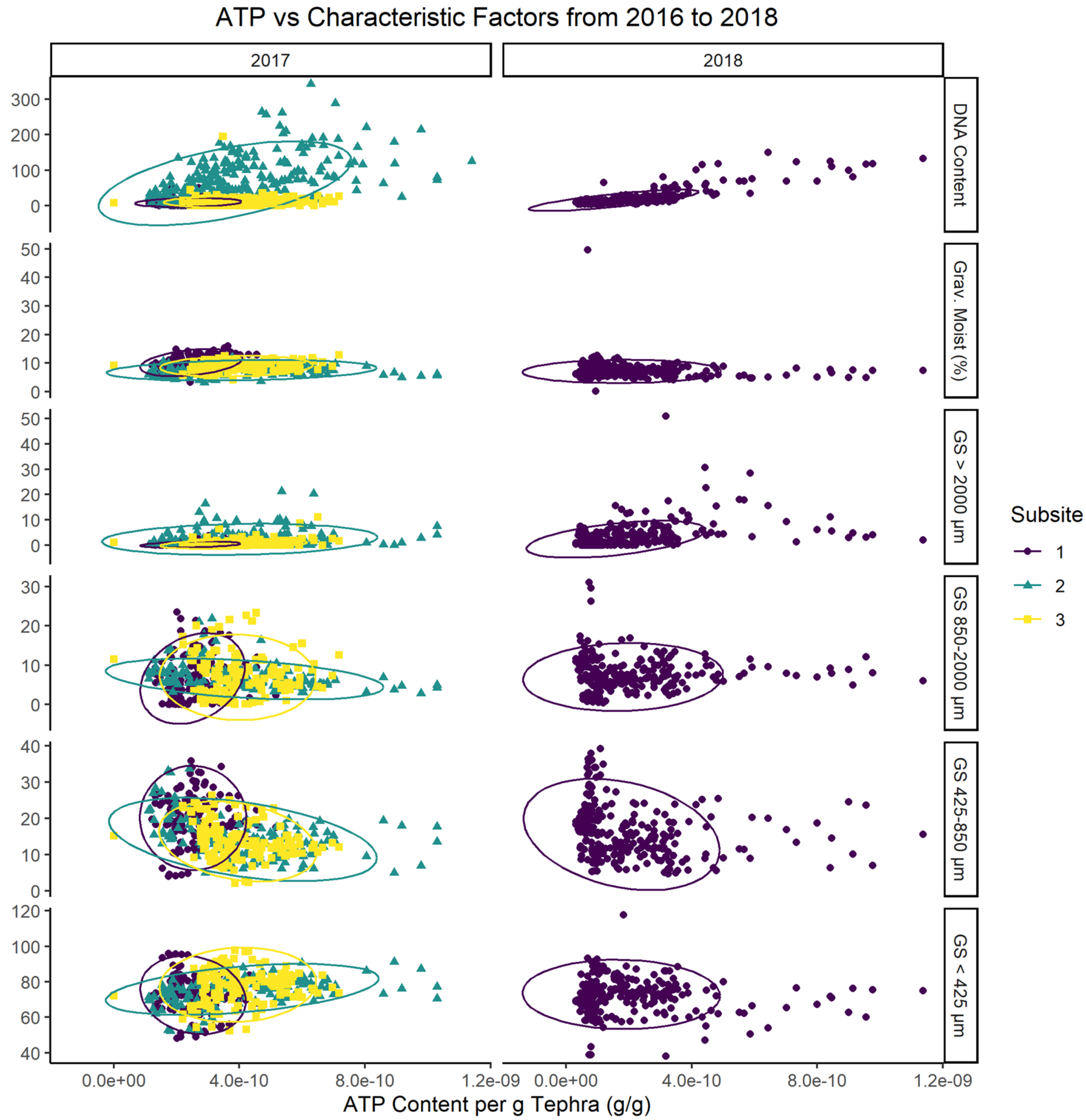

Figure 4-7 – Distributions of ATP Content Over Time. *For each year of data, ATP was plotted against each other characteristic factor: dsDNA, gravimetric moisture, and grain size fractions. Each color represents a 100 m triangle (subsite), and ellipses were plotted to encompass trends of significance.*